



# **Impact of Aluminium Adhesive Joints for the Automotive Industry as a Function of Environmental Conditions and Adherend Thickness**

**Submitted by:**

*Daniel Neto Rosendo*

A dissertation submitted for master's degree of  
mechanical engineering – FEUP

**Supervisor:**

Lucas F M da Silva

**Co-Supervisor:**

Guilherme Viana

July 2015



# Abstract

The use of adhesive joints in the automotive industry has been increasingly important over the years. Other more traditional bonding methods such as welding or riveting cannot compete with certain characteristics that only adhesive bonding can provide. An adhesive joint has a good stress distribution and, when used appropriately, behaves surprisingly well under impact and cyclical loads or fatigue, all while being lighter than its counterparts. Weight is an issue in the automotive industry since concerns regarding environmental impact and fuel efficiency of vehicles are emerging, which leads to an effort among manufacturers to develop lighter and more economic vehicles without compromising luxury or safety features.

In order to properly design an adequate adhesively bonded structure for the automotive industry it is required to predict its behaviour when subjected to different conditions by analysing its deformation as well the normal and shear load distribution throughout the adhesive and the energy the joint is able to absorb. This thesis focuses on evaluating the impact of aluminium adhesive joints as a function of temperature and moisture in order to understand how these conditions affect their mechanical properties and behaviour. After preparations of the required specimens (using two different adhesives and adherend thicknesses), several tests have been made in order to determine these properties and compare them to the predictions made using analytical methods. These tests were repeated in several combinations of different temperatures and moisture so that the effect of these properties can be conveniently interpreted.

It was observed that higher temperatures strongly increase the ductility of the adhesive, but mixed with moisture this can degrade them. Moisture can increase the energy absorbed through increased plastic deformation of the adhesive and improve behaviour at low temperatures. Thinner adherends at normal conditions withstand a large energy due to their plastic deformation.

*Keywords:* adhesive joint, structural adhesive, impact, single-lap joint, temperature, moisture.



# Resumo

A utilização de juntas adesivas na indústria automóvel tem sido cada vez mais importante ao longo dos anos. Outros métodos de ligação mais tradicionais como soldadura ou rebiteamento não são capazes de proporcionar certas características que apenas podem ser obtidas em ligações adesivas. Estas conferem boas distribuições de tensão e, quando usadas adequadamente, têm bom comportamento sob impacto ou cargas cíclicas de fadiga, sendo mais leves do que as alternativas. O peso dos veículos é um problema a considerar na indústria automóvel já que recentemente têm surgido preocupações relativas ao impacto ambiental e consumo de combustível dos automóveis, o que leva os fabricantes a desenvolver veículos mais leves e económicos sem comprometer a sua luxúria ou segurança.

Para projetar uma estrutura ligada por juntas adesivas para a indústria automóvel é necessário prever o seu comportamento quando está sujeita a diferentes condições, analisando a sua deformação e a distribuição de tensões normais e de corte ao longo do adesivo, bem como a energia que a junta é capaz de absorver. Esta tese foca-se em avaliar o impacto de juntas adesivas de alumínio em função da humidade e temperatura de modo a compreender como estas condições afetam as suas propriedades mecânicas e comportamento. Após as preparações dos provetes necessários (usando dois adesivos e espessuras de substrato diferentes), vários testes foram realizados para determinar estas propriedades e compará-las com as previsões feitas por métodos analíticos. Estes testes foram repetidos com várias combinações de temperaturas e níveis de humidade para que o efeito destas propriedades possam ser convenientemente interpretadas.

Foi verificado que temperaturas mais altas aumentam a ductilidade do adesivo, mas, com humidade, este pode ser degradado. A humidade aumenta a energia absorvida com o aumento da deformação plástica do adesivo para além de melhorar o comportamento da junta a baixas temperaturas. Substratos de espessura inferior, em condições normais de temperatura e humidade absorvem grandes quantidades de energia devido à sua deformação plástica.

*Palavras-chave:* junta adesiva, adesivo estrutural, impacto, junta de sobreposição simples, temperatura, humidade



# Acknowledgements

I would like to gratefully thank Prof. Lucas da Silva for his support throughout the development of this thesis. With his mentoring, guidance and willingness to patiently help in every aspect of the research, all difficulties and problems that arose were fluently overcome.

To my co-supervisor, Eng. Guilherme Viana, my sincere gratitude for the many hours spent teaching, helping and advising during every step of the thesis development. His assistance during the experimental work was invaluable towards the successful completion of my work.

I would like to acknowledge the staff from the LET laboratory, especially Mr. Miguel Figueiredo, for the meaningful assistance performing the impact tests.

I would also like to thank the personnel of the FEUP Adhesives Group for their selfless availability to help and support me in any situation that would arise. In particular, I commend Rodrigo, Tânia and Joana for their willingness to help and for the countless hours spent in my company making the development of this thesis a pleasant and all around enjoyable experience.

Finally, I would like to express my gratitude to all my friends and family who have supported me through every stage of my master's degree throughout the years. It's their care and understanding that enabled the accomplishment of this important step of my life.





# Contents

<b>1. Introduction .....</b>	<b>1</b>
1.1. Motivation.....	1
1.2. Objectives of the research .....	1
1.3. Research methodology.....	2
1.4. Thesis structure .....	3
<b>2. Literature Review .....</b>	<b>5</b>
2.1. Adhesive joints .....	5
2.2. Adhesive and adhesive joint properties.....	8
2.2.1. Structural adhesives .....	9
2.2.2. Adherend properties .....	11
2.3. Analysis of adhesive Joints .....	12
2.3.1. Linear elastic analysis .....	13
2.3.2. Volkersen's analysis.....	13
2.3.3. Goland and Reissner analysis .....	14
2.3.4. Adams et al. predictive model.....	15
2.4. Joints properties and failure.....	17
2.4.1. Adhesive joints properties.....	17
2.4.2. Impact loads .....	22
2.4.3. Effect of temperature.....	24
2.4.4. Effect of moisture .....	29
2.5. Testing methods.....	31
2.5.1. Water absorption tests on bulk specimens.....	32
2.5.2. Single lap joints for quasi-static and impact testing.....	34
2.5.3. Quasi-static testing of single lap joints.....	35
2.5.4. Impact testing of single lap joints.....	35
<b>3. Experimental Details .....</b>	<b>37</b>
3.1. Testing variables .....	37
3.2. Materials .....	37
3.2.1. Adhesives.....	37
3.2.2. Adherends .....	40
3.3. Water absorption tests.....	42
3.3.1. Experimental procedure .....	42
3.3.2. Experimental results and diffusivity .....	44
3.3.3. Water content prediction.....	47
3.4. Specimens manufacture.....	52
3.4.1. Single lap joints geometry .....	52
3.4.2. Surface preparation.....	54
3.4.3. Manufacture process.....	56
3.5. Tensile tests (quasi-static).....	58

3.5.1.	Experimental procedure .....	58
3.6.	<i>Impact tests</i> .....	59
3.6.1.	Experimental procedure .....	59
<b>4.</b>	<b>Experimental Results and Discussion</b> .....	<b>65</b>
4.1.	<i>Maximum load of the impact and quasi-static tests</i> .....	65
4.1.1.	Maximum loads under different strain-rate conditions .....	65
4.1.2.	Maximum load predictions – quasi-static .....	71
4.1.3.	Maximum load predictions – impact.....	74
4.2.	<i>Absorbed energy under impact</i> .....	77
<b>5.</b>	<b>Conclusions</b> .....	<b>83</b>
<b>6.</b>	<b>Future Work</b> .....	<b>85</b>
	<b>References</b> .....	<b>87</b>
	<b>Appendix A: Results of the quasi-static tests</b> .....	<b>89</b>
	<b>Appendix B: Results of the impact tests</b> .....	<b>97</b>

# List of Figures

Figure 1. Structure of an adhesive joint.....	5
Figure 2. Comparison between stresses distribution in riveted and adhesively bonded plates [1].....	6
Figure 3. Some types of stress an adhesive joint can be subjected to [1]. .....	7
Figure 4. Examples of different types of fracture [2]. .....	8
Figure 5. Adhesive deformation in a single lap joint considering rigid substrates and constant shear stress [9]. .....	13
Figure 6. Adhesive deformation in a single lap joint considering elastic substrates [9]. .....	14
Figure 7. Stress distribution on a single lap joint according to Goland and Reissner’s analysis model [9]. .....	15
Figure 8. Graphical representation of the predictive model of Adams et al. for single lap joints [11].	16
Figure 9. Stress distribution along the overlap of a single lap joint for a stiff and a flexible adhesive [1]. .....	17
Figure 10. Failure load of adhesive joints as a function of their exposure time to water after different surface treatments [13]. .....	19
Figure 11. Shear and peel stresses along the overlap length of a joint with 2 mm thick adherends...	20
Figure 12. Shear and peel stresses along the overlap length of a joint with 5 mm thick adherends...	20
Figure 13. Strength of SLJs in tension vs. overlap length for AV 119 adhesive and different adherend materials [15]. .....	22
Figure 14. Load vs displacement graphs for the same single lap joint, using mild steel adherends, with a strain rate of 1mm/min and 4.47m/s [16]. .....	23
Figure 15. Impact for lap shear aluminium alloy specimens [17]. .....	24
Figure 16. Adhesive strengths of several adhesives as a function of temperature - (A) tensile strength (measured with dogbone specimens); (B) shear strength (measured with TAST) [6]. .....	27
Figure 17. Adhesive ductility of several adhesives as a function of temperature - (A) tensile (measured with dogbone specimens); (B) shear (measured with TAST) [6]. .....	28
Figure 18. Moisture intake of the adhesive of a single lap joint [12]. .....	29
Figure 19. Variation of an adhesive's properties as its moisture content increases [12]. .....	30
Figure 20. Tg as a function of time submerged of the AV119 adhesive. ....	31
Figure 21. Geometry of a bulk specimen for water absorption testing. ....	32
Figure 22. Example of moisture absorption graphs for bismaleimide at several temperatures [25].	33
Figure 23. Standard geometry of a single lap joint. ....	34
Figure 24. Stress-strain curves for the SikaPower 4720 and Nagase XNR 6852E-2 [26]. ....	38
Figure 25. Comparison between stress strain curves at 1 and 100 mm/min for the (A) XNR 6852E-2 and (B) SikaPower 4720 adhesives [26]. .....	39
Figure 26. Stress-strain curve for the 6082-T6 aluminium at 1 mm/min. ....	41
Figure 27. Load-displacement curve obtained from an impact test of the 6082-T6 aluminium.....	42
Figure 28. Schematic representation of the mould used to produce bulk specimens [3]. ....	43
Figure 29. Bulk specimen for the XNR 6852E-2 water absorption test. ....	44
Figure 30. Average mass uptake of the bulk specimens of Nagase XNR 6852E-2 over time. ....	45
Figure 31. Comparison of moisture intake for the Nagase XNR 6852E-2 at 30°C and 50°C.....	46
Figure 32. Modelled area of the adhesive layer and directions from which water is absorbed. ....	48
Figure 33. Mesh used for the water uptake simulations. ....	48

Figure 34. Water absorption in 3 different points of the XNR 6852E-2 adhesive layer. ....	49
Figure 35. Average water content on the XNR 6852E-2 adhesive layer. ....	50
Figure 36. Water absorption in 3 different points of the SikaPower 4720 adhesive layer. ....	51
Figure 37. Average water content on the SikaPower 4720 adhesive layer. ....	52
Figure 38. Dimensions of the single lap joints used for testing. ....	53
Figure 39. Schematic illustration of the setup used for the anodization process. ....	55
Figure 40. 2mm adherend after surface preparation (The left, lighter section has been anodized). ..	55
Figure 41. Positioning of spacers and strips relative to the joints in the mould. ....	56
Figure 42. Optimized setup used for the joints with 2 mm adherends. ....	56
Figure 43. Hidraulic hot plates press with a mould inside. ....	57
Figure 44. Finished single lap joint using the SikaPower 4720 adhesive and 5 mm thick adherends. .	58
Figure 45. Single lap joint mounted for a quasi-static tensile test. ....	59
Figure 46. Process of electromagnetic induction heating [30]. ....	60
Figure 47. Equipment used for the induction heating system/close-up of the "pancake" induction coil used [2]. ....	61
Figure 48. Single lap joint mounted and waiting to be heated up before a high temperature impact test. ....	62
Figure 49. Nitrogen being sprayed onto a single lap joint ready to be tested under impact. ....	63
Figure 50. Maximum loads obtained from all the tests – Nagase XNR 6852E-2 with 2 mm adherends. ....	66
Figure 51. Maximum loads obtained from all the tests – Nagase XNR 6852E-2 with 5 mm adherends. ....	66
Figure 52. Adherend yielding after quasi-static testing of a SLJ using SikaPower 4720 with 2 mm adherends (-20 °C; moist) ....	67
Figure 53. Failure mode after quasi-static testing of a SLJ with XNR 6852E-2 at low temperature (5 mm adherends; moist). ....	68
Figure 54. Load-displacement curves of SLJs under impact using XNR 6852E-2 with 5 mm adherends under dry conditions and (A) -20 °C and (B) 80°C. ....	68
Figure 55. Figure 46. Maximum loads obtained from all the tests – SikaPower 4720 with 2 mm adherends. ....	69
Figure 56. Maximum loads obtained from all the tests – SikaPower 4720 with 5 mm adherends. ....	69
Figure 57. Adhesive failure after quasi-static testing of a SLJ with SikaPower 4720 at low temperature (2 mm adherends; dry). ....	70
Figure 58. Load-displacement curve of a quasi-static test of a SLJ with SikaPower 4720 at high temperature (2 mm adherends; moist). ....	70
Figure 59. Maximum load prediction using Adams et al. predictive model for the static tests – Nagase XNR 6852E-2 with 2 mm adherends. ....	72
Figure 60. Maximum load prediction using Adams et al. predictive model for the static tests - Nagase XNR 6852E-2 with 5 mm adherends. ....	72
Figure 61. Maximum load prediction using Adams et al. predictive model for the static tests – SikaPower 4720 with 2 mm adherends. ....	73
Figure 62. Maximum load prediction using Adams et al. predictive model for the static tests – SikaPower 4720 with 5 mm adherends. ....	73
Figure 63. Maximum load prediction using Adams et al. predictive model for the impact tests – Nagase XNR 6852E-2 with 2 mm adherends. ....	75
Figure 64. Maximum load prediction using Adams et al. predictive model for the impact tests – Nagase XNR 6852E-2 with 5 mm adherends. ....	75

Figure 65. Maximum load prediction using Adams et al. predictive model for the static tests – SikaPower 4720 with 2 mm adherends. ....	76
Figure 66. Maximum load prediction using Adams et al. predictive model for the static tests – SikaPower 4720 with 5 mm adherends. ....	76
Figure 67. Energy absorbed under impact for the joints with the XNR 6852E-2 adhesive. ....	78
Figure 68. Energy absorbed under impact for the joints with the SikaPower 4720 adhesive.....	78
Figure 69. Adhesive failure under impact of a SLJ with SikaPower 4720 at low temperature (2 mm adherends; dry).....	79
Figure 70. Adherend yielding after impact on a joint made with the Nagase XNR 6852E-2 adhesive (2 mm adherends; dry; room temperature) .....	80
Figure 71. Energy absorbed as a function of maximum load at -20°C.....	81
Figure 72. Energy absorbed as a function of maximum load at room temperature. ....	81
Figure 73. Energy absorbed as a function of maximum load at 80°C.....	82



# List of Tables

Table 1. General mechanical properties of commonly used structural adhesives.* .....	10
Table 2. General mechanical properties of commonly used adherend materials. ....	12
Table 3. Variables considered for testing the joints.....	37
Table 4. Basic properties of the SikaPower 4720 and the XNR 6852E-2 at 1 mm/min strain rate [26].	38
Table 5. Basic properties of the SikaPower 4720 and the XNR 6852E-2 at 100 mm/min strain rate [26]. .....	39
Table 6. Coefficients of diffusion and corresponding saturation levels for the XNR 6852E-2 adhesive.	47
Table 7. Coefficient of diffusion and corresponding saturation level for the SikaPower 4720 adhesive. .....	47
Table 8. Experimental and predicted maximum loads under quasi-static conditions. ....	71
Table 9. Experimental and predicted maximum loads under impact conditions. ....	74





# List of Acronyms and Symbols

## Abbreviations

SLJ – Single Lap Joint

FEA – Finite Element Analysis

PAA – Phosphoric Acid Anodization

RT – Room Temperature

## Symbols

$b$  – Joint width

$l$  – Overlap length

$t$  – Adherend thickness

$\tau$  – Shear stress

$\tau_y$  – Yield strength

$\sigma$  – Tensile stress

$\varepsilon$  – Strain

$P$  – Applied load

$k$  – Bending moment factor

$E$  – Adherend's Young's modulus

$T_g$  – Glass transition temperature

$d$  – Bulk specimen thickness

$m$  – Bulk specimen weight

$c_s$  – Adhesive's moisture saturation level



# 1. Introduction

## 1.1. Motivation

Nowadays, the automotive industry has been assessing different methods of reducing the weight of their structures in order to improve environmental impact and fuel efficiency. By using adhesive bonding, different materials can be joined while providing smooth surfaces and improving corrosion and fatigue resistances and, most of all, granting a uniform stress distribution. Adhesives are also the only way to joint composite materials efficiently. When designing a joint using structural adhesives for the automotive industry, one of the most important factors to consider is its resistance to impact load. High toughness of the adhesive is important in these situations and as such epoxy adhesives are commonly used. Even though pure epoxy resins are brittle, technological advances have allowed them to be produced with improved toughness without forfeiting too much of the joint strength.

The varying environmental conditions that adhesively bonded structures made for the automotive industry are subjected to during their lifetime is a major concern. It is extremely important to know how different conditions affect the behaviour of the joints considering that, under high strain-rate, the different temperatures and moisture absorption levels of the adhesive can affect its behaviour. Experimental testing of joints under impact load while exposed to these different conditions is, for these reasons, very important in order to design the most efficient possible structures using adhesive bonding.

## 1.2. Objectives of the research

The objective of this study is to analyse the behaviour of adhesive bonded joints under several conditions that emulate environmental changes or situations that could appear in real situations for the automotive industry, focusing mainly on impact loads.

Two different new adhesives were studied, which have suitable properties for this type of application though, after further analysis, may behave differently under some important condition changes like different temperatures or moisture level. To understand how the bending of the substrates affects the joints' behaviour and strength, different adherend thicknesses were also used. Finally, to compare how the strain-rate affects the failure of the adhesive joint, tensile quasi-static tests were performed.

### 1.3. Research methodology

To accomplish the purpose of this work described in the previous section, a predetermined series of tasks were carried out in the following order:

- 1) Bibliographic review of adhesive bonding in general, including the study of the required materials and testing methods and especially how the variable conditions may affect the bonded joints;
- 2) Manufacture of the joints required to perform the tests under all conditions, after studying an optimized and efficient way to do so and to prepare the materials;
- 3) Perform the water absorption tests required to determine the unknown diffusion properties of one of the adhesives;
- 4) Determination and testing of the methods used to heat up and cool down the joints for the different temperature tests;
- 5) Perform the quasi-static tensile tests of the adhesive joints for all of the required combinations;
- 6) Perform the impact tests of the adhesive joints for all of the required combinations;
- 7) Organize and analyse the results from the several tests and compare them to the predicted calculated values.

## 1.4. Thesis structure

This thesis is divided into several sections, organized in the following manner:

**Chapter 2 – Literature Review:** This section summarily reviews the state of adhesive bonding compared to other methods. Adhesives and adhesive joints are also described as well as the most relevant analytical methods to study their stress distribution under load. This section also reviews how the different variables under which the joints will be tested are expected to affect their behaviour and, finally, the testing methods that are most adequate to obtain the required results will also be described.

**Chapter 3 – Experimental Details:** Initially all the testing variables are summarized as a way to review exactly what needs to be tested. After the characterization of the required materials, all experimental procedures are described, from the manufacturing of the joints to all the tests that are performed, including the required equipment and techniques used to obtain the required conditions at the time of testing. This section also summarizes the results from the several tests in a way to facilitate the comparison between the different testing conditions.

**Chapter 4 – Experimental Results and Discussion:** This section presents a more in-depth analysis of the results obtained in the previous chapter and evaluates if they correspond to what was expected after the literature review. To verify the accuracy of the experimental results, failure predictions using an analytical prediction method are made for the basic tests and compared to what was obtained.

**Chapter 5 – Conclusions:** Brief summary of the results obtained from the previous sections. The difference between the adhesives' behaviour is explained as well as how each variable affected each adhesive.

**Chapter 6 – Future work:** Suggestions are made for what can be done to further investigate the covered theme of the thesis and how the research of impact on single lap joints can be improved.



## 2. Literature Review

This chapter succinctly reviews the properties of the material used for performing the required tests and as analyses the types of specimens used throughout the study and the required methods of prediction and testing. The effect of the conditions that vary among the tested joints were also reviewed.

### 2.1. Adhesive joints

An adhesive can be generally described as a material capable of sustaining two surfaces of another material together, keeping them from being separated [1]. Even though there are several substances capable of such behaviour, it is interesting for application in a diverse amount of industries to study adhesives which withstand a substantial load (~7 MPa shear strength). These are named structural adhesives and are used for a large amount of applications. The most important of which are the epoxy adhesives which present the highest strengths and the have the most varied purposes.

An adhesive joint (Figure 1) is composed by the adhesive and the materials that it's bonding – the adherends or substrates. The region closer to the contact point between the adhesive and the adherend is the interphase, and the plane that divides their surfaces is named interface.

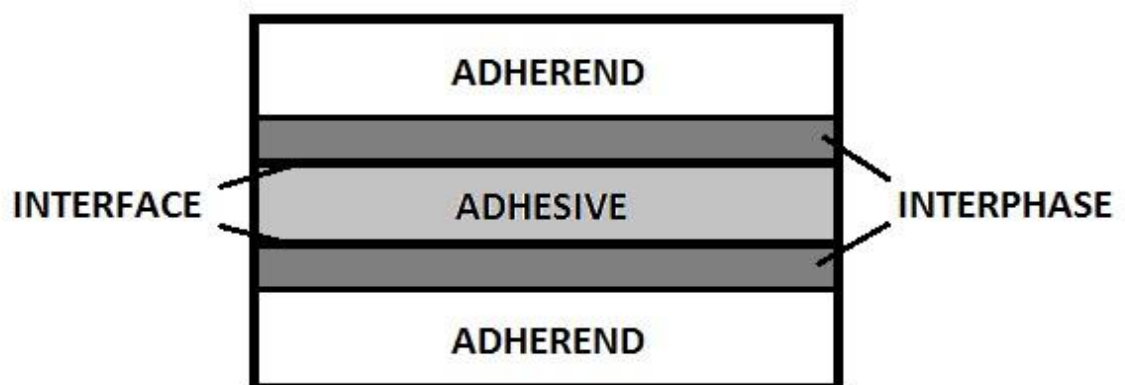


Figure 1. Structure of an adhesive joint.

By appropriately applying adhesive joints in the automotive industry it is possible to improve design options while joining different materials such as aluminium with steel or copper, even with very different expansion coefficients (due to the adhesives' flexibility) or thin plates, all while being accessibly possible to create automatic processes to apply them. It is also the only method that can be used to efficiently bond composite materials. This allows the creation of lightweight structures without sacrificing their resistance, expanding possibilities in several industries and, in the case of the automotive industry, granting the opportunity to create more fuel efficient vehicles which in turn reduce environmental issues which have been of considerable concern over the several last years. Furthermore, one of the most notable advantages of using adhesive joints is how evenly distributed it is possible to have the stresses throughout the bonded zone, as is visible in Figure 2.

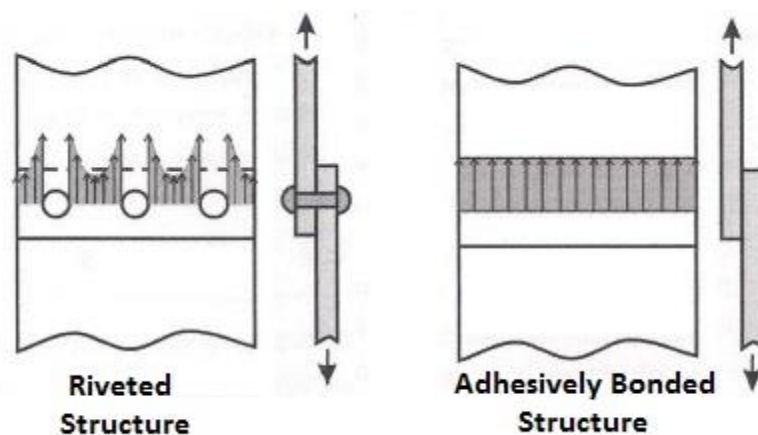


Figure 2. Comparison between stresses distribution in riveted and adhesively bonded plates [1].

Even though they have many advantages, there are certain aspects that need to be carefully assessed before implementing adhesively bonded joints. In many cases the materials' surfaces must be previously treated in order to make sure that the adhesion will be sufficiently strong to hold the joint. It is also extremely important to understand that adhesives, due to their polymeric nature, are very sensitive to heat and humidity variations so selecting which adhesive to use in each situation is a crucial step when designing an adhesively bonded structure. Another important factor to consider is that adhesives are weak to certain kinds of load. It is necessary to avoid



localized stresses on the adhesive and, most of all, cleavage and peel stresses (Figure 3).

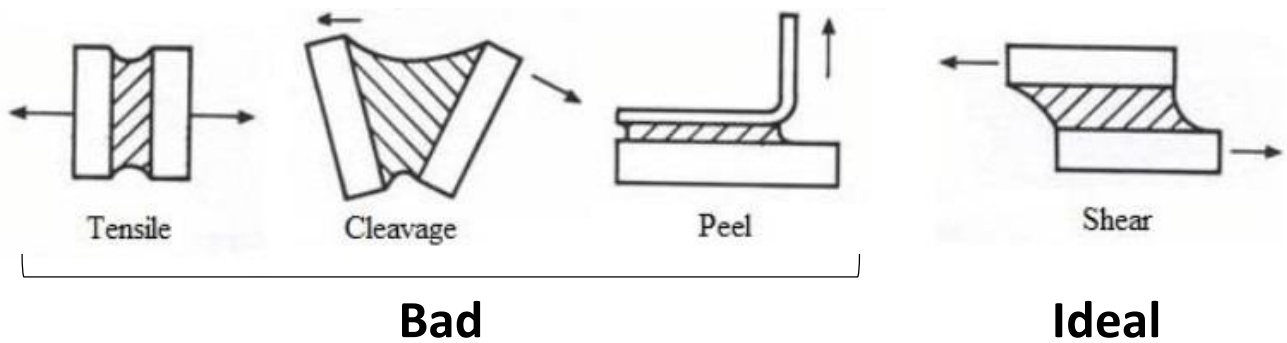


Figure 3. Some types of stress an adhesive joint can be subjected to [1].

In order to study the failure of an adhesive joint, it is necessary to understand its failure modes (Figure 4). The intermolecular forces that exist inside only one substance are known as *cohesion forces* while the forces between two different materials are responsible for their adhesion [1]. This means that when an adhesive joint fails it can do so cohesively at the adhesive or adherend, or it can fail adhesively at the interface.

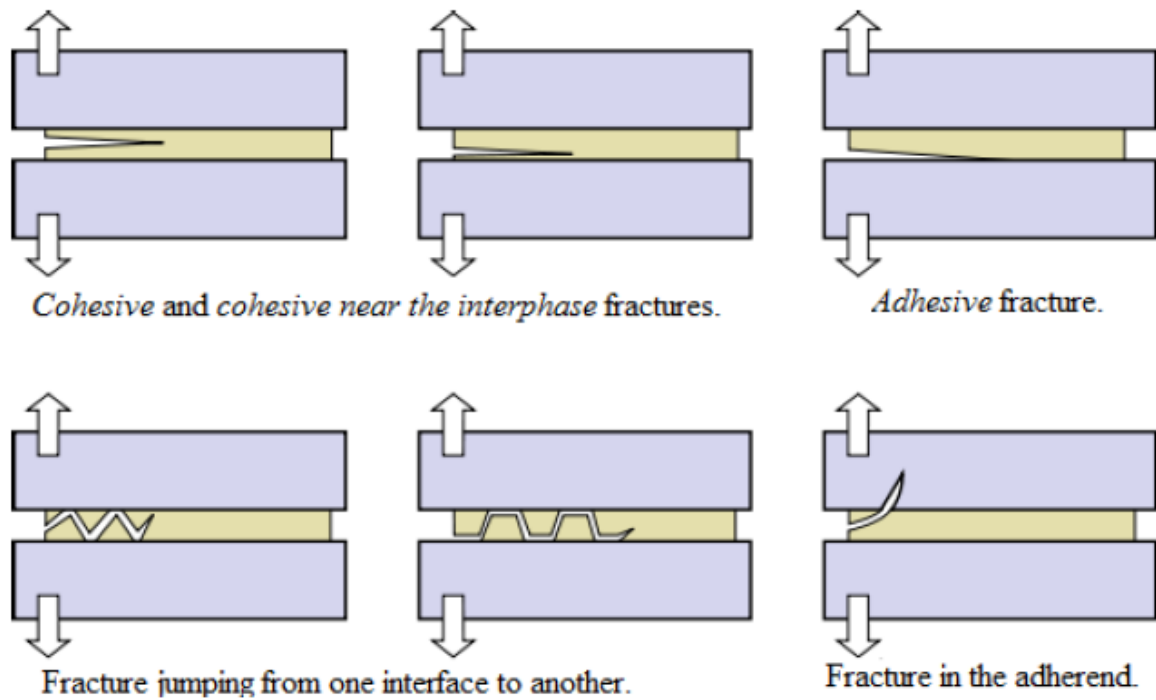


Figure 4. Examples of different types of fracture [2].

## 2.2. Adhesive and adhesive joint properties

There are a wide variety of adhesives available with different properties and adequate for different situations. They are polymeric by nature and formed by small groups of atoms – monomers – which can be rearranged in a great number of viable combinations, allowing a high variety of polymers to exist. Furthermore, these adhesives can also be mixed [3]. This results in a number of different classifications from which to organize them.

Even though there are several natural adhesives such as starch or natural rubber which can be extracted from their corresponding natural resources, the industry has designed their own, more efficient adhesives, suitable for different functionalities. They can then be classified as thermoplastics, thermosets and elastomers (rubbers), depending on their intermolecular strength and molecular structure. One of the main differences in their behaviour lies on their glass transition temperature ( $T_g$ ) [2].

Adhesives can also be classified based on their chemical families (such as epoxy or silicone), their curing method (chemical reaction, solvent loss or cooling for instance), and their physical form (single or dual component) [1, 4].

Regarding their role in the industry we can yet classify them by their application. Non-structural adhesives, depending on their function, can be hot melt, pressure sensitive or water-based adhesives [1]. Structural adhesives are designed to transfer load between two adherends and in order to be classified as such, they must have a shear strength higher than 5-7 MPa. These are the most important to research in the context of this study.

### 2.2.1. Structural adhesives

A structural adhesive is a cross-linked/thermosetting polymer even though some thermoplastics are used as such [5]. Since a correctly made adhesive joint is produced carefully and with proper surface preparation of the adherends, its failure is generally at the adhesive (cohesive failure at the adhesive, as mentioned above), meaning that the strength of an adhesive joint is directly related to the strength of its adhesive. Also, the adhesive's material is generally not as stiff as the adherend's, and as a consequence a significant part of the elongation may come from the strain of the adhesive.

Ductile adhesives can usually be stronger than other, stronger but less ductile ones, even though normally this wouldn't be the case for more ductile and flexible adhesives. This happens due to these being able to more efficiently distribute the stress throughout the overlap (causing plastic deformation on the adherend) [1, 6]. This is one of the reasons why the selection process of the adhesive to be used on a certain application is of extreme importance and should be carefully assessed. Fortunately there are several types of adhesives with diversified mechanical properties (Table 1).

Table 1. General mechanical properties of commonly used structural adhesives.\*

Common adhesives	Density [kg/m <sup>3</sup> ]	Young's modulus [GPa]	Shear modulus [GPa]	Tensile strength [MPa]
Epoxy	1.15*10 <sup>3</sup>	2.8	1.2	60
Polyurethane	1.18*10 <sup>3</sup>	0.02	0.008	40

\*Values composed from several databases and textbooks.

Each application normally has more than one suitable adhesive. There are surface treatments that can be performed to improve the joints' performance in certain conditions and some adhesives, such as epoxies, are versatile and can bond adherends of different materials [7], but each of the categories listed above is composed of a wide variety of specific adhesives. It is necessary to take into account the materials that need to be bonded, application costs, aesthetics, health requirements, fabrication process and other factors – selecting the adequate adhesive requires a significant amount of experience but it is helpful to have a general idea of the main properties that make each category unique:

**Epoxy:** These adhesives are the most important in the industry and can present a one- or two-part physical form. They have very good strength and toughness, corrosion resistance, while presenting good dimensional stability and low shrinkage. The one-part epoxies normally cure at a high temperature (~150°C) but for a relatively short amount of time, while two-part epoxies cure at room temperature for a longer amount of time, even though this can sometimes be reduced with a higher temperature. These two-part systems need to be mixed before being applied, a process that can be automated as well as its application. Their service temperature is -40°C to 100°C for one-part and -40°C to 180°C for two-part epoxies. This type of adhesive is mostly used in aircraft, land vehicles such as cars and trains, and sports.

**Polyurethane:** These adhesives are normally used due to their good strength and toughness at low service temperatures (-200°C to 80°C), as well as their wetting ability. They can also appear as one- or two-part systems and are cured at room temperature. The main disadvantages of using a polyurethane is their poor heat resistance and non-practical curing method, through moisture, which is not ideal for

wider joints in which the water has trouble penetrating the whole overlap area. They are used when the joints will be used under small loads and in cryogenic applications, as well as in the automotive and shoe industries.

Even though these are the currently most used categories, there are several factors that can lead to a better choice regarding the type of adhesive to be used. Once again, this should be carefully assessed to efficiently design an adhesively bonded structure.

### 2.2.2. Adherend properties

As it has already been mentioned, an adhesive joint generally fails cohesively at the adhesive due to it having less strength than the adherends it is bonding. In certain applications, however, in order to absorb more energy, the adherends need to have some elongation and be more flexible. When the joints are loaded over a large area, the adhesive can be providing a high enough strength so that the material of the substrate is deforming instead of the adhesive [7]. This means that the strength of the adhesive joint as a whole is not only dependant of the strength of the adhesive but of a combination of the strength of the adhesive and the substrates.

An adherend material with low Young's and shear moduli will suffer high deformation, especially at the edges of the overlap since that is where the load transfer begins and so causes a higher effect due to the differential straining in the adhesive [1, 8]. Since the adherend yielding can also lead to failure, its materials' strength is also essential to evaluate when determining the joint's strength. Table 2 presents the values for these properties for some of the most commonly used materials in structural adhesive bonding.

Table 2. General mechanical properties of commonly used adherend materials.

<b>Material</b>	<b>Relative density</b>	<b>Young's modulus [GPa]</b>	<b>Shear modulus [GPa]</b>	<b>Tensile strength [MPa]</b>
Mild Steel	7.8	208	80	400
Hard Steel	7.7	200	80	650
Aluminium	2.7	70	26	300
Carbon fibre reinforced composite	1.6	100	40	800

### 2.3. Analysis of adhesive Joints

In order to design the most efficient joints, it is crucial to understand how to predict their behaviour upon failure. For the more complex joints' geometries or joints with more elaborate materials, a numerical method such as the finite elements method (FEM) is the most preferable. However, in order to obtain a faster and easier solution, a closed-form analysis method can be used [1, 9].

The simplest way to obtain the properties of an adhesive and study its behaviour is by using single lap joint (SLJ) specimens. They have a very simple configuration, are similar to a lot of joints used in the industry and have been used as a standard specimen to analyse adhesive joints so, considering the main purpose of this research, the main analytical methods for studying SLJs will be reviewed.

Some simplifications are made for most analysis: Substrates are considered to only deform due to tension and bending, and adhesive stresses are being reduced to only peel and shear, both considered constant throughout the adhesive width.

### 2.3.1. Linear elastic analysis

The simplest and most common analysis of a SLJ consists in considering that the substrates are not deformable when compared to the adhesive, which is much softer, meaning that the shear stress across the adhesive layer is constant (Figure 5).

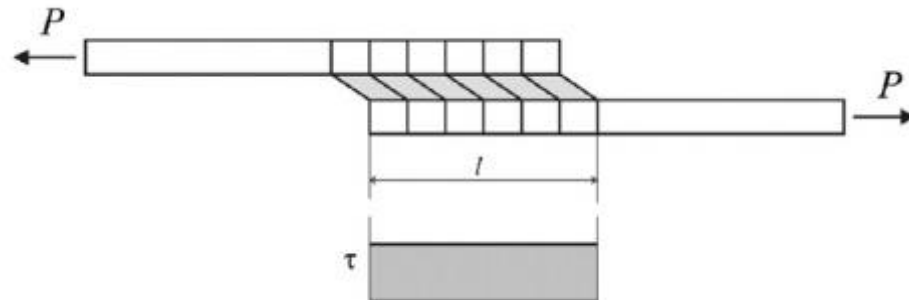


Figure 5. Adhesive deformation in a single lap joint considering rigid substrates and constant shear stress [9].

Considering  $P$  to be the applied tensile force,  $l$  the joint's overlap length and considering  $b$  as the specimen's thickness, the adhesive shear stress can be calculated by Equation 2.1:

$$\tau = \frac{P}{b.l} \quad (2.1)$$

Despite the fact that this method is not the most accurate, it is still very commonly used as a quick method to roughly predict the adhesive's shear strength.

### 2.3.2. Volkersen's analysis

In contrast to the linear elastic model, the Volkersen's analysis considers the adherends to be elastic. This introduces a shear stress differential across the overlap of the SLJ and, by considering the joint to be in pure tension (excluding the substrates' bending moment), the adhesive is considered to be under pure shear stress [9, 10].

The non-constant strain along the overlap due to the substrates' elasticity and therefore increased deformation near the adhesive's edges provokes a stress distribution on the adhesive as illustrated in Figure 6.

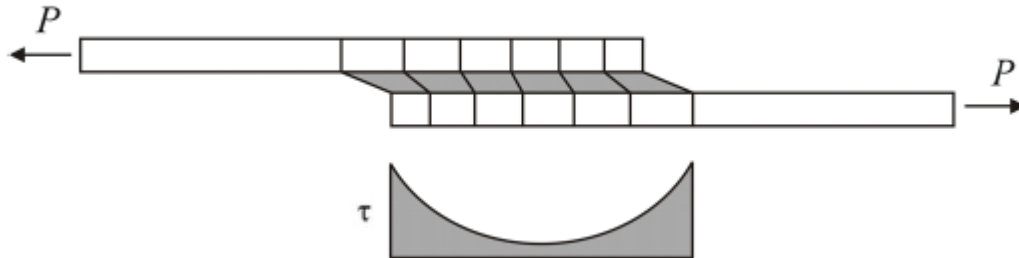


Figure 6. Adhesive deformation in a single lap joint considering elastic substrates [9].

This analysis model does not consider the bending of the substrates or their shear deformation, which are important aspects to consider when analysing an adhesive joint, especially when the adherends have low shear and transverse moduli [9, 10]. The Volkersen's model is more suitable for double lap joints, where the adherends' bending moment is not as significant as in SLJs.

### 2.3.3. Goland and Reissner analysis

This analysis is a more complex yet refined model since it considers adherend bending which in turn introduces peel stresses in the adhesive layer. The resulting bending moment in the SLJ is caused by its eccentric load path and makes the joint rotate. The applied load is therefore no longer aligned with the shear stress plane in the bonded area, which is evident in Figure 7. This method also takes into account how the bending moment decreases as the joint rotates so it is appropriate for adherends whose materials present large elastic deflections [9].



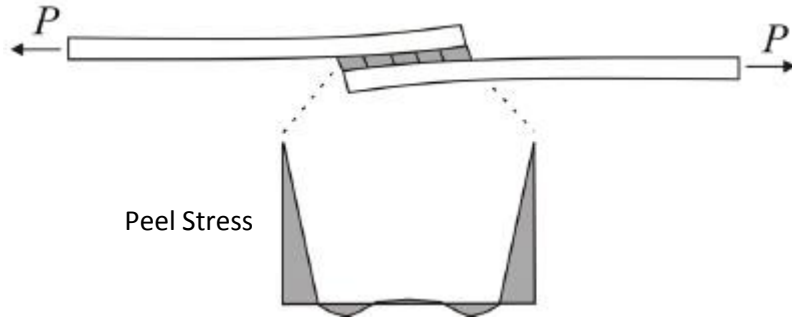


Figure 7. Stress distribution on a single lap joint according to Goland and Reissner's analysis model [9].

#### 2.3.4. Adams et al. predictive model

As opposed to the previous methods, the predictive model of Adams et al. considers adherend yielding and is described as followed [10]. The load that corresponds to the global yielding of the adhesive (adhesive totally plastically deformed) is given by:

$$P_a = \tau_y bl \quad (2.2)$$

where  $P_a$  is adhesive joint's failure load,  $\tau_y$  is the yield strength of the adhesive,  $b$  is the joint's width and  $l$  is the overlap length.

The direct tensile stress ( $\sigma_t$ ) acting on the adherend resulting from the applied load ( $P$ ) is given by:

$$\sigma_t = \frac{P}{bt} \quad (2.3)$$

where  $t$  is the adherend's thickness.

In the case of substrate bending (as per Goland and Reissner), the bending moment ( $M$ ) causes stress in the inner adherend ( $\sigma_s$ ), that is given by:

$$\sigma_s = \frac{6M}{bt^2} ; \quad M = \frac{kpt}{2} \quad (2.4)$$

where  $k$  is the bending moment factor which reduces from unity as the lap rotates from the load.

The sum of the direct stress  $\sigma_t$  and the bending stress  $\sigma_s$  represents the global stress acting on the adherend. The maximum load for adherend yielding is therefore given by:

$$P_s = \frac{\sigma_y bt}{(1+3k)} \quad (2.5)$$

where  $\sigma_y$  is the yield strength of the adherend.

For low loads and short overlaps, where  $k$  is approximately 1:

$$P_s = \frac{\sigma_y bt}{4} \quad (2.6)$$

When the case is the opposite and the overlap length is significantly higher than the adherend thickness ( $l/t \geq 20$ ), the value of  $k$  is approximately 0:

$$P_s = \sigma_y bt \quad (2.7)$$

Figure 8 is the graphical representation of these equations, showing the failure load of the joint due to adherend or adhesive global yielding as function of overlap length.

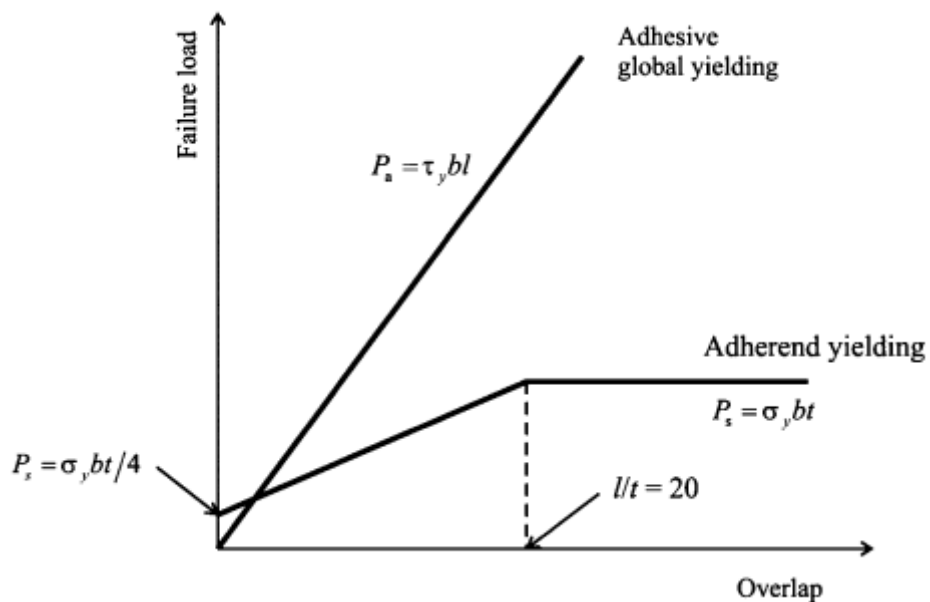


Figure 8. Graphical representation of the predictive model of Adams et al. for single lap joints [11].

## 2.4. Joints properties and failure

One of the main purposes of this study is to analyse the differences in how an adhesive joint behaves when certain variables are added or changed, both in the manufacturing of the joint and at the time of testing. This section will review all of these parameters and in what ways they affect the strength of the joints so that their failure can more easily be predicted.

### 2.4.1. Adhesive joints properties

#### 2.4.1.1. Adhesive properties

Even though a flexible but ductile adhesive is normally weaker than a stronger and less ductile one, it is usually more suitable for structural adhesive bonding. As it has been mentioned in the analysis of adhesive joints, the strain along the overlap is not constant and is increased nearer to the edges, where the bending moment due to the elasticity of the adherends is more pronounced. Figure 9 shows that by using a ductile and flexible adhesive, this stress distribution along the overlap is more uniform than when using stiffer adhesive, leading to a stronger joint even if the adhesive is not as strong.

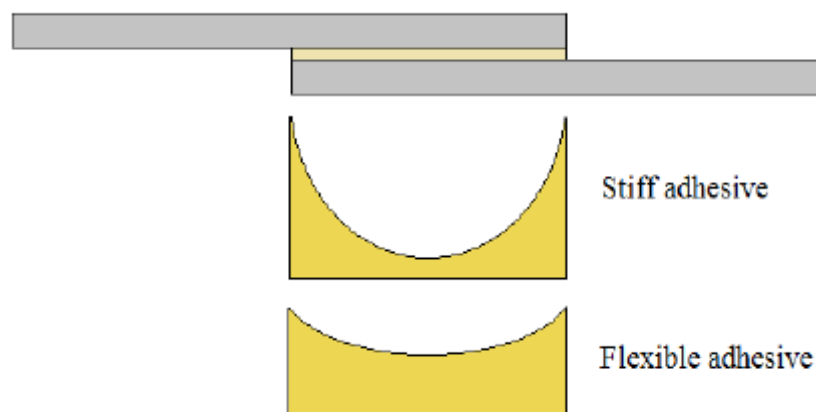


Figure 9. Stress distribution along the overlap of a single lap joint for a stiff and a flexible adhesive [1].

There are several properties of a single lap joint that can affect its durability under fatigue but using a ductile adhesive instead of a brittle one is an important step towards guaranteeing this important factor.

#### *2.4.1.2. Adherend surface preparation*

When an adhesive joint fails, in order to maximize the load required to do so, the failure mode should be cohesive. In order to increase the required energy to deteriorate the adhesive-adherend plane and avoid adhesive failures, the surface of the adherend should be carefully treated on the region that will be bonded.

One way of doing this is increasing the area of contact between the adhesive and the adherends. Without changing the overlap length, this can be done by intentionally creating a roughness at the adherends' surface, which is normally done by either using sandpaper or sandblasting. It is also important to degrease the surface and make sure that it is clean at the time of adhesive application.

Especially when wetting is expected to occur, these treatments may not suffice, as macro roughness, voids on the interface and poor spreading capability of the adhesive may cause an interfacial failure of the joint. Several studies have shown that for aluminium adherends, Phosphoric Acid Anodization (PAA) is an effective way to produce a good durability by forming a "micro-composite" structure of adhesive and oxide structure. By using PAA treatments, the failure mechanism involves the uppermost region of the oxide layer which is the weakest due to hydration that can be reduced by priming after the PAA treatment [12].

Figure 10 compares the reduction rate of maximum failure load of adhesive joints during their time exposed to water, after different kinds or combinations of surface treatments.

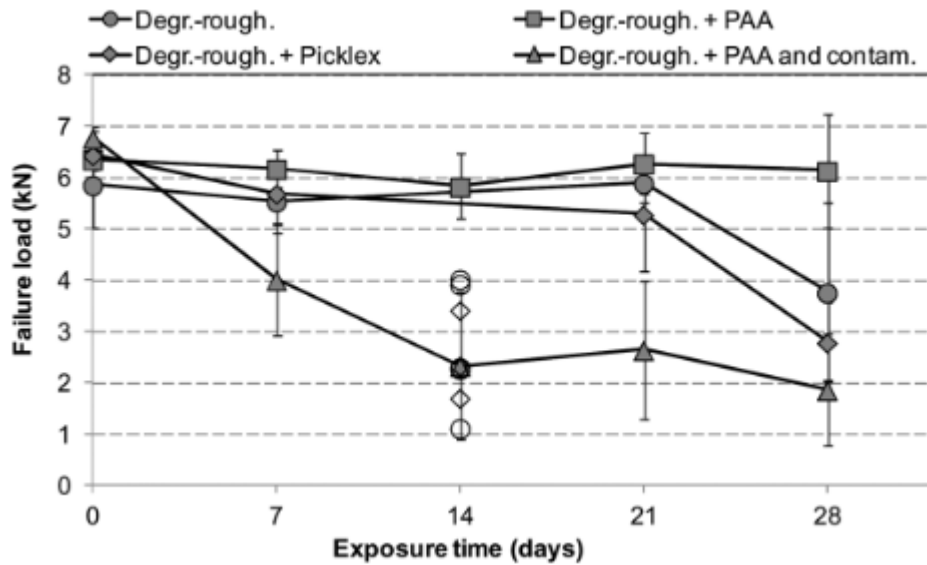


Figure 10. Failure load of adhesive joints as a function of their exposure time to water after different surface treatments [13].

#### 2.4.1.3. Adherend thickness

To verify the effect of adherend thickness on a SLJ, two simulations were made using the JointDesigner [14] website, where two SLJs were modelled under the exact same conditions except the adherend thickness which was of 2 mm and 5 mm (Figures 11 and 12), respectively, and analysed using the Goland and Reissner analytical model. These are the results along the overlap:

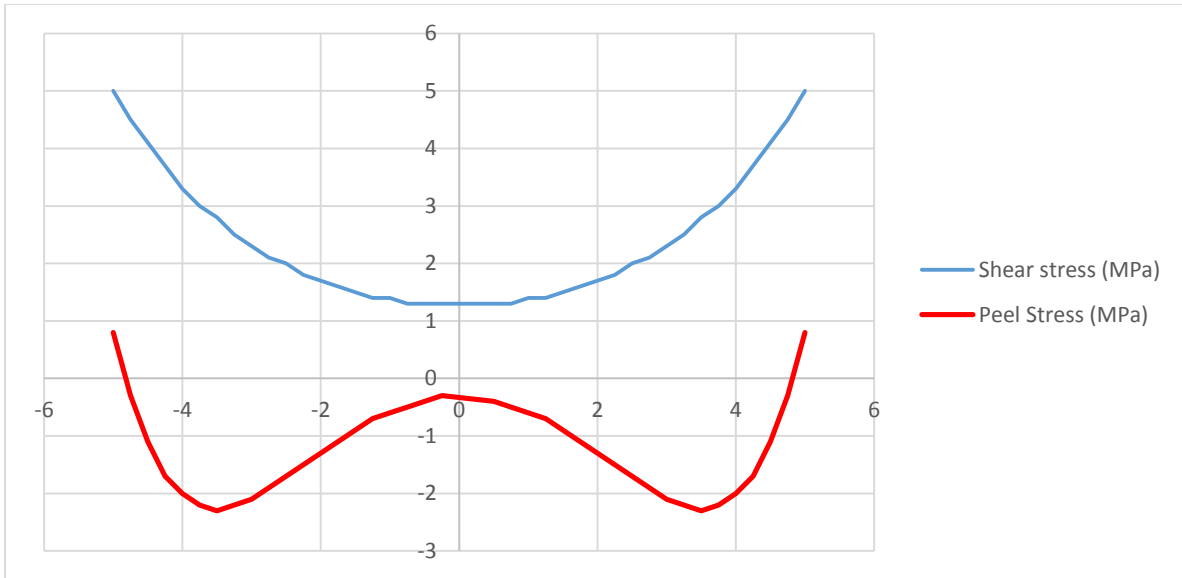


Figure 11. Shear and peel stresses along the overlap length of a joint with 2 mm thick adherends.

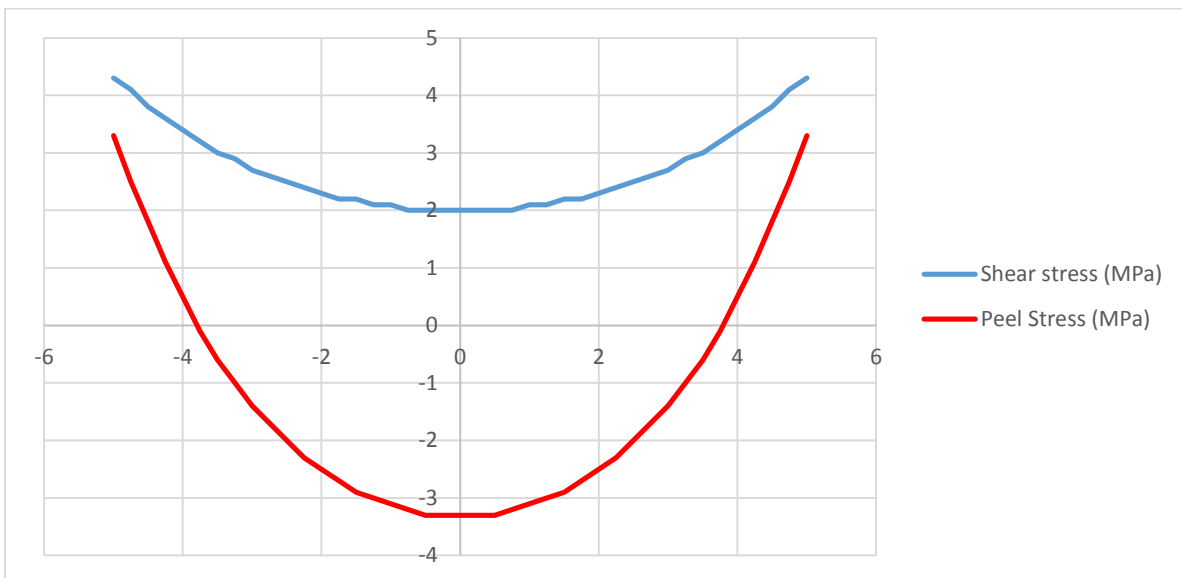


Figure 12. Shear and peel stresses along the overlap length of a joint with 5 mm thick adherends.

The shear stress is better distributed on the joints with thicker adherends, meaning their maximum values are lower while, on the other hand, their peel stress is higher on the edges and centre of the overlap length. As adherend thickness increases so the type of failure changes – low thicknesses mean the failure will be due to the adherend bending, while higher thicknesses provoke adhesive shear failures or, for the highest adherend thicknesses, adhesive peel failures.

#### 2.4.1.4. *Overlap length*

Depending on the material behaviour of both the adherend and the adhesive, the overlap length can have a varying level of influence on the joint's strength.

For elastic adherends, the influence depends greatly on the adhesive's properties. A ductile adhesive will deform plastically as the load it is subjected to increases, redistributing the stress until failure, which will occur with a global yielding of the adhesive and meaning the joint's strength will largely depend on the overlap. When a more brittle adhesive is used, the stress is not as well distributed along the overlap length and instead concentrated on its edges. In this case increasing the overlap length barely changes stress distribution, so it doesn't effectively affect the joint's strength. Other solutions should be adopted in this case, like using a different, more ductile adhesive on the edges while maintaining a strong adhesive in the middle, or using an adhesive whose properties progressively change along the overlap.

When the adherends are not as elastic, they may yield and as such their yield strength is what determines the failure load. In this situation the bending moment is a decisive factor in the maximum load and it depends strongly on the overlap length.

Even though for long overlaps and for the most brittle or extremely ductile adhesives more complicated analytical models should be used, it is possible to use simple calculations to predict the failure load. The predictive model of Adams et al. [11], described in Chapter 2.3.4., uses these calculations in order to figure the failure load for SLJs under tensile stress. For overlap lengths lower than 40 mm and bondline thicknesses under 1 mm, this method has proven to consistently portray the experimental results, when considering the global yielding of the adhesive and yielding of the substrate. For more brittle adhesives, other models, such as Volkersen's are more suitable [9].

The effect of overlap length on a joint's strength has been studied and is accessible in literature. Figure 13 shows results from a study [15] where the strength of SLJs with adherends of several materials are presented as a function of overlap length.

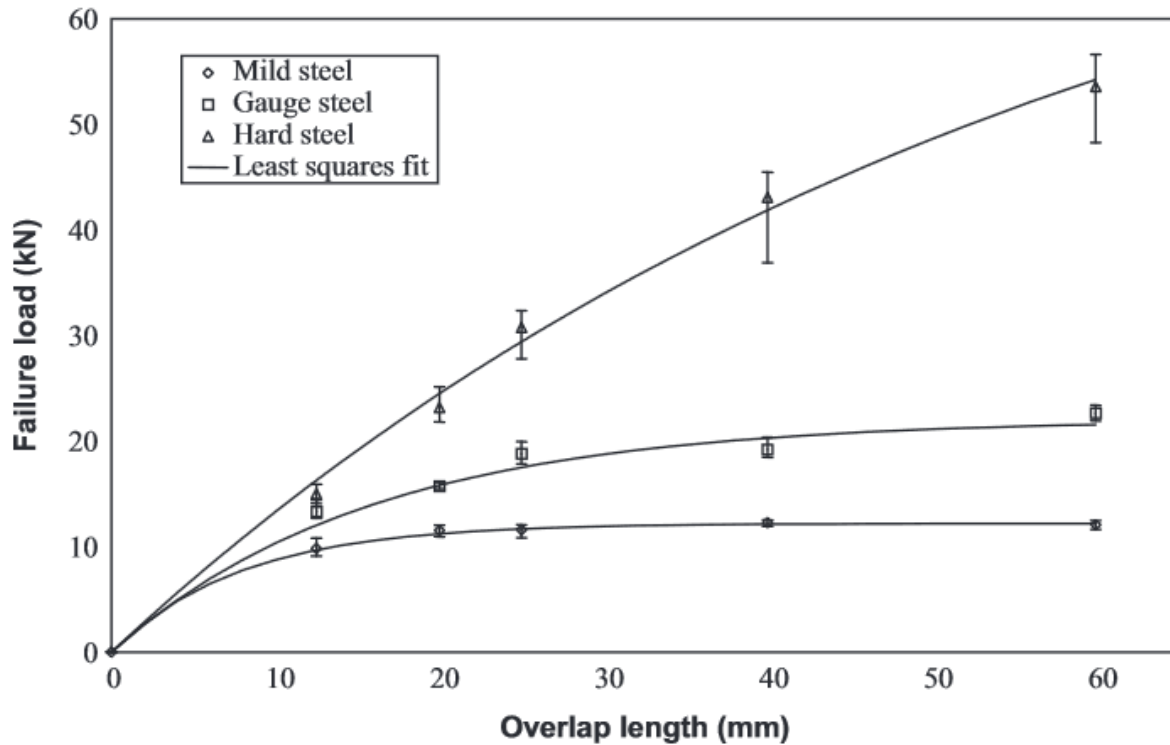


Figure 13. Strength of SLJs in tension vs. overlap length for AV 119 adhesive and different adherend materials [15].

As the overlap length increases so does the failure load until a plateau is reached. An increase in overlap reduces the adherend bending and distributes the tension across a larger area.

#### 2.4.2. Impact loads

When the strain-rate applied on a SLJ varies, so do its mechanical properties. In the automotive industry it is especially important to understand these variations since the joints should not be fractured in case of an accident, allowing the vehicles to maintain integrity. When studying impact loads, the energy that the joints are capable of absorbing is an important factor, since this energy is, in case of a car crash, not transferred to the passengers, improving their safety.

Predicting adhesive's properties under impact loads is not as accessible as in quasi-static conditions, even though there is available literature for certain conditions



and materials and, after some experiments, the difference in values can be extrapolated.

Focusing on SLJ drop weight impact tests using ductile epoxy adhesives with high elongation, the failure mode is generally the same as with low-speed, quasi-static loads. Nevertheless, due to their sensitivity to high strain rates, they do not deform as much, reducing the absorbed energy but increasing the maximum load before failure [16] (Figure 14).

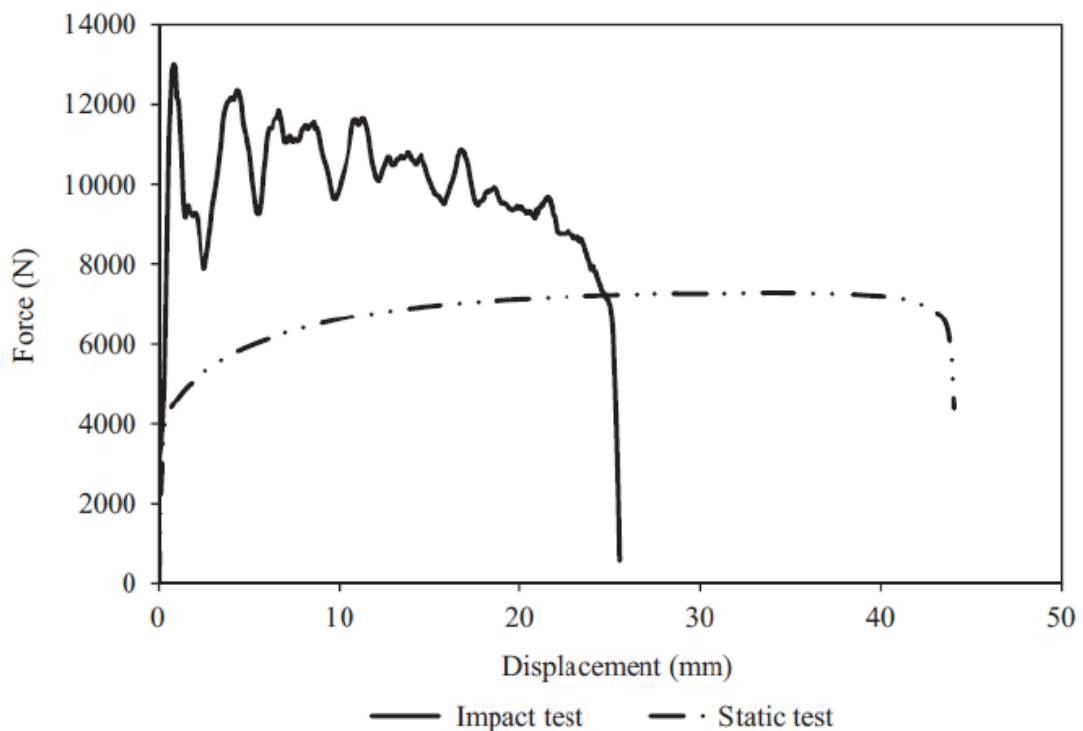


Figure 14. Load vs displacement graphs for the same single lap joint, using mild steel adherends, with a strain rate of 1mm/min and 4.47m/s [16].

The energy absorbed in the adhesive is normally very small. Its function is to hold the two adherends together while they deform plastically in tension. A joint with high yield strength adherends will therefore have good strength even when coupled with a low ductility adhesive but this is not the case for ductile adherends which will fail at low loads [17].

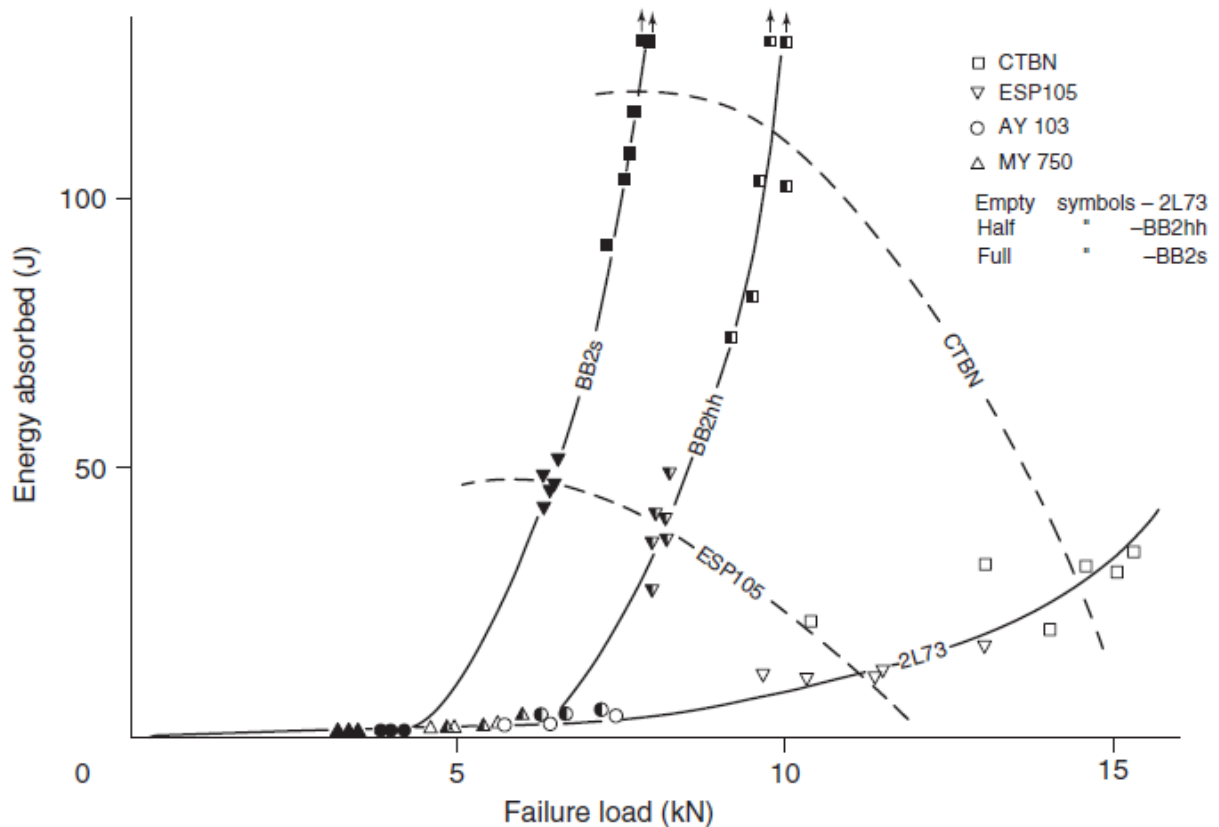


Figure 15. Impact for lap shear aluminium alloy specimens [17].

Figure 15 shows the results of pendulum impact tests where the energy absorbed as a function of joint strength is represented for a range of adhesives and adherends. Low ductility adhesives provide a decent joint strength but very little energy absorption. The highest energy absorption values are obtained from the rubber-toughened adhesive with ductile aluminium adherends. A high-grade aluminium alloy used in the aircraft industry provided the highest strength joints, but only allowed little energy absorption because of its high yield strength [17].

### 2.4.3. Effect of temperature

Most adhesives are sensitive to temperature, whether during the curing process or while they're in service. This means that it is an extremely important factor to consider while designing an adhesive bond and it is essential to know which properties

of the adhesive are relevant when considering which one to apply for more adverse service conditions.

**Glass transition temperature:** The glass transition temperature,  $T_g$ , is the most critical value referring to temperature in polymers. It is a property of the amorphous part and marks the transition from a glass-like to a rubber-like structure. In amorphous polymers, when they go above the  $T_g$ , the long coiled molecular chains can rearrange and extend, causing fast stress relaxation due to the viscoelastic nature of the polymer, lowering its moduli and strength. This is mostly unwanted in rigid structures so structural adhesives should normally work below their  $T_g$  [1, 3, 11].

**Decomposition temperature:** At this temperature the adhesive will completely degrade and its mechanical properties will no longer be relevant.

**Thermal expansion:** If the thermal expansion coefficient of the adhesive is not close to the one of the substrates, additional interfacial stresses are created which can lead to a premature failure of the joint. Since this coefficient is generally higher for the adhesive when compared to the most commonly used materials for the substrates, this is an important factor to consider when creating an adhesively bonded structure. By the addition of mineral fillers, this expansion can be reduced [1].

Especially in the automotive industry, it is crucial to understand how the mechanical properties of an adhesive and therefore a joint's strength can vary as their service temperature goes up or down. As it has already been mentioned, it is of extreme importance not to go past an adhesive's glass transition temperature,  $T_g$ , and even at temperatures close to this value its properties may effectively harm an adhesive joint's strength. It is also necessary to consider the thermal expansion coefficients of both the adhesive and the adherends since dissimilar values will create additional stresses which can compromise the joint's strength when it's submitted to different temperatures [18, 19].

When manufacturing an adhesive joint, its necessary service temperature should be carefully determined beforehand. In the case of the automotive industry, where their temperatures range from  $-40^{\circ}\text{C}$  to  $80^{\circ}\text{C}$  [20], both the highest and lowest temperature may negatively affect the strength of the adhesive joints. The adhesive's strength is lowered as the temperature gets too high (once again, especially close to its  $T_g$ ), while at lower temperatures thermal stresses start becoming relevant. It is known that SLJs stiffness, when tested at low temperature using an epoxy adhesive, are more affected by the adherends' response than by the adhesive's modulus [21].

In the case of SLJs where the adherend will yield when loaded, lower temperatures can improve the strength of the joint. Since in these cases the maximum load the joint can support is highly dependent on the yield point of the substrates' material, this failure load goes up as the temperatures decrease, as long as the limiting factor doesn't become the adhesive's properties.

Several studies have been made relating adhesives' properties to their working temperature. Figure 16 shows the results of a study [6] displaying how the strength of some adhesives are affected.

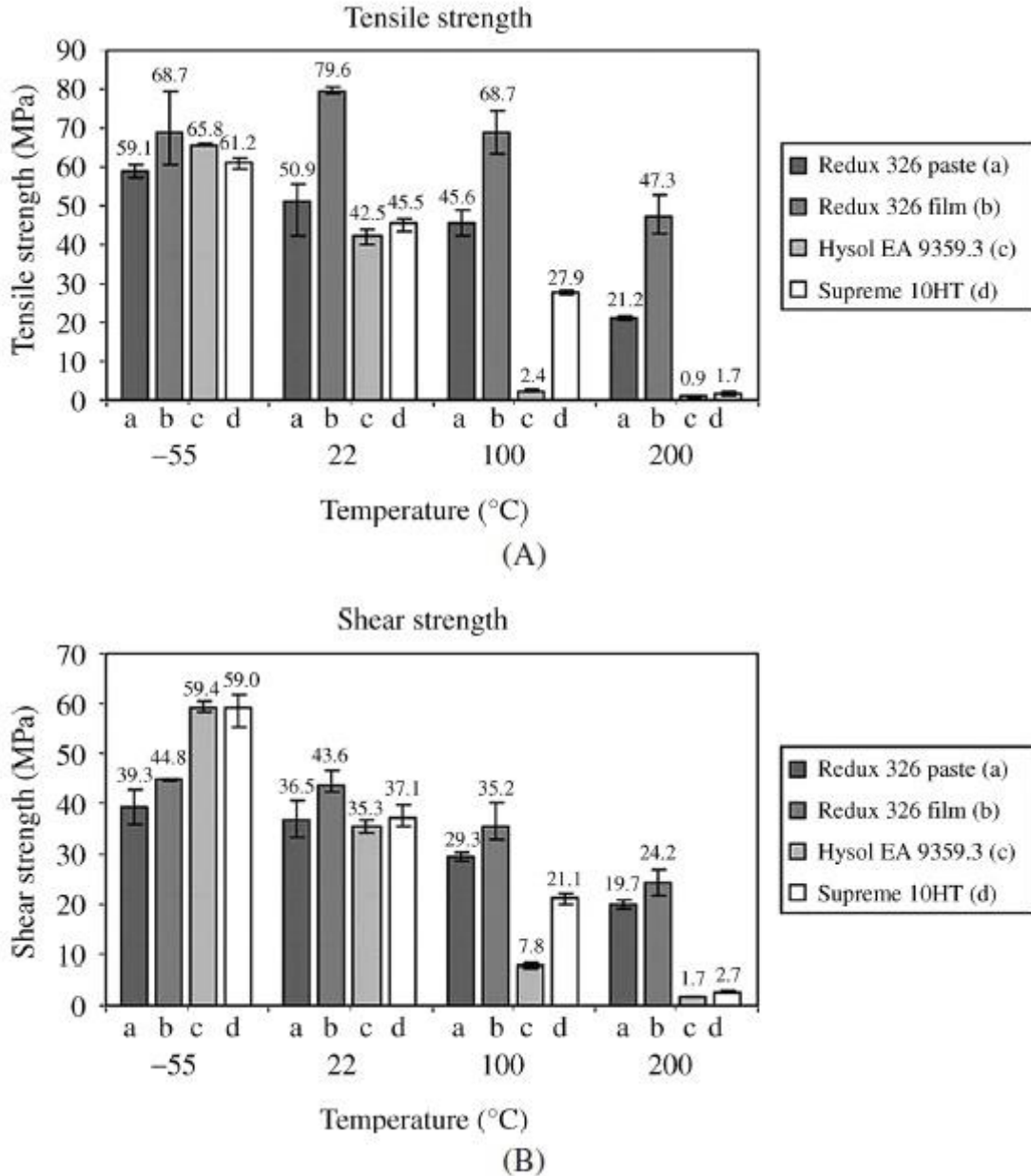


Figure 16. Adhesive strengths of several adhesives as a function of temperature - (A) tensile strength (measured with dogbone specimens); (B) shear strength (measured with TAST) [6].

Results show that as the temperature approaches the adhesive's  $T_g$ , its strength reduces significantly. It is clear that the  $T_g$  of the Hysol EA 9359.3 adhesive is lower than 100 °C and that of the Supreme 10HT adhesive is between 100 °C and 200 °C, since at 100 °C it is still relatively strong. Below their respective  $T_g$  the adhesives are still stiff and strong while above that value they are soft and the load they can carry is extremely reduced [6].

Ductility tests were also performed, from which the results are presented in Figure 17.

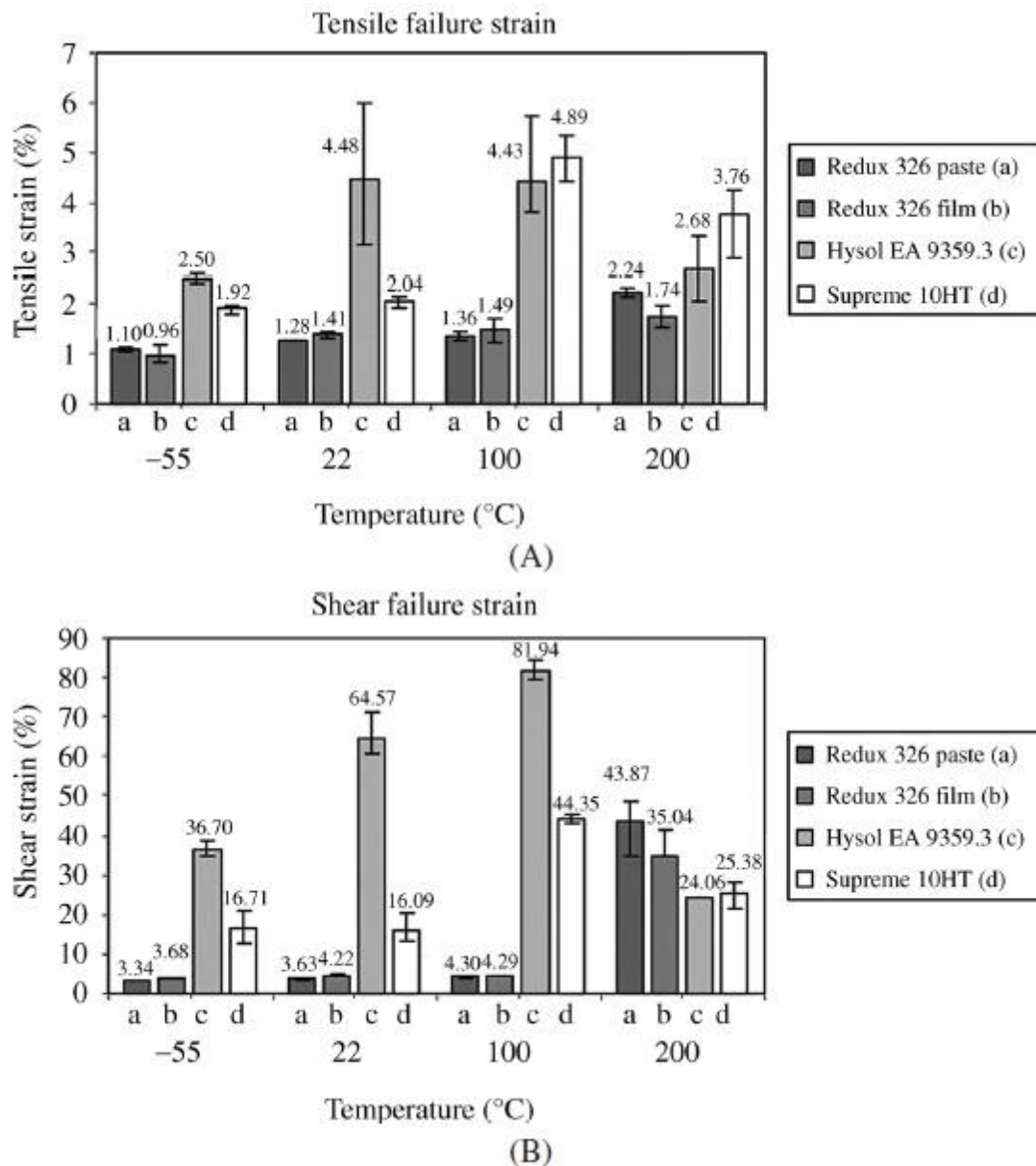


Figure 17. Adhesive ductility of several adhesives as a function of temperature - (A) tensile (measured with dogbone specimens); (B) shear (measured with TAST) [6].

Results show how the ductility increases with temperature. This behaviour is clear with the Redux 326 adhesives, both in paste and film form. The Hysol EA 9359.3 and Supreme 10HT adhesives, however, present a decrease in strain at 200 °C, as if they have become brittle. It can therefore be concluded that above their  $T_g$ , polymers have a decrease in strain to failure even though they are extremely soft [6].

#### 2.4.4. Effect of moisture

Diffusion is a process in which the random motion of a substance's molecules transports matter from one place to another over time [22]. This means that, when in contact with water in the form of liquid or vapour, and often driven by the concentration gradient, this water can be transported to and penetrate the adhesive layer of an adhesive joint (Figure 18).

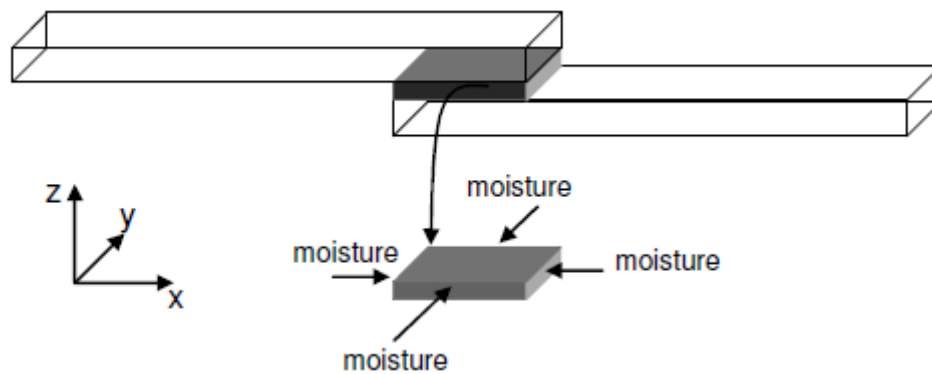


Figure 18. Moisture intake of the adhesive of a single lap joint [12].

When referring to the water absorption rate of an adhesive under certain conditions, it is normally accompanied by its coefficient of moisture diffusion,  $D$ , and generally described by Fick's first law:

$$F_x = -D \frac{dc}{dx} \quad (2.8)$$

where  $x$  is the diffusion path and  $c$  the moisture concentration that can be described along time,  $t$ , by Fick's second law:

$$\frac{\delta c}{\delta t} = D \frac{\delta^2 c}{\delta x^2} \quad (2.9)$$

Even though some adhesives don't follow the Fickian law of diffusion, an efficient way to determine the coefficient of diffusion is by measuring the water uptake of a bulk adhesive specimen. During the initial stages it should follow a linear rate of absorption which can be used to calculate the diffusion using an expansion of Equation 2.9. Certain adhesives may change behaviour after some time, presenting a dual-Fick behaviour (or triple, etc.) and a different coefficient of diffusion after a determined amount of water absorption. These changes in behaviour should be carefully assessed so that the amount of moisture content in the adhesive can be accurately calculated.

Figure 19 shows that as the amount of moisture in the adhesive increases, its properties are also modified. This is generally unwanted since these changes may significantly reduce the joint's strength.

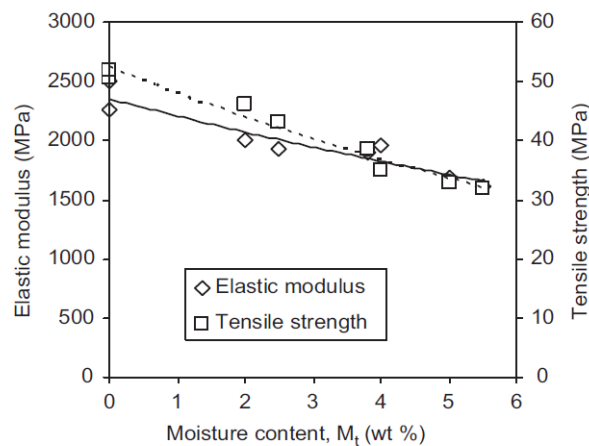


Figure 19. Variation of an adhesive's properties as its moisture content increases [12].

Water uptake rate and maximum uptake both increase as temperature raises. This means the maximum saturation level is higher which in some adhesives leads to an increased amount of swelling (volumetric change due to moisture content alone, independently of thermal expansion [23]), that can create additional stresses and reduce the strength of the joint.

It is also important to notice that, as the moisture content of the adhesive increases, its glass transition temperature,  $T_g$ , gradually decreases, which can also compromise the joint under certain conditions. Figure 20 shows the results of a study



[24] which shows the variation of an adhesive's  $T_g$  as a function of time submerged in two different fluids.

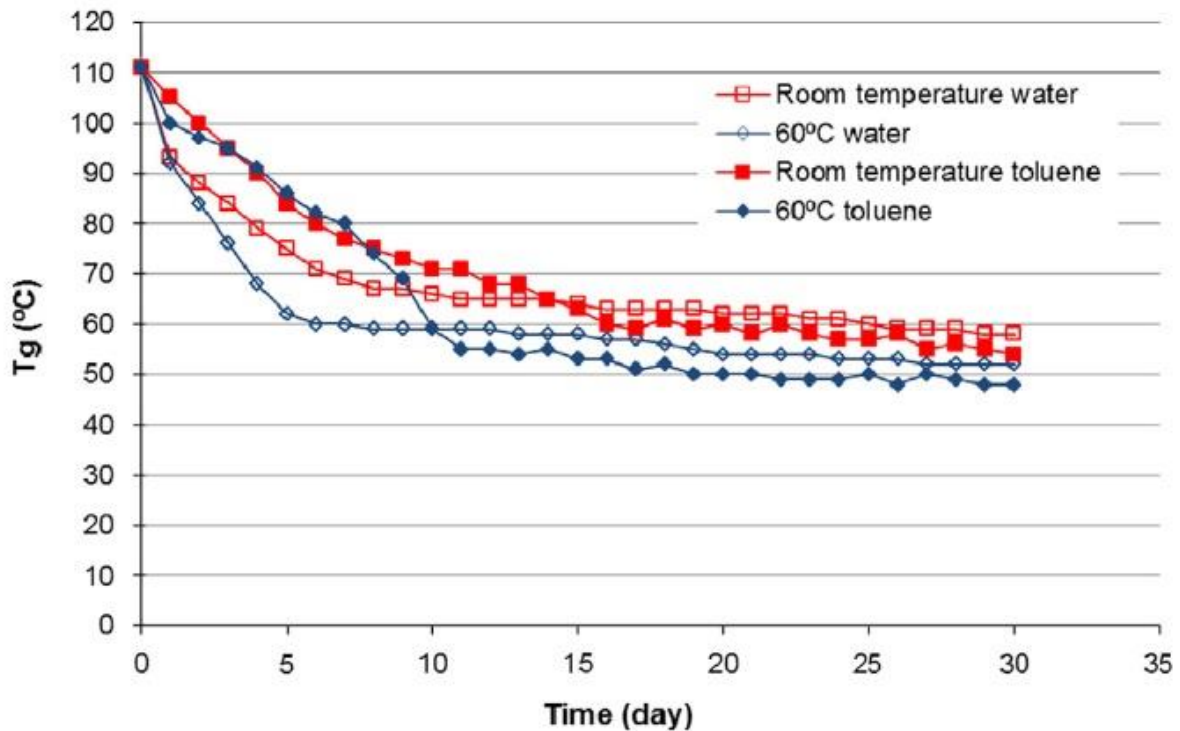


Figure 20.  $T_g$  as a function of time submerged of the AV119 adhesive.

As time passes and the amount of water content of the adhesive increases, there is a clear decrease in the adhesive's  $T_g$ . As the adhesive becomes close to saturation and the moisture level does not increase as fast, the  $T_g$  variation comes close to a plateau.

## 2.5. Testing methods

The main purpose of this study is to determine how the adhesive joints' behaviour changes when subjected to a diverse amount of condition combinations by analysing their mechanical properties. Even though there are plenty of methods nowadays to predict these behaviours analytically, there are always certain results that can be unpredictable, for which the most efficient way to study the behaviour of an

adhesive joint is by performing tests where it can be subjected to certain controlled environments, simulating what they will be influenced by in reality.

Even though the central objective is to study these adhesive joints under impact, other tests were also performed in order to analyse the differences in properties under different conditions, as well as to determine certain properties of the adhesives.

### 2.5.1. Water absorption tests on bulk specimens

As it was just mentioned in the previous section, moisture can have a big effect in the mechanical or even geometrical properties of an adhesive. For this reason, it is crucial to know at which rate each adhesive will absorb moisture from its surroundings and how this will affect it. Following the standard ISO 62:2008, this segment will explain an efficient procedure to measure the water acquisition of an adhesive in order to determine these properties.

To conduct this experiment, bulk specimens are used, which are specimens made exclusively of the adhesive that is to be tested. These can be cut from a plate of adhesive and can be square shaped with a  $60\pm 1$  mm side length and  $1\pm 0.1$  mm width (figure 21), even though these values can be adjusted to closer resemble a specific situation or joint.

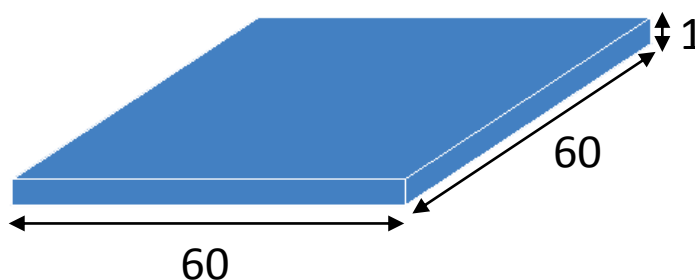


Figure 21. Geometry of a bulk specimen for water absorption testing.

At least 3 specimens should be manufactured from which to determine average values and obtain a more accurate representation of the actual ones.

Once the bulk specimens are completed, they should be completely dried out before beginning the measurements. This can be done by maintaining them at high temperature during a few days or by maintaining them in a desiccator or a controlled environment with low humidity. After cleaning their surfaces thoroughly they should be weighed and their exact thickness measured. The fluid in which they are being submerged should avoid being contaminated at all costs. In order to avoid too much concentration of contamination from components released from the specimens, the volume of distilled water should correspond to at least 8mL for each squared centimetre of the specimen's total surface, and never less than 300mL per specimen.

The measurements should initially be made every 2 to 6 hours, depending on the coefficient of diffusion, since at first the water absorption is the highest. As it reduces, the differences in weight of the specimens will also reduce so the time between measurements may increase. The results can be presented as a graph showing weight increase percentage as a function of time and thickness. Once again, notice that the coefficient of diffusion will vary with the temperature at which the test is made – for most adhesives, the higher the temperature, the higher the rate at which water will be absorbed by the adhesive and the higher the saturation point (Figure 22).

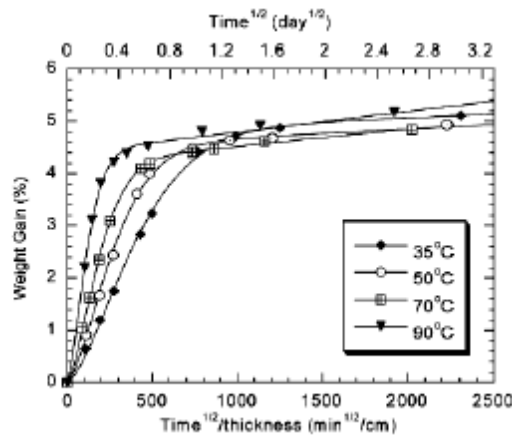


Figure 22. Example of moisture absorption graphs for bismaleimide at several temperatures [25].

## 2.5.2. Single lap joints for quasi-static and impact testing

One of the most important properties of an adhesive for use in the automotive industry is its shear strength. Since it's the best way to maximize their strength, adhesive joints are positioned in such a way so that the load is applied to them as in a unidirectional manner, along the tensile direction, and the adhesive's behaviour is ultimately decided by its shear strength. The most effective yet simple way to emulate the joints as used in the industry for testing is by using single lap joints. They are cost-effective and the fastest to manufacture, while providing accurate enough results to analyse and predict the joints' performance when subjected to the real demands they are designed for.

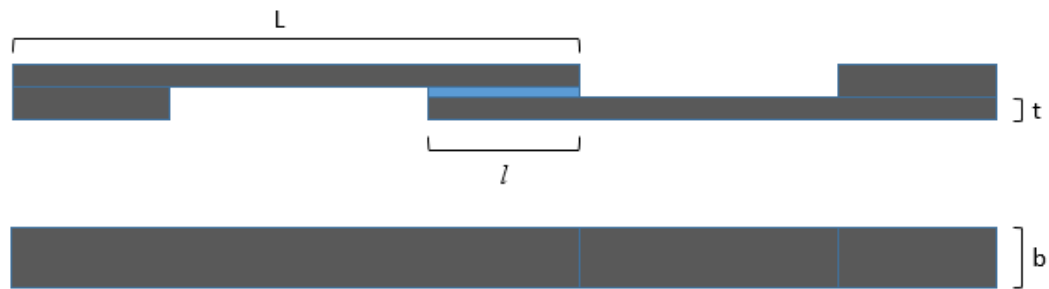


Figure 23. Standard geometry of a single lap joint.

On a single lap joint (see Figure 23), the adherends overlap in a small area ( $l \times b$ ) at the end of their length, where the adhesive bonds them together. This area, as well as the bondline thickness (thickness of the adhesive layer), are decisive in the performance of the joint and extremely important when designing a SLJ for testing. As already mentioned, the thickness of the adherends ( $t$ ) is also critical since the additional stresses caused by their bending may completely modify the maximum load a joint can endure. At the other end of the adherends, in order to guarantee that the applied load is aligned with the centre plane of the adhesive bond, small tabs are bonded whose thickness is the same as the substrate's plus the bondline thickness of the adhesive. This is the section that is gripped by the testing machine and corresponds to the height of the joint on the overlap area. Even though there are several standards defining exactly which geometries to use when manufacturing SLJs

for testing, variations are generally used as a way to resemble the real structure more accurately [2].

### 2.5.3. Quasi-static testing of single lap joints

Quasi-static testing consists in applying a longitudinal deformation to the SLJ while measuring the increase of applied load over time and as the displacement increases. The load can be measured using a load cell and the displacement is made at low speeds (generally 1 mm per minute), hence the name. The results of this test consist therefore in a load-displacement curve [17].

This curve can vary meaningfully as both the conditions in which the SLJ is tested (such as temperature and moisture) as well as its design (geometry as mentioned above and materials, for example) are modified. By adjusting these parameters accordingly, accurate depictions of the joint's behaviour in reality can be made, meaning that it is possible to obtain a rigorous estimate of the joint's shear behaviour in the real conditions it will be used on [17].

Quasi-static testing will be important in the context of this study as it will be used to compare the difference of the joints' strength as a function of its loading conditions, namely the load application rate.

### 2.5.4. Impact testing of single lap joints

In the automotive industry, adhesively bonded structures may be subjected to a different loading condition since a car crash for example can cause the joints to abruptly sustain a large load. This type of solicitation is not intentional and as such might not but should be accounted for when designing an adhesive joint. It is therefore important to understand how the joint will behave by emulating this loading condition and performing impact tests.

There are several kinds of impact testing available and which one is more appropriate depends on several factors. For instance, if the impact loading is expected from the regular use of the bonded structure, we typically want to avoid damaging it – it is designed to suffer impact loads. This is not the case in the automotive industry and, for this study, we will approach an appropriate testing method used for exceptional impact loads, the drop weight impact test.

The drop weight impact test is a very common form of measuring shear impact loading conditions since it is simple yet reliable and accurate. A weight is positioned vertically above the specimen that is to be tested, where its mass and height can be adjusted allowing the impact velocity and energy to be regulated. After being released, the weight is guided towards and collides with a special device which is attached to the specimen, transferring to it the load it receives. A drop weight impact testing machine typically measures the load using a load cell as well as the displacement, calculating the energy absorbed by the specimen before either the weight stops by colliding with it or the joint fails. In the same way as in the quasi-static test described previously, in this test the load is applied in one direction and, in addition to the adjustable parameters, this makes for an effective method of simulating conditions in which the joints may be exposed to during their service lifetime.

## 3. Experimental Details

### 3.1. Testing variables

The objective of this work is to study how the different conditions affect the single lap joints. In order to do so, the conditions presented on Table 3 were considered and the tests were made using their possible combinations:

*Table 3. Variables considered for testing the joints.*

<b>Adherend thickness</b>	2 mm and 5 mm
<b>Adhesive used</b>	Nagase XNR 6852E-2 and SikaPower 4720
<b>Temperature</b>	-20 °C, 80 °C and Room Temp. ~23 °C
<b>Humidity</b>	Dry and Moist
<b>Tests</b>	Quasi-static and Impact

The adhesive thickness is constant and equals 0.2 mm.

### 3.2. Materials

#### 3.2.1. Adhesives

For this study, two different structural adhesives were analysed so that their differences in behaviour can be analysed.

The first adhesive is the SikaPower 4720, supplied by SIKA® (Vila Nova de Gaia, Portugal). This is a two-part epoxy adhesive which cures at room temperature for 24 hours.

The adhesive XNR 6852E-2 was also used, supplied by NAGASE CHEMTEX® (Osaka, Japan). This one-part system is an epoxy adhesive that cures at 150°C for 3 hours and is a prototype that has been in development for several versions. These crash resistant adhesives present a particular linear structure, allowing more freedom of movement to the chains, unlike the network structure of a regular epoxy adhesive.

The studied adhesives' properties have been determined in a previous work [26] and can be consulted in literature. Their properties are presented in Table 4:

Table 4. Basic properties of the SikaPower 4720 and the XNR 6852E-2 at 1 mm/min strain rate [26].

Adhesive	Young's modulus (MPa)	Tensile strength (MPa)
SikaPower 4720	2170	32
XNR 6852E-2	1830	41

These values were obtained from traction tests made with dogbone bulk specimens, of which the results are presented in Figure 24, comparing the stress-strain curves of each adhesive.

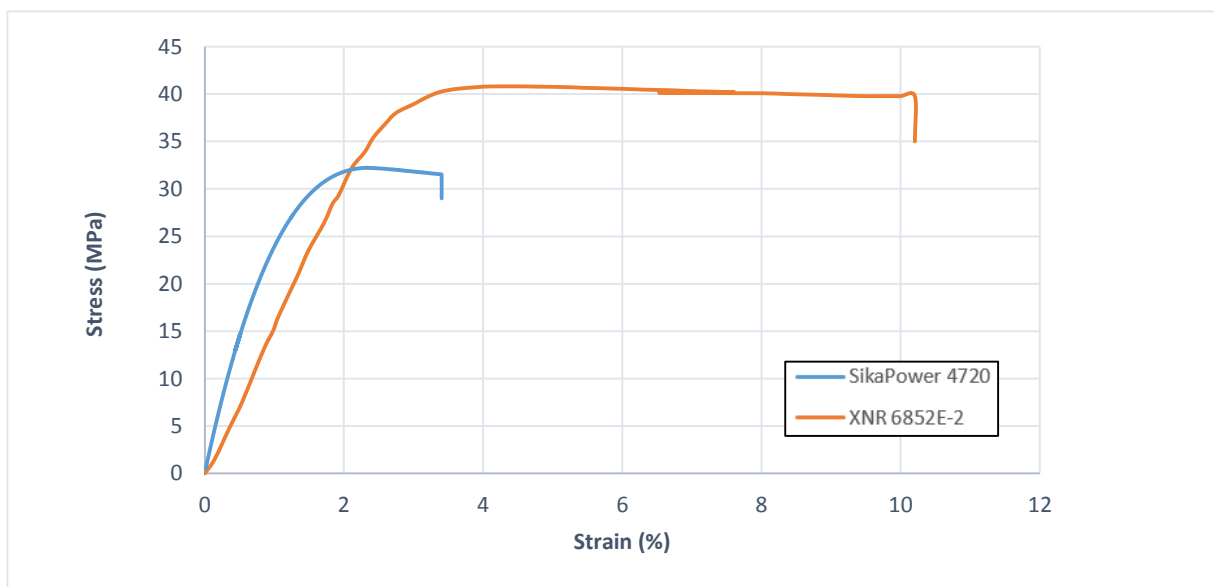


Figure 24. Stress-strain curves for the SikaPower 4720 and Nagase XNR 6852E-2 [26].



To verify how these properties vary with strain rate, they were also obtained for a higher value, 100 mm/min. Even though this strain rate will not be used for this study, the relation between these values allow the properties at impact velocity to be extrapolated to predict the joints' behaviour. These values are presented in Table 5.

Table 5. Basic properties of the SikaPower 4720 and the XNR 6852E-2 at 100 mm/min strain rate [26].

Adhesive	Young's modulus (MPa)	Tensile strength (MPa)
SikaPower 4720	2431	38
XNR 6852E-2	1803	46

Figure 25 shows the results from the traction tests from which these values were obtained and how the strain rate affects their behaviour during the tests.

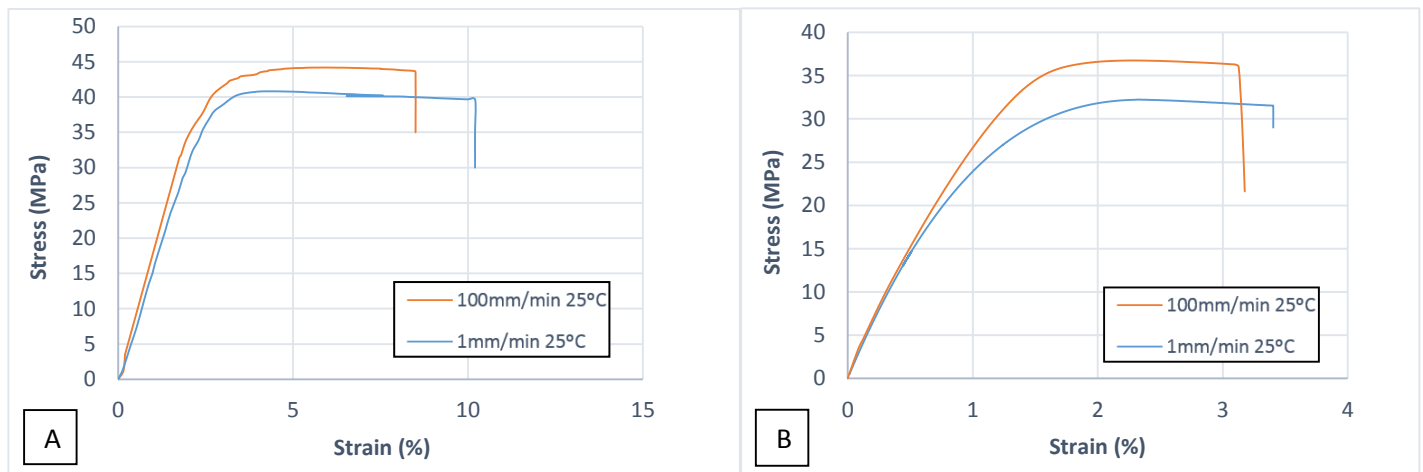


Figure 25. Comparison between stress strain curves at 1 and 100 mm/min for the (A) XNR 6852E-2 and (B) SikaPower 4720 adhesives [26].

Both adhesives show that as the strain rate increases so does their tensile strength but the maximum strain before failure is reduced.

Another important property of the adhesives, considering they are being studied at high temperatures, is their  $T_g$ . Knowing this value allows us to predict if the joints will show a drastic decrease in strength when being tested at high temperature. These values are unknown and tests should be performed to determine them. For this work it was assumed that the  $T_g$  for the SikaPower 4720 is the maximum temperature at which its manufacturer recommends it to be used which is 60 °C. For the XNR 6852E-

2, it was assumed that the  $T_g$  is approximately the same as its previous version, the Nagase XNR 6852. This value has been determined in other studies [16] and is equal to  $102.6 \pm 0.1$  °C. Considering that the high temperature tests are being performed at 80 °C, it is expected for the joints with SikaPower 4720 adhesive to perform poorly during the high temperature tests while the joints with Nagase XNR 6852E-2 will not be affected by the changes caused by reaching the  $T_g$ .

### 3.2.2. Adherends

The used adherends are made of the aluminium 6082-T6. It is a medium strength structural alloy that is commonly used for machining. Due to its good properties it is mainly used in high stressed applications, which is the case of the transport industry. Considering its strength, it is expected that there will be adherend yielding in certain combinations of conditions, which will prove to be useful to study the effect of yielding on the joint's strength.

Figure 26 presents the material's stress-strain curve from which it was possible to determine its yield strength of 300 MPa.

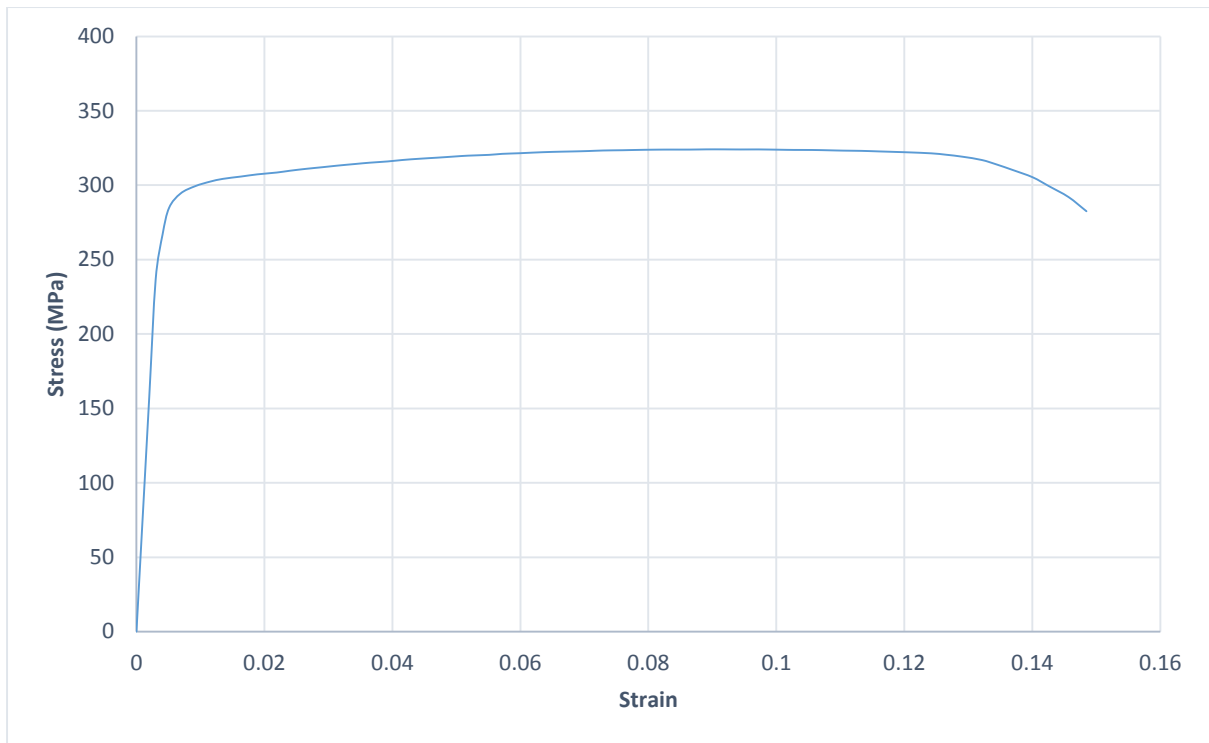


Figure 26. Stress-strain curve for the 6082-T6 aluminium at 1 mm/min.

Since the strength of the adherends at high strain-rate was unknown, a series of impact tests were performed using specimens made out of the aluminium alone (9 x 2 mm section), using the same conditions that will be used to test the adhesives (described later in Section 3.6.1). The typical curve obtained from these tests is presented in Figure 27.

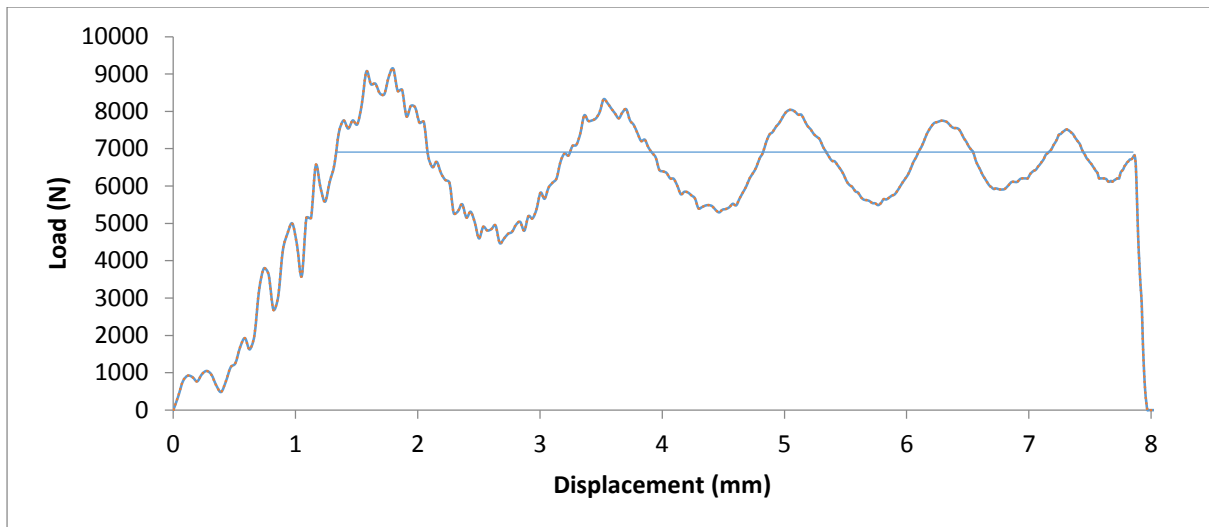


Figure 27. Load-displacement curve obtained from an impact test of the 6082-T6 aluminium.

The maximum load was determined by the average value obtained from the vibrations at the peak of the curve, marked in Figure 27, and is equal to 7015 N. Adapting Equation 2.1. for the adherend:

$$\tau = \frac{P}{b * t} = \frac{7015}{2 * 9} = 390 \text{ MPa}$$

The aluminium's yield strength under impact is therefore 390 MPa.

### 3.3. Water absorption tests

#### 3.3.1. Experimental procedure

To perform the tests in humid conditions, the amount of time that the specimens were submerged for was constant. Depending on the coefficient of diffusion of the adhesive, the saturation level of the joint will vary and can be determined, so there will be joints with two different levels of moisture, depending on the coefficient of diffusion of the adhesive used on that particular joint.

While the coefficient of diffusion of the SikaPower 4720 is already known from previous studies, the value for the XNR 6852E-2 is unknown and must be determined. To do so, the steps described in Section 2.5.1 to perform water absorption tests on the XNR 6852E-2 adhesive were followed.

To produce the testable bulk specimens, a different mould was used (Figure 28).

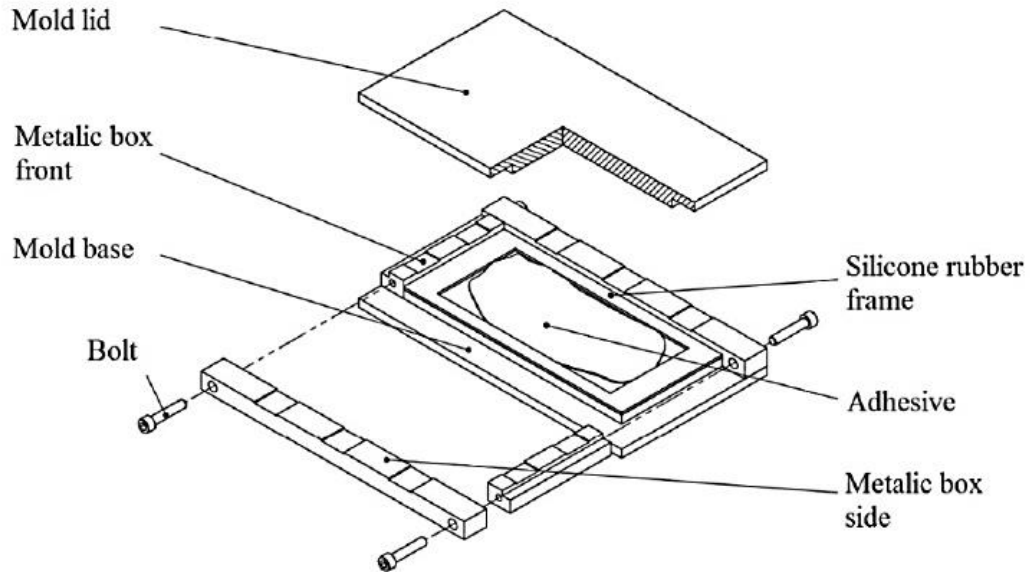


Figure 28. Schematic representation of the mould used to produce bulk specimens [3].

The mould allows to create two plates of adhesive at a time, from which the desired bulk dimensions were machined (60 X 60 mm). Once again, mould release agent was used to avoid unwanted bonding and silicone frames were used to prevent the adhesive from flowing out (see Figure 28). The thickness of the plates, controlled by these frames, was not perfectly constant so this will later be accounted for. Three specimens were tested to obtain more accurate results.



*Figure 29. Bulk specimen for the XNR 6852E-2 water absorption test.*

After being produced and machined, the specimens (Figure 29) were placed among silica gel for at least a week to make sure that they were completely dry at the beginning of the test.

After gently abrading their surfaces with sandpaper and making sure they are clean, their initial weight and thickness were measured using a precise scale capable of measuring 4 decimal places and a calliper, respectively. They were then submerged in a jar of distilled water where they remained until saturated at a temperature of 32.5°C, the same temperature at which the joints will be submerged while ageing. This means this is the temperature for which the coefficient of diffusion will be determined.

Initially, their weight and thickness were remeasured every 2 hours and, as they absorbed more and their mass growth rate reduced, the interval between measurements decreased.

### 3.3.2. Experimental results and diffusivity

The first conclusion was that the increase in size of the XNR 6852E-2 adhesive was too small to be measured with a micrometer as it took in the water from its surroundings, which is good since it reduces additional stresses when being used in a joint. The obtained curve from the specimens is presented in Figure 30. The y axis represents the mass uptake, in percentage, relative to the initial mass of the specimen, given by Equation 3.1.

$$uptake = \frac{m - m_0}{m_0} * 100 \quad (3.1)$$

where  $m$  is the specimen's weight at that specific point and  $m_0$  is its initial weight.

The xx axis is the square root of the elapsed time divided by the specimen's thickness. These values were obtained during a period of 30 days, after which the specimens had clearly reached their saturated values.

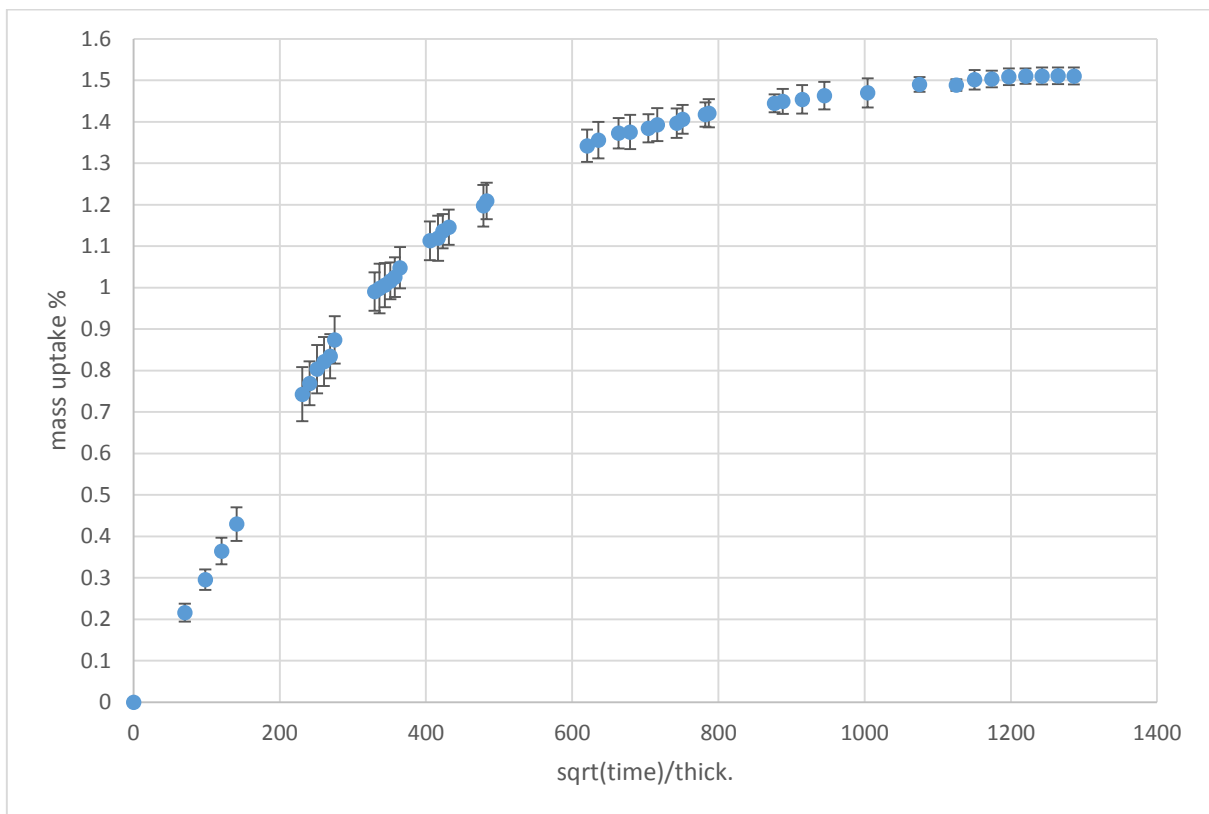


Figure 30. Average mass uptake of the bulk specimens of Nagase XNR 6852E-2 over time.

In order to verify if these values are logical and the absorption does indeed increase as pointed out in Section 2.4.4, the results for a specimen tested at 32.5°C were compared to a similar one from which was tested in identical conditions but at 50°C (Figure 31).

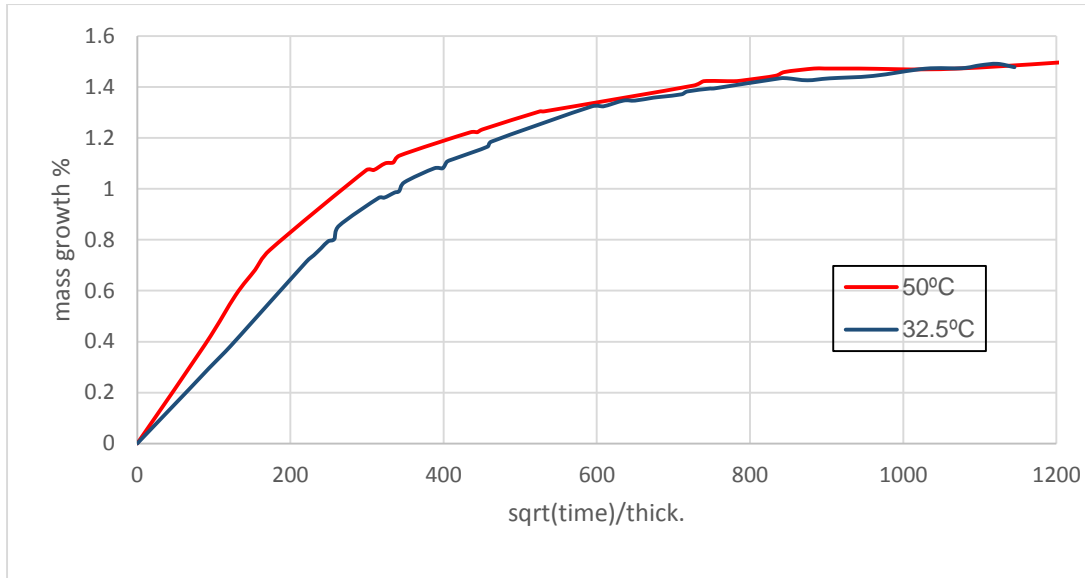


Figure 31. Comparison of moisture intake for the Nagase XNR 6852E-2 at 30°C and 50°C.

Especially in the beginning stage, the water intake is clearly higher for the 50 °C specimen. This means that, as expected the coefficient of diffusion is higher for the higher temperature, even though the maximum intake is the same. The 50 °C specimen also reached saturation slightly faster than the 32.5 °C one.

To determine the coefficient of diffusion, a dual Fick behaviour was assumed based on the results - the adhesive presents a linear intake rate of water in the initial stages which later becomes a constant curve until saturation. This means that two coefficients of diffusion would need to be calculated to properly predict the amount of water in the joints' adhesive after a certain amount of time. These were calculated for the saturation point  $c_s$  using Equation 3.2.

$$c(t) = c_s - c_s \frac{8}{\pi^2} \sum_{k=1}^{20} \frac{1}{(2k-1)^2} \exp \left[ -\frac{(2k-1)^2 D \pi^2}{d^2} t \right] \quad (3.2)$$

where  $D$  is the coefficient of diffusion and  $d$  is the specimen thickness.

The obtained values for the diffusion coefficients and corresponding saturation are presented on Table 6:



Table 6. Coefficients of diffusion and corresponding saturation levels for the XNR 6852E-2 adhesive.

	Coefficient of diffusion (m <sup>2</sup> /s)		Maximum saturation (%)	
	Average	St. deviation	Average	St. Deviation
<b>First Fick</b>	1.60 x 10 <sup>-12</sup>	1.34 x 10 <sup>-13</sup>	0.96	0.01
<b>Second Fick</b>	1.27 x 10 <sup>-13</sup>	2.55 x 10 <sup>-14</sup>	0.55	0.02

The values for the SikaPower 4720 (single Fick) were already known from previous studies and are presented in Table 7:

Table 7. Coefficient of diffusion and corresponding saturation level for the SikaPower 4720 adhesive.

	Coefficient of diffusion (m <sup>2</sup> /s)	Maximum saturation (%)
<b>SikaPower 4720</b>	8.94 x 10 <sup>-14</sup>	32.5

These are the values needed to predict the amount of water contained in the adhesive of a joint after a certain amount of time.

### 3.3.3. Water content prediction

The next step is to obtain the water content of the joints that are going to be tested after ageing to know exactly what is being tested. This was done using the Abaqus<sup>®</sup> finite element analysis software and the procedure will be described for each adhesive. To hasten the simulation process, only a fourth of the adhesive layer was modelled (Figure 32) and the water uptake from two sides was considered. Since it is horizontally and vertically symmetrical, the values can correctly be predicted for the whole adhesive area.

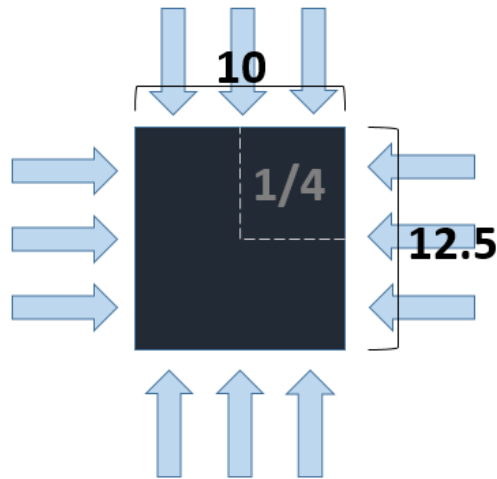


Figure 32. Modelled area of the adhesive layer and directions from which water is absorbed.

To perform the simulations a few parameters were inferred. The mathematics behind heat transfer and mass diffusion are the same so a material's temperature is equivalent to its water content percentage, meaning its thermal diffusivity is equivalent to its coefficient of mass diffusion. A 4-node linear heat transfer quadrilateral element type could therefore be used, available in the Abaqus® library as DC2D4. The used mesh was made of 12500 elements and the model was made in 2D, as shown in Figure 33.

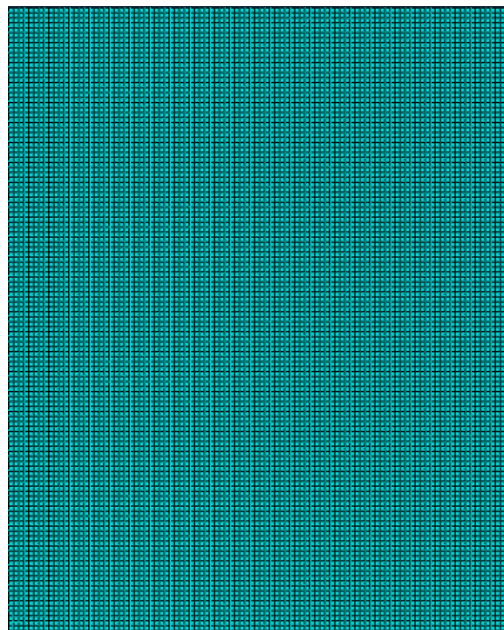
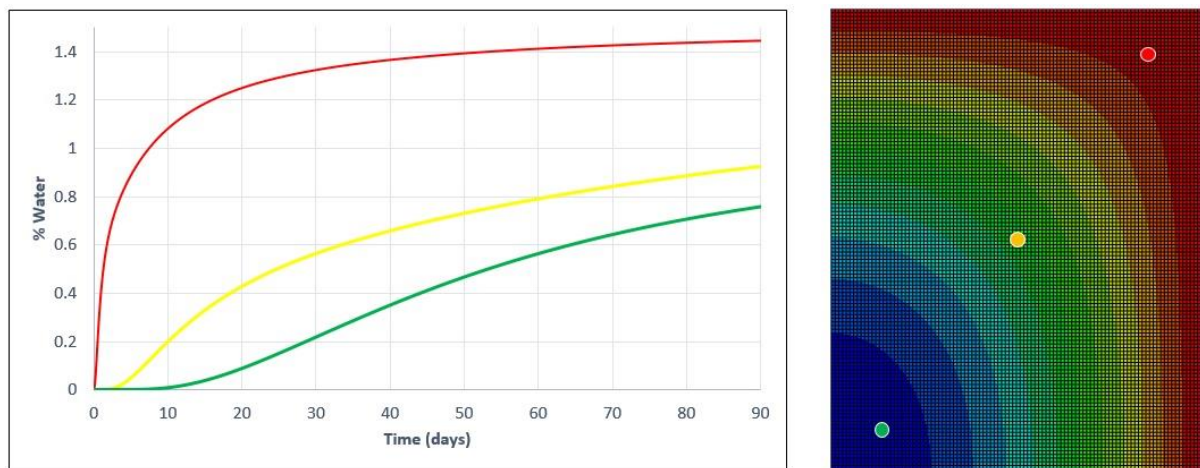


Figure 33. Mesh used for the water uptake simulations.

## Nagase XNR 6852E-2

Because of the dual Fick behaviour of this adhesive two simulations were conducted, one for each behaviour, which were afterwards combined to obtain the correct amount of water absorbed. A lot of information can be extracted from these simulations. For instance, it is possible to obtain the gained water in any exact point of the adhesive as time passes or the average throughout the whole layer.

Figure 34 shows the different rates at which the water penetrates the adhesive at 3 different points.



*Figure 34. Water absorption in 3 different points of the XNR 6852E-2 adhesive layer.*

On the right side, three points are marked – The red point is closest to the edge of the adhesive layer and the green point is closer to the centre. The yellow point represents a middle ground. The graph to the left shows the evolution of water absorbed as time passes for each one of these points, represented by their respective colour. As expected, the closer the point is to the centre of the layer, the longer it takes for the percentage of water to begin increasing. The red point is the fastest to reach saturation level while the green one takes the longest.

To know the water percentage in the adhesive of the joints that are tested after ageing, considering the adhesive geometry represented in Figure 32 with 2 mm

thickness, a similar graph (Figure 35) can be drawn with the average values for all the points of the adhesive.

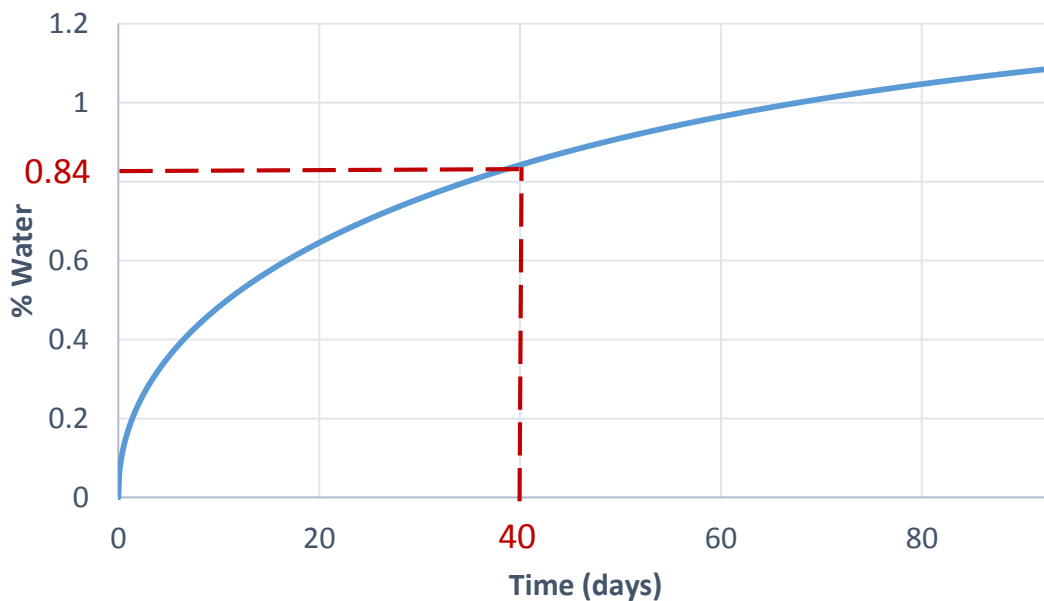


Figure 35. Average water content on the XNR 6852E-2 adhesive layer.

The marked point corresponds to the amount of time the ageing joints remained submerged before being tested and the corresponding average water content of the adhesive.

It can be concluded that after ageing for 40 days, the joints made with the XNR 6852E-2 adhesive will have 0.84 % of water content.

### **SikaPower 4720**

For this adhesive the procedure is identical to the previous one, though it is slightly simpler due to the adhesive presenting a single Fick behaviour. Once again, it is possible to obtain the water percentage throughout the adhesive layer as time passes for any point in the adhesive (Figure 36).

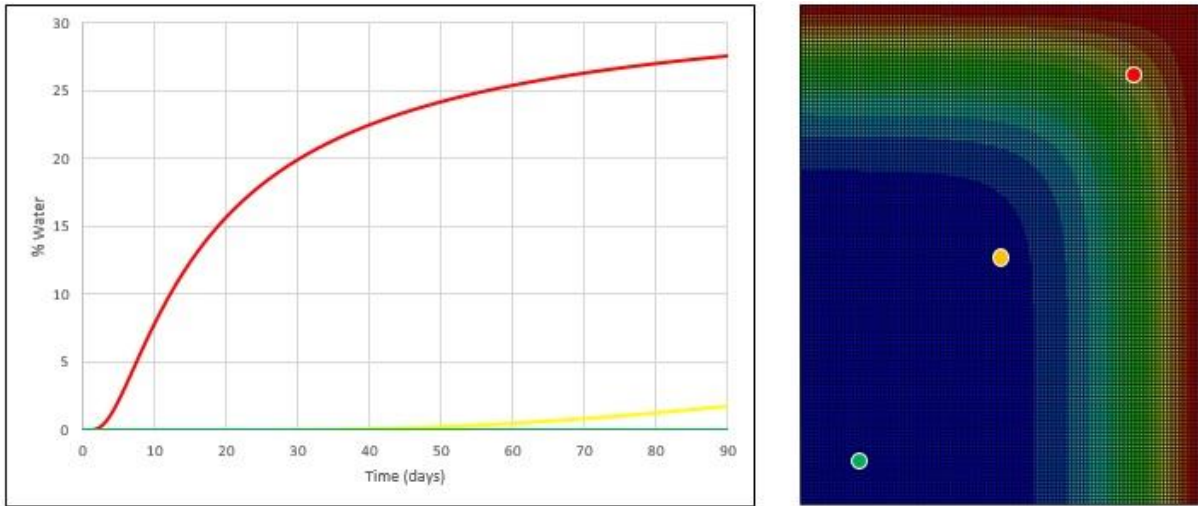


Figure 36. Water absorption in 3 different points of the SikaPower 4720 adhesive layer.

This adhesive has a lower coefficient of diffusion but a higher maximum saturation, making it take longer to reach maximum water content and for the points in the interior of the layer to begin absorbing water. For this reason, the yellow point has a very low amount of water gain over the first three months and the green point has virtually none, while the red point, closer to the border, has a very high amount of water content after this period of time.

Figure 37 shows the average values of water content throughout the whole adhesive layer:

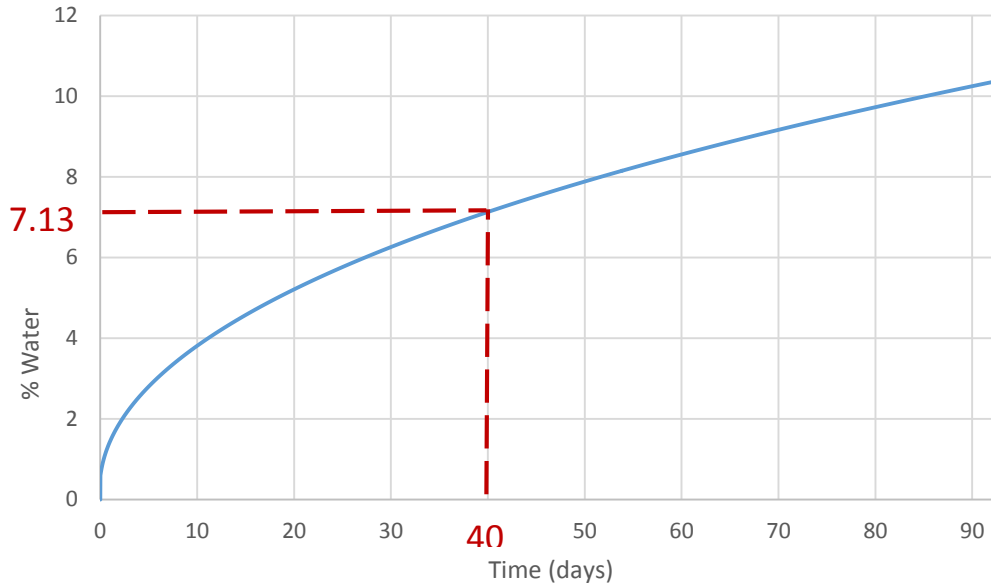


Figure 37. Average water content on the SikaPower 4720 adhesive layer.

It can be concluded that after ageing for 40 days, the joints made with the SikaPower 4720 adhesive will have 7.13 % of water content.

### 3.4. Specimens manufacture

#### 3.4.1. Single lap joints geometry

To perform the required tests, enough single lap joints were manufactured to experiment with all the possible combinations of adhesive, adherend thickness, temperature, humidity and stress rate (quasi-static and impact tests). The geometry of the SLJs is shown in Figure 38.

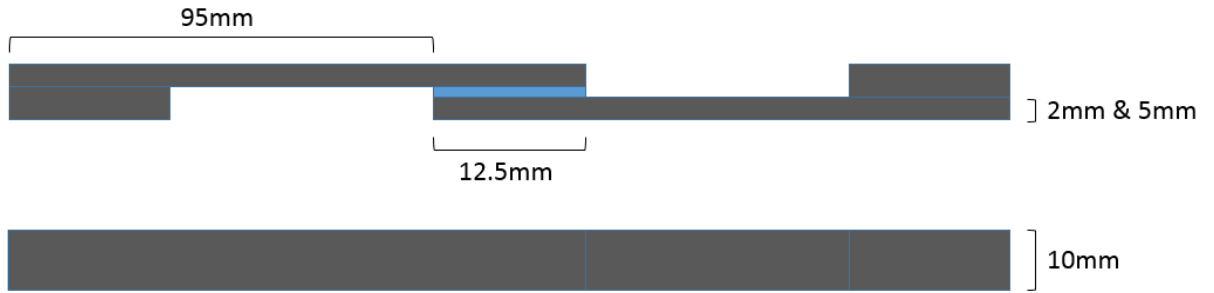


Figure 38. Dimensions of the single lap joints used for testing.

By using a small substrate width of 10 mm, it is ensured that the overlap area is small enough so that the adhesive can absorb a significant amount of water in a short period of time, speeding up the tests in humid conditions. The chosen adhesive layer thickness of 0.2 mm was determined for the same reason. Due to the large amount of required specimens, these relatively small dimensions are ideal to hasten their manufacturing process.

The substrate thicknesses were one of the testing variables established in a way so that there was yielding on some cases only. To do so, some basic calculations were made and the closest substrate thicknesses available to ensure that there would or would not be adherend yielding were used.

Recalling the calculations used on the method presented by Adams et al. [10], plastic deformation of the substrates will occur as long as the load that leads to global yielding of the adhesive, given by Equation 2.2, is lower or equal to the load needed for the aluminium to break, which can be determined by Equation 2.3. With this condition it can be guaranteed that there will be plastic deformation of the substrate:

$$\tau_y bl = \sigma_t bt \quad (3.3)$$

where  $\tau_y$  is the adhesive's shear strength estimated from its tensile strength using the Von Mises approximation,  $b$  and  $l$  are the joint's width and overlap length, respectively,  $\sigma_t$  is the adherend's yield strength and  $t$  is the adherend's thickness, to be determined. Substituting the values:

$$23.87 * 10 * 12.5 = 300 * 10 * t \Rightarrow t = 1 \text{ mm}$$

The adherend thickness that ensures adherend yielding is therefore 1 mm. The closest thickness granted by the provider is of 2 mm.

To select a thickness that will guarantee that there will only be plastic deformation of the substrate, a bending factor was considered. According to Goland and Reissner, the minimum bending factor along the overlap length is of 0.25 [10], so applying this value when calculating the aluminium's yielding load ensures that it will not plastically deform. Therefore:

$$23.87 * 10 * 12.5 = 300 * 10 * t * 0.25 \Rightarrow t = 4 \text{ mm}$$

While 4 mm thick adherends would guarantee that the failure is due only to the deformation of the adhesive, the closest thickness provided is of 5 mm.

### 3.4.2. Surface preparation

The first and extremely important step for manufacturing the single lap joints is to ensure that the adherends' surfaces are properly prepared so that their adherence is guaranteed, avoiding adhesive failures at the interface. This was done first by using sandpaper to create surface roughness on the section of the substrate that would be in contact with the adhesive, on the overlap area, followed by degreasing using acetone. Since the adherends have relatively small dimensions, this was done easily by using a regular household ultrasonic cleaner. Finally, each adherend was subjected to a phosphoric acid anodization (PAA) treatment to further improve adhesion, especially since some joints would be tested under humid conditions.

The PAA treatment was done following the standard ASTM D3933. First, a phosphoric acid solution was prepared with a concentration of 12% of phosphoric acid mixed with distilled water. Using a 16V power supply, the setup illustrated in Figure 39 was used.



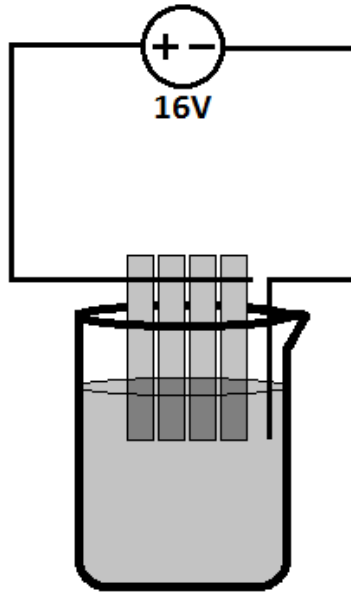


*Figure 39. Schematic illustration of the setup used for the anodization process.*

After 25 minutes submerged in the solution with this setup, the adherends presented a clear change in appearance. After carefully drying them, in order to avoid ruining the treated surface, they were wrapped in aluminium foil until ready for the joint manufacture (they should not spend more than 3 days before being bonded so that the anodization's effect is not lost). The visual difference after surface treatment can be seen in Figure 40.



*Figure 40. 2mm adherend after surface preparation (The left, lighter section has been anodized).*

### 3.4.3. Manufacture process

To create the joints with the intended dimensions, a mould was used in which the specimens were placed using spacers that guarantee the overlap length as well as steel strips that assure that the adhesive thickness is the intended (Figure 41).



Figure 41. Positioning of spacers and strips relative to the joints in the mould.

The spacers are made from the spare material used to make the substrates so they have the same thickness of 2 or 5 mm, depending on the joint. Their length is equal to the adherends' minus the overlap length of 12.5 mm, totalling 95 mm. The strips have the same thickness as the intended adhesive thickness of 0.2 mm, which means that this will be the gap between adherends that the adhesive will fill in.

Due to the large amount of specimens needed to satisfy all condition combinations, optimization methods were explored to hasten the manufacturing process. It was noticed that using the setup described earlier would waste a considerable amount of space on the mould for the 2 mm adherends. The joints occupied less than half of the available vertical space. The solution that was thought of was to assemble two setups above one another, properly separated from each other (Figure 42), effectively doubling the amount of manufactured joints with 2 mm adherends manufactured at a time.

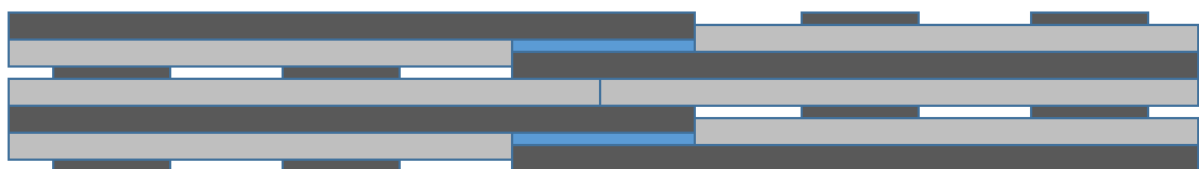


Figure 42. Optimized setup used for the joints with 2 mm adherends.

To make sure that there would be enough available specimens to accurately test all property combinations, it was established that at least 5 joints should be manufactured for each, totalling 240 SLJs for the 24 combinations described earlier, for both the quasi-static and impact tests. Each mould supports 12 joints side by side at a time, but half of them (the ones with 2 mm thick adherends) can be fit 24 at a time. This equals a total of 26 moulds since joints with different adhesives could not be manufactured in the same batch due to different curing conditions.

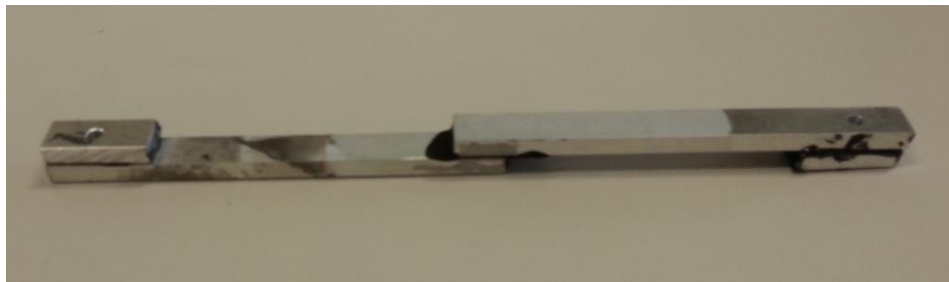
To guarantee that the excess adhesive doesn't bond to the mould and aid in the process of removing the joints from it, mould release agent was applied on the mould and its components. After positioning the adherends in the mould, it was placed under pressure using a hydraulic hot plates press (Figure 43) and, depending on the adhesive, was heated (for the Nagase adhesive) or not (for the Sika adhesive) to begin the curing process.



Figure 43. Hidraulic hot plates press with a mould inside.

When the joints were completely cured, the excess adhesive was removed from the edges of the overlap and the tabs were attached, also using the SikaPower 4720, to ensure that the load applied during the tests is aligned with the centre plane of the adhesive and to facilitate the gripping of the specimens.

The specimens are now ready to be tested or, in the case of the ones for humid conditions, to be submerged in water.



*Figure 44. Finished single lap joint using the SikaPower 4720 adhesive and 5 mm thick adherends.*

### 3.5. Tensile tests (quasi-static)

#### 3.5.1. Experimental procedure

For the quasi-static tests, the used machine was an INSTRON® model 3367 (Norwood, Massachusetts, USA), capable of applying loads up to 30 kN and measuring the displacement during the test.

It includes a heating chamber which could be automatically heated or cooled down for the different temperature tests and adjustable grips to use for both the thinner and thicker (2 mm and 5 mm) adherends. The low temperature tests required the acquisition of liquid nitrogen that was sprayed onto the joints through a hose that could be connected to the chamber. Due to the tests being performed inside the heating chamber, it would not be practical to use a thermocouple to verify when the joints reached the required temperature. Instead, a thermographic camera was used. The infrared images it provided showed the exact temperature on the overlap of the SLJ,

which was covered with a black electric tape to avoid reflections (see Figure 45) that could induce wrong readings. These tests were performed at a speed of 1 mm/min.



*Figure 45. Single lap joint mounted for a quasi-static tensile test.*

## 3.6. Impact tests

### 3.6.1. Experimental procedure

#### *3.6.1.1. Testing equipment and procedure*

As already mentioned, the method used for impact testing was the drop weight impact test. The machine used to conduct the tests was the Rosand<sup>®</sup> Instrumented falling weight impact tester, type 5 H.V. (Stourbridge, West Midlands, U.K.).

The adhesive joint is attached to the holding device at the bottom section of the machine using a special tool that takes the impact and transfers the load to the specimen. The impactor is guided down from the top section towards the specimen while attached to a configurable mass and a load cell that will measure the transmitted load.

For the joints tested in this study, it was determined that 20 J of impact energy would be more than enough for all specimens to fail and be successfully tested, so a mass of 26 kg was set on the impactor. The height was also adjusted so that the impact speed was 1.24 m/s – high enough to provide decent impact results but not too high as to provoke too much vibrations for the load cell to accurately measure the load. To further increase accuracy, at least 3 and up to 5 specimens for each combination of conditions was tested, depending on the coherence of the performed tests' results.

### 3.6.1.2. Heating system

To perform the high temperature impact tests, the bonded area of the joint needed to be at 80°C at the time the load is applied, to ensure that the adhesive is tested with its properties modified by the high temperature. Previous studies [2, 27, 28] involving temperature suggest that by heating through electromagnetic induction (Figure 46), a homogenous and constant temperature can be obtained throughout the adhesive.

To use this method, an electric current circulating through a coil made of conductive material generates a magnetic field which is more intense in the centre of said coil. When a ferromagnetic material is positioned in the magnetic field, electric currents – Foucault currents – are induced in the material, agitating its particles and heating it up by Joule effect [29].

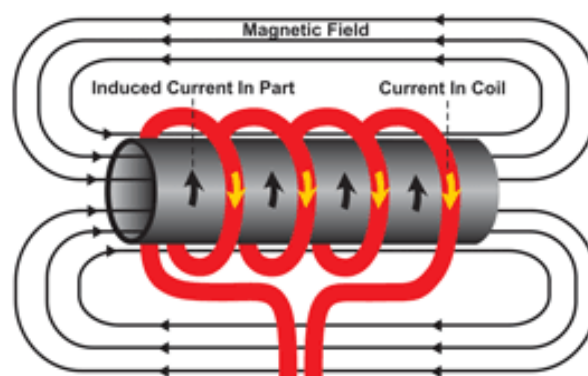


Figure 46. Process of electromagnetic induction heating [30].

This was a cheap and quick way to heat up the required specimens and, by using a coil with the correct geometry, could be used with any of the specimens to be tested without any form of physical contact. The heating was also homogenous and easily controlled by adjusting the electric current.

The used equipment (Figure 47) consists in a power supply which rectifies and regulates the alternating current it receives, feeding it to the frequency converter where the magnetic field is generated. The recommended frequency varies based on the material's thickness – thinner components need higher frequencies (100 – 400 kHz) whereas for thicker ones, lower frequencies are recommended (5 – 30 kHz). To regulate the application voltage or frequency, a heating station was used where, by using a water circuit, the induction coil was refrigerated [2, 29].



Figure 47. Equipment used for the induction heating system/close-up of the "pancake" induction coil used [2].

The induction coil is made of copper and has a hollow interior so that the water from the refrigeration system can circulate in its interior. This “pancake” geometry was the most suitable found to accommodate both the SLJs and the testing machine’s holding system since it managed to easily provide the adhesive’s required 80°C homogeneously and without physical contact.



*Figure 48. Single lap joint mounted and waiting to be heated up before a high temperature impact test.*

After mounting the specimen on the support and placing the coil in position (Figure 48), the heating system was turned on for a couple of minutes until the specimen reached a slightly higher temperature than the intended 80°C. The few seconds between removing the coil and triggering the impact machine would cool the adhesive down to the planned temperature.

To measure this temperature during the procedure, a thermocouple would be the simplest solution but the interference with the magnetic field wouldn't allow it. Instead, the same solution as in the quasi-static tests was adopted – a thermographic camera was used.

#### *3.6.1.3. Cooling system*

In order to perform the low temperature tests, the specimens would require to be at -20°C at the time of impact. To do so, the selected method was to use the liquid nitrogen to manually spray the surface of the overlap until the adhesive was at the required temperature. The nitrogen was contained under pressure and at extremely low temperatures in a bottle and sprayed directly from the hose (Figure 49).





*Figure 49. Nitrogen being sprayed onto a single lap joint ready to be tested under impact.*

Just as in the high temperature tests, the required temperature was slightly overshoot so that the few seconds between removing the cooling equipment and triggering the machine would ensure that the adhesive would be at roughly  $-20^{\circ}\text{C}$  at the time of impact. In this case, to measure the temperature, a thermocouple was used, attached as close as possible to the joint's overlap to measure the current temperature as accurately as possible.

This method proved to be fast and easy, though not as accurate since the overlap was being cooled from the outside surface as opposed to the heating system which heated it uniformly.



## 4. Experimental Results and Discussion

This chapter covers the results of the tests described in chapter 3 by discussing and comparing them with their analytical predictions. A summary of all results will be presented here, while the individual results for each test and their respective failure modes can be consulted in the appendices.

### 4.1. Maximum load of the impact and quasi-static tests

#### 4.1.1. Maximum loads under different strain-rate conditions

The first results analysed are the maximum load of each kind of joint presented in a way so that the effect of temperature, moisture, adherend thickness and strain-rate is easily observable for both adhesives.

Figures 50 and 51 show the results for the SLJs with the XNR 6852E-2 adhesive.

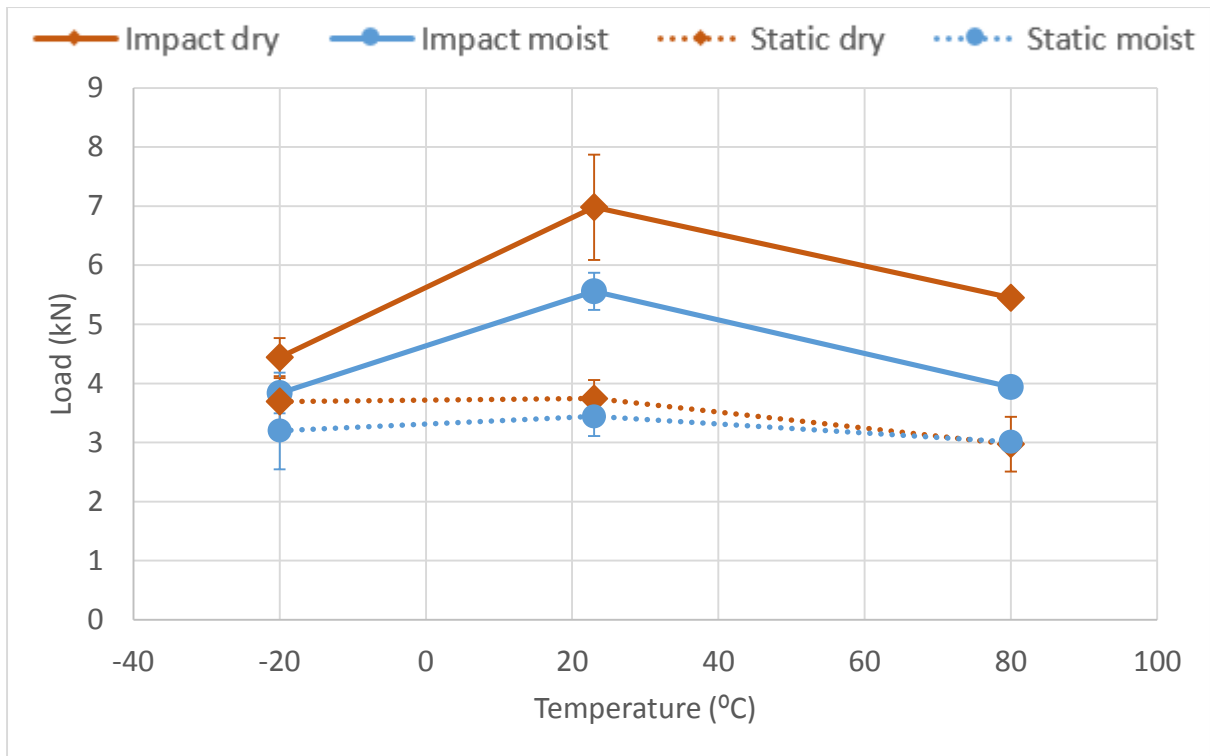


Figure 50. Maximum loads obtained from all the tests – Nagase XNR 6852E-2 with 2 mm adherends.

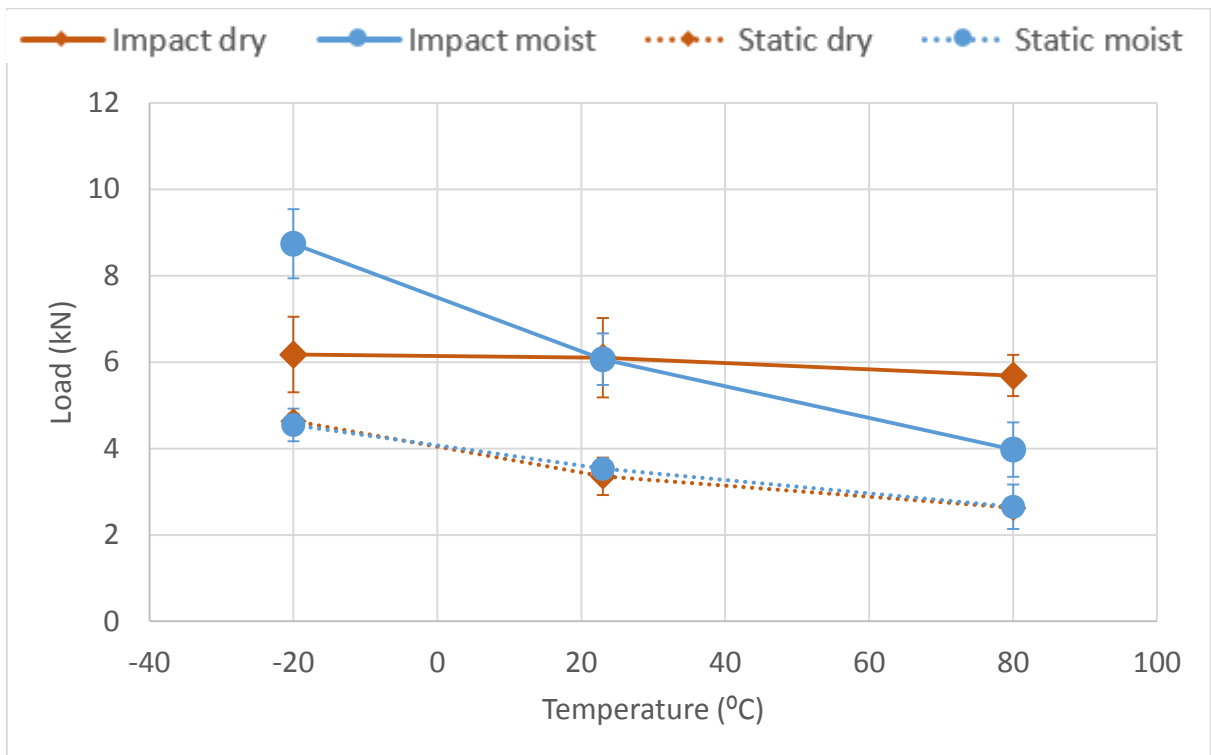


Figure 51. Maximum loads obtained from all the tests – Nagase XNR 6852E-2 with 5 mm adherends.

Results show that, for the joints with 2 mm thick adherends (Figure 50), the relation between maximum loads is linear – the joints take a higher load before failure under impact than quasi-static conditions and the dry joints are stronger than the moist ones. It is also noticeable that at room temperature the joints are the strongest since at low temperature the adhesive loses ductility and at high temperature, closer to its  $T_g$ , it loses mechanical qualities. These effects from temperature variation are most noticeable at a higher strain-rate. In both the quasi-static and impact tests, the adherend yielding is clearly visible (Figure 52) for the dry tests performed at room temperature as well as low temperature which increases the yielding of the aluminium. For these conditions, the failure is controlled by the adherend.



*Figure 52. Adherend yielding after quasi-static testing of a SLJ using SikaPower 4720 with 2 mm adherends (-20 °C; moist)*

For the joints with 5 mm thick adherends (Figure 51), where the stress distribution throughout the joint is more linear due to less elastic deformation of the aluminium, relation between results are different, but the maximum loads are generally higher. In this case, the strongest joints are the low temperature moist ones, an effect that becomes more apparent as strain-rate goes up. However the dry joints, under impact, show no variation in behaviour as temperature varies.

In both cases, moisture level barely affects results in the quasi-static tests. The Nagase adhesive generally has failure modes more towards the interface as temperature varies – higher temperature results show plenty of mixed failure modes (see appendixes) and lower temperatures usually result in failures closer to the interface or even some mixed failures. Figure 53 shows an example of a failure at low temperature on a wet joint, where the effect of the moisture distribution throughout the layer is clearly visible.



Figure 53. Failure mode after quasi-static testing of a SLJ with XNR 6852E-2 at low temperature (5 mm adherends; moist).

The increase in ductility with temperature is very noticeable in both the load-displacement curves and the failure modes of the joints, as seen in Figure 54.

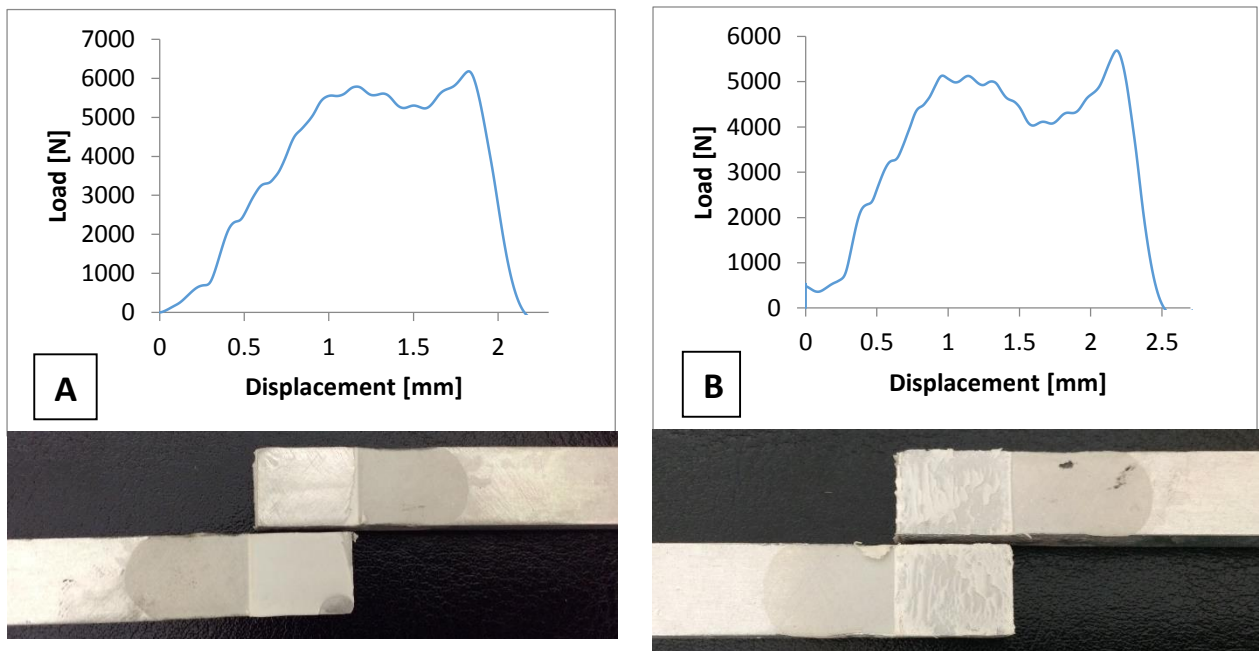


Figure 54. Load-displacement curves of SLJs under impact using XNR 6852E-2 with 5 mm adherends under dry conditions and (A) -20 °C and (B) 80°C.

The behaviour obtained from a ductile failure is noticeable from the increase in displacement before failure as well as a less uniform distribution of the remaining adhesive.

Figures 55 and 56 show the results for the SLJs with the SikaPower 4720 adhesive.

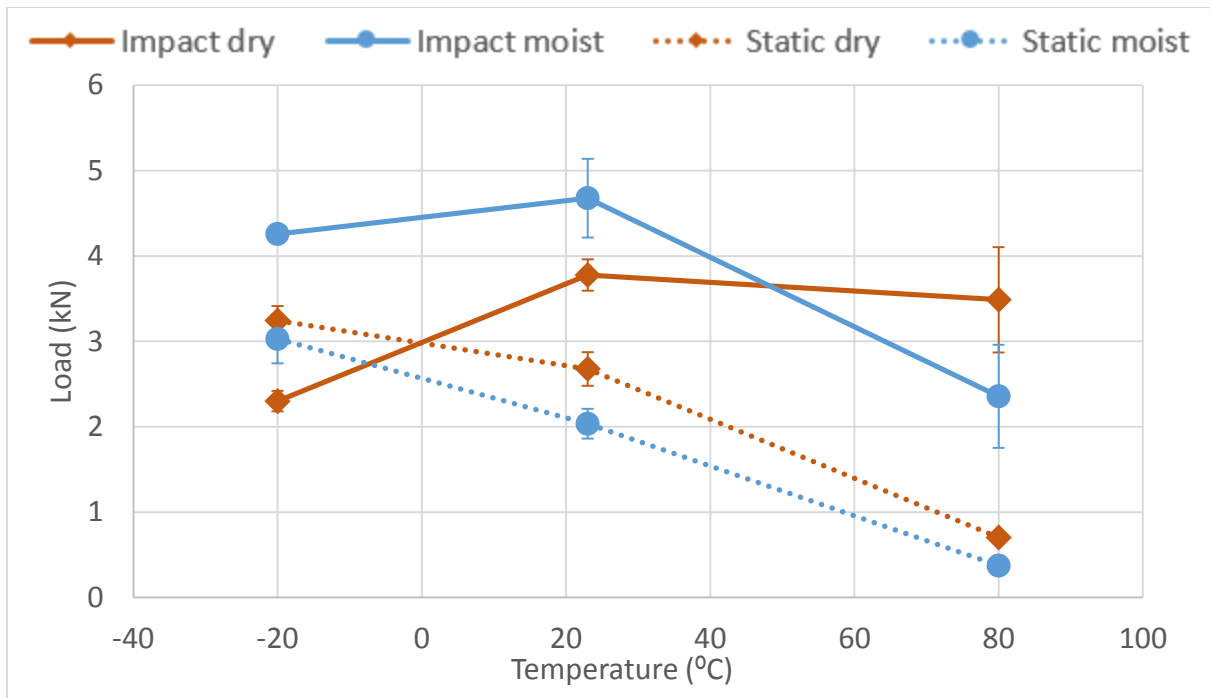


Figure 55. Maximum loads obtained from all the tests – SikaPower 4720 with 2 mm adherends.

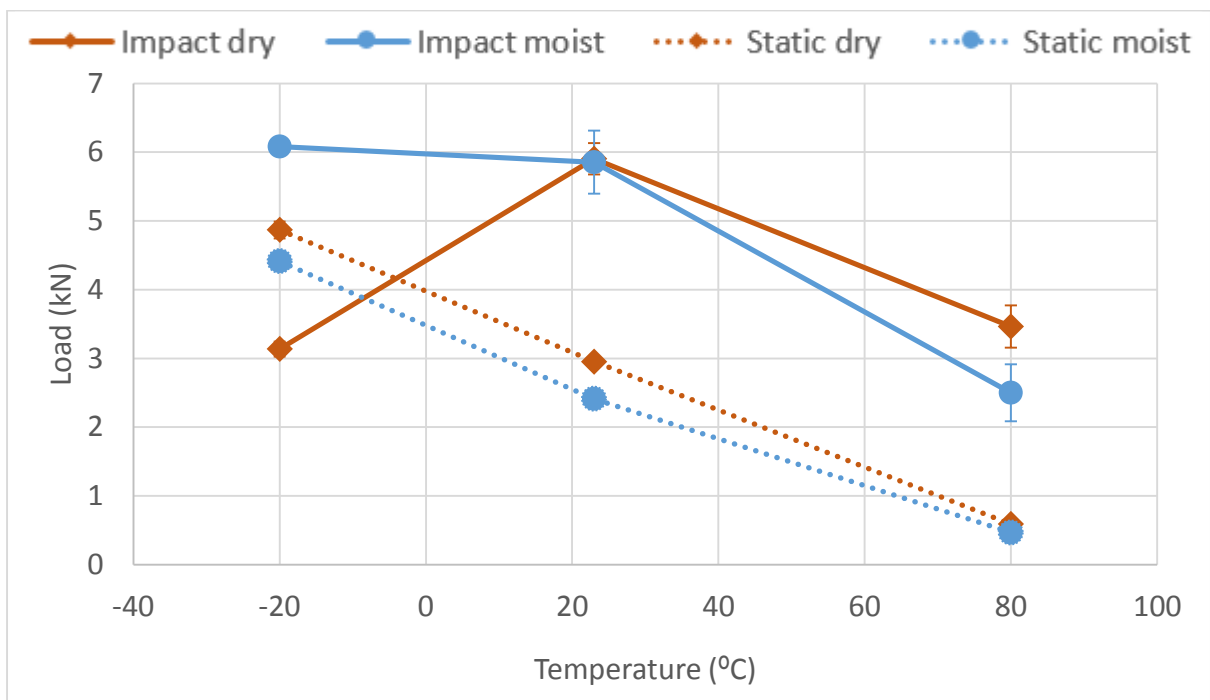


Figure 56. Maximum loads obtained from all the tests – SikaPower 4720 with 5 mm adherends.

As a first observation both graphs are much more similar to each other than the XNR 6852E-2 ones. This means the SikaPower 4720 adhesive is not as dependant

on the adherend thickness due to the generally lower maximum loads which lead to a decrease in elastic deformation of the aluminium and therefore the stress distribution is more uniform. At low temperatures the abnormal adhesive failures don't allow for much conclusions to be drawn, even though the joints seem to be strong at low strain-rates or with moisture. Figure 57 shows an interfacial failure where the adhesive disappears from the joints, losing adhesion from both adherends simultaneously.



Figure 57. Adhesive failure after quasi-static testing of a SLJ with SikaPower 4720 at low temperature (2 mm adherends; dry).

At high temperature, the adhesive has clearly passed its  $T_g$ , for which the maximum load the joints can withstand is reduced. The effect of working at a higher temperature than its  $T_g$  is very strain-rate dependant though and under impact the joints still withstood a high maximum load. The effect on the load-displacement curve of a joint working above its  $T_g$  is clear, as the failure isn't as abrupt and the load reduction after failure is more gradual due to its rubbery behaviour, as seen in Figure 58.

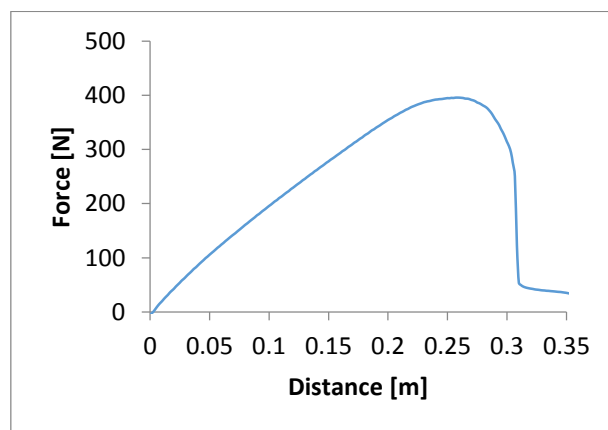


Figure 58. Load-displacement curve of a quasi-static test of a SLJ with SikaPower 4720 at high temperature (2 mm adherends; moist).

Due to the lower maximum loads, there was no yielding of the adherends in any test using the SikaPower 4720 adhesive.



#### 4.1.2. Maximum load predictions – quasi-static

Using the Adams et al. predictive model described in chapter 2.3.4., the values obtained for maximum load can be predicted. This was done for the joints tested at room temperature and at a dry state, where the materials' properties are either accessible or easily determined.

The yield strength used for the adherends was 300 MPa, and the shear strength of the adhesives, obtained from other studies, were 22.9 MPa and 27.8 MPa for the Sika and Nagase adhesives, respectively. The comparison between the experimental and predicted loads is presented in Table 8.

*Table 8. Experimental and predicted maximum loads under quasi-static conditions.*

<b>Adhesive</b>	<b>Adherend thickness (mm)</b>	<b>Experimental max. load (N)</b>	<b>Predicted max. load (N)</b>
Nagase XNR 6852E-2	2 mm	3893	2906
	5 mm	3355	3475
SikaPower 4720	2 mm	2718	2863
	5 mm	2953	2863

A visual representation of the predicted values allows us to better understand how the joints' failure would be controlled by either the adhesive or adherends as a function of overlap length (Figures 59-62).

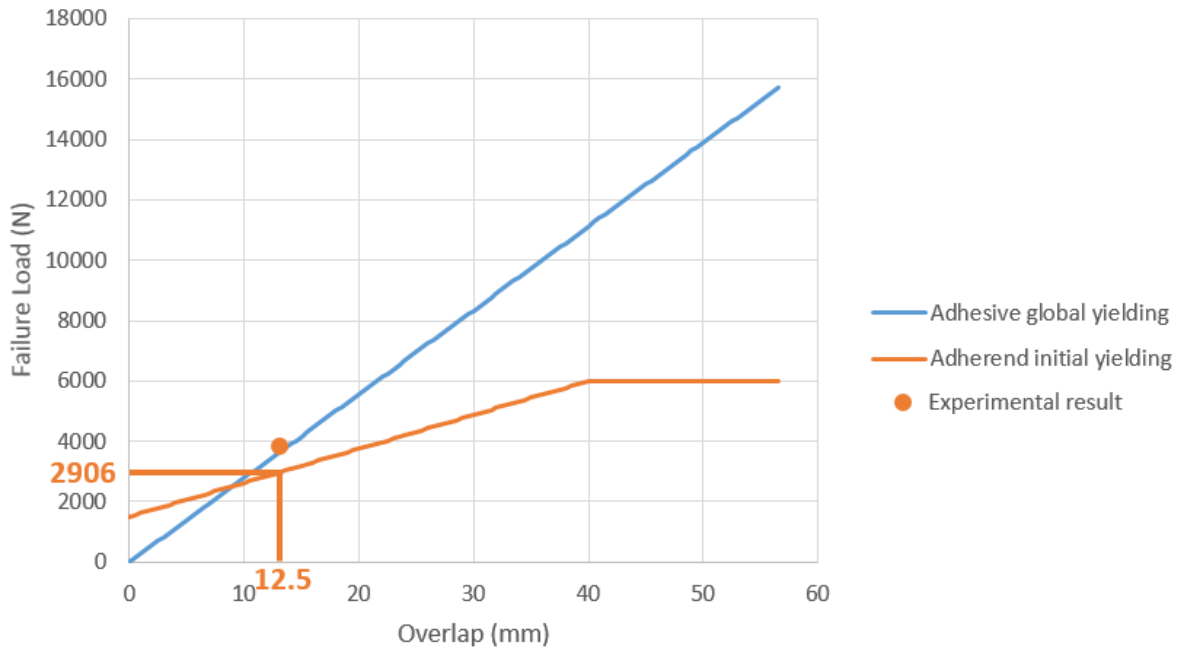


Figure 59. Maximum load prediction using Adams et al. predictive model for the static tests – Nagase XNR 6852E-2 with 2 mm adherends.

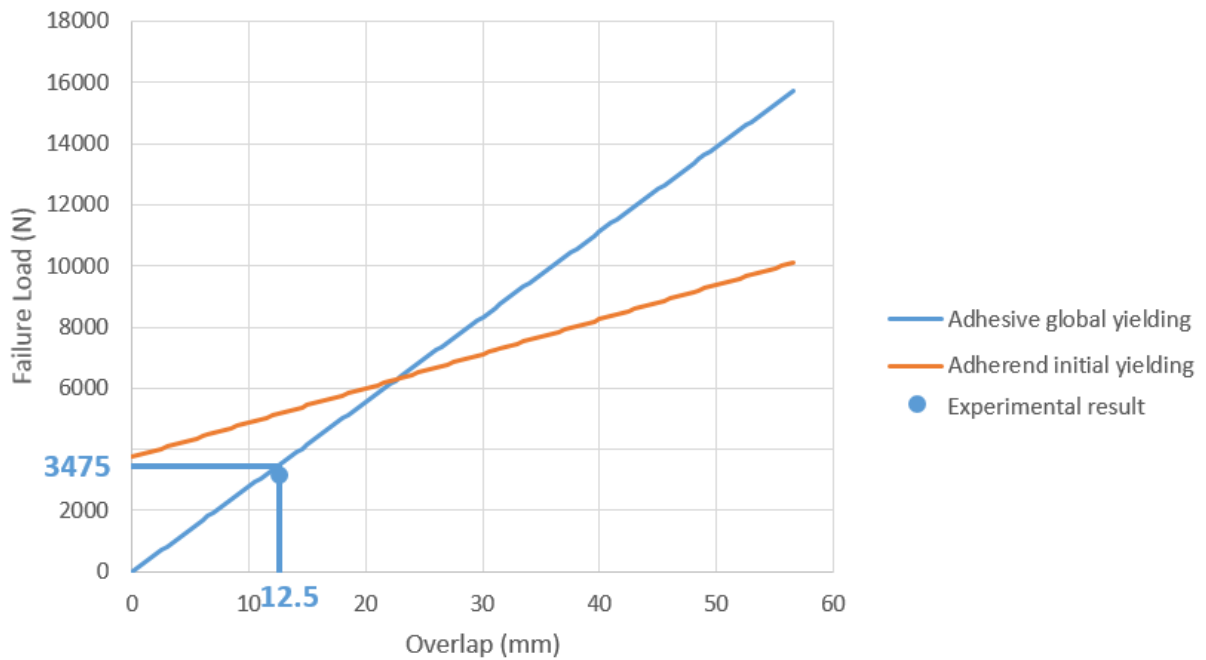


Figure 60. Maximum load prediction using Adams et al. predictive model for the static tests - Nagase XNR 6852E-2 with 5 mm adherends.

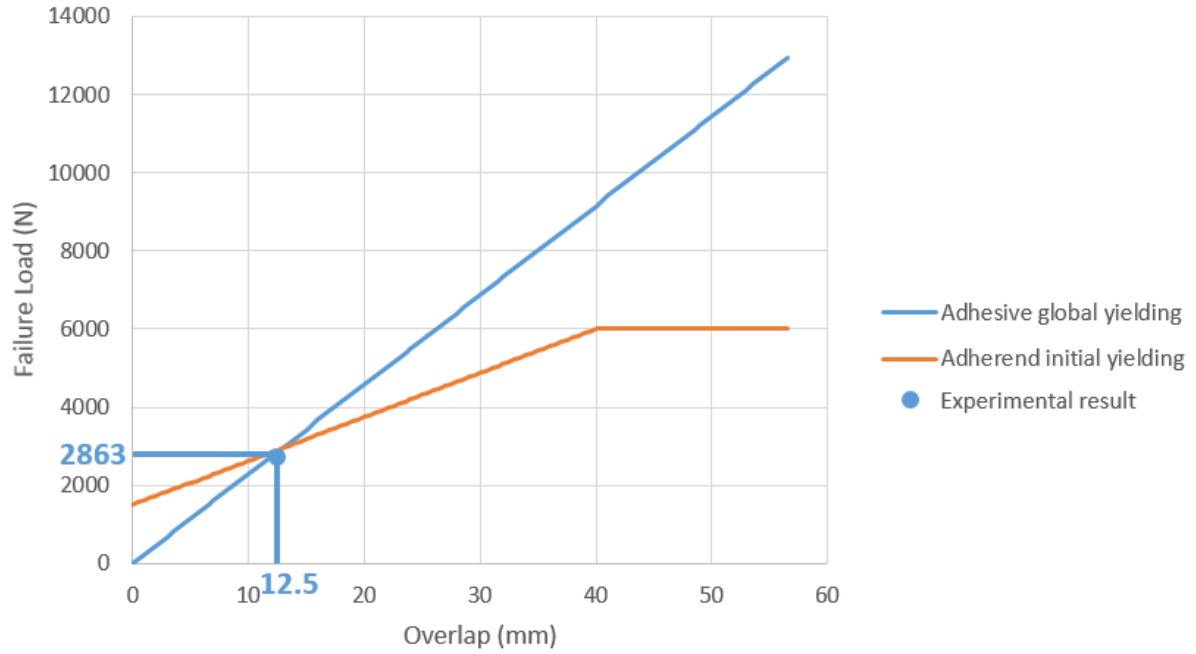


Figure 61. Maximum load prediction using Adams et al. predictive model for the static tests – SikaPower 4720 with 2 mm adherends.

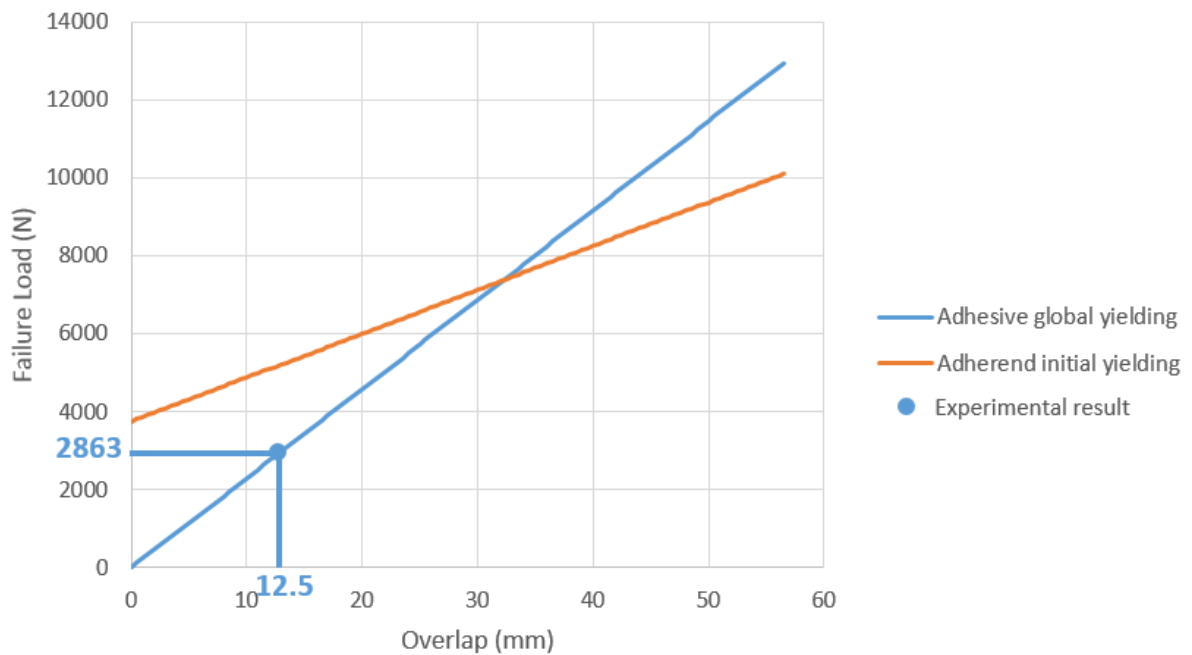


Figure 62. Maximum load prediction using Adams et al. predictive model for the static tests – SikaPower 4720 with 5 mm adherends.

It can be concluded that this predictive model, applied to the quasi-static tensile tests does indeed correctly forecast if the failure will be caused by the adherend

yielding or solely by the adhesive's properties. In the latter case, the predicted values correspond correctly to the amounts verified experimentally, but there is some inconsistency when it comes to the maximum load at which the yielding will cause failure.

#### 4.1.3. Maximum load predictions – impact

The same predictive model could be used for the same joints under impact conditions, but the properties for the high strain rate of 1.24 m/s are not directly available in literature.

The tensile strength of the aluminium adherends was obtained by performing impact tests on specimens made out of the same aluminium. By measuring the maximum applied load and the respective deformation, its tensile strength at the same strain-rate it was submitted to in the impact tests could be directly determined. This value is equal to 390 MPa.

For the adhesives' properties, a different method was used. Using the relation between the available values for 1 mm/min and 100 mm/min, their shear strength was obtained by logarithmic extrapolation. The obtained strengths were 41.6 and 32.2 MPa respectively for the Nagase and the Sika adhesives. The comparison between the experimental and predicted loads is presented in Table 9.

*Table 9. Experimental and predicted maximum loads under impact conditions.*

<b>Adhesive</b>	<b>Adherend thickness (mm)</b>	<b>Experimental max. load (N)</b>	<b>Predicted max. load (N)</b>
Nagase XNR 6852E-2	2 mm	6981	3778
	5 mm	6100	5201
SikaPower 4720	2 mm	3777	3778
	5 mm	5904	4028

The graphs showing each individual result are presented in Figures 63-66.

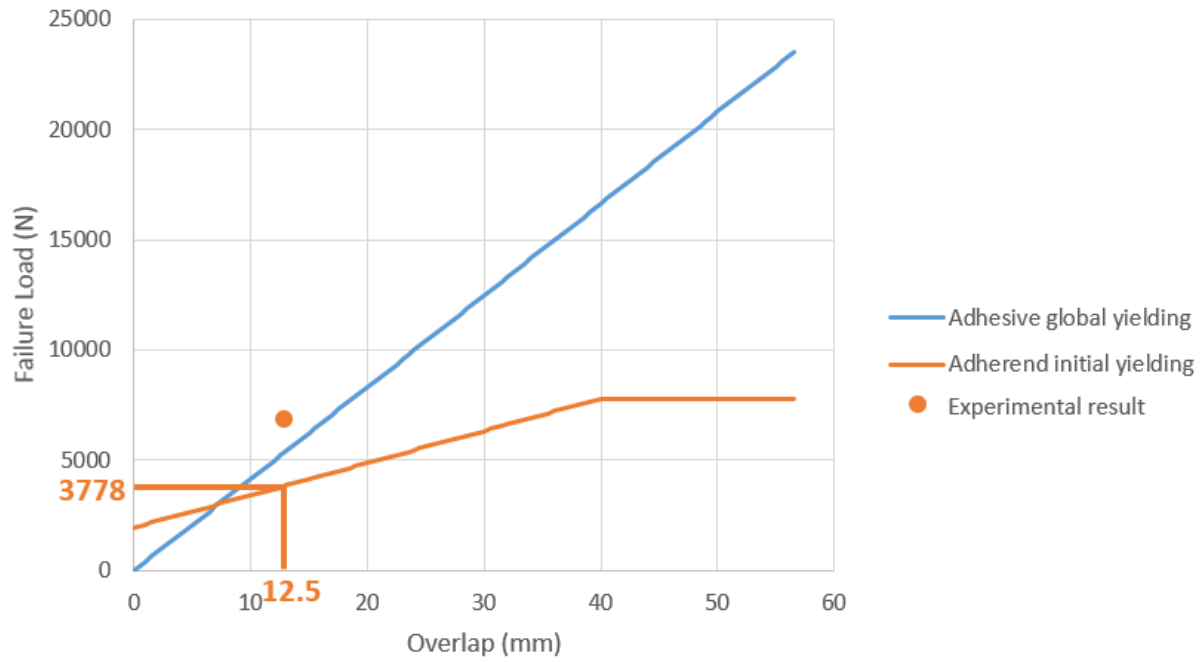


Figure 63. Maximum load prediction using Adams et al. predictive model for the impact tests – Nagase XNR 6852E-2 with 2 mm adherends.

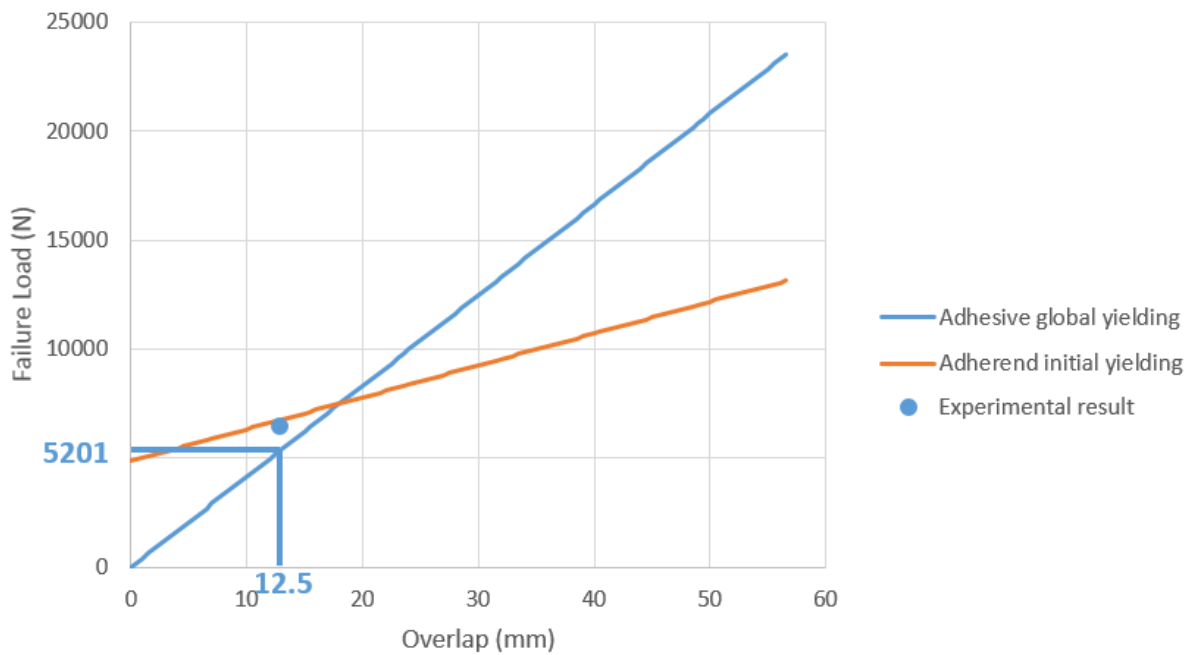


Figure 64. Maximum load prediction using Adams et al. predictive model for the impact tests – Nagase XNR 6852E-2 with 5 mm adherends.

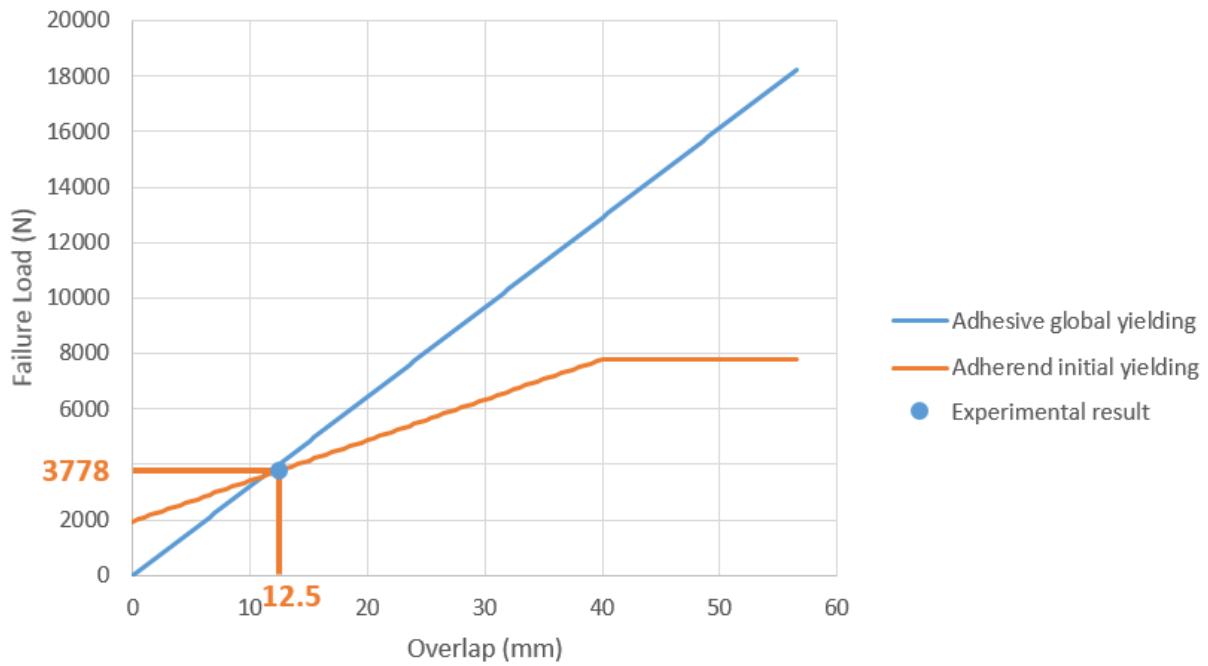


Figure 65. Maximum load prediction using Adams et al. predictive model for the static tests – SikaPower 4720 with 2 mm adherends.

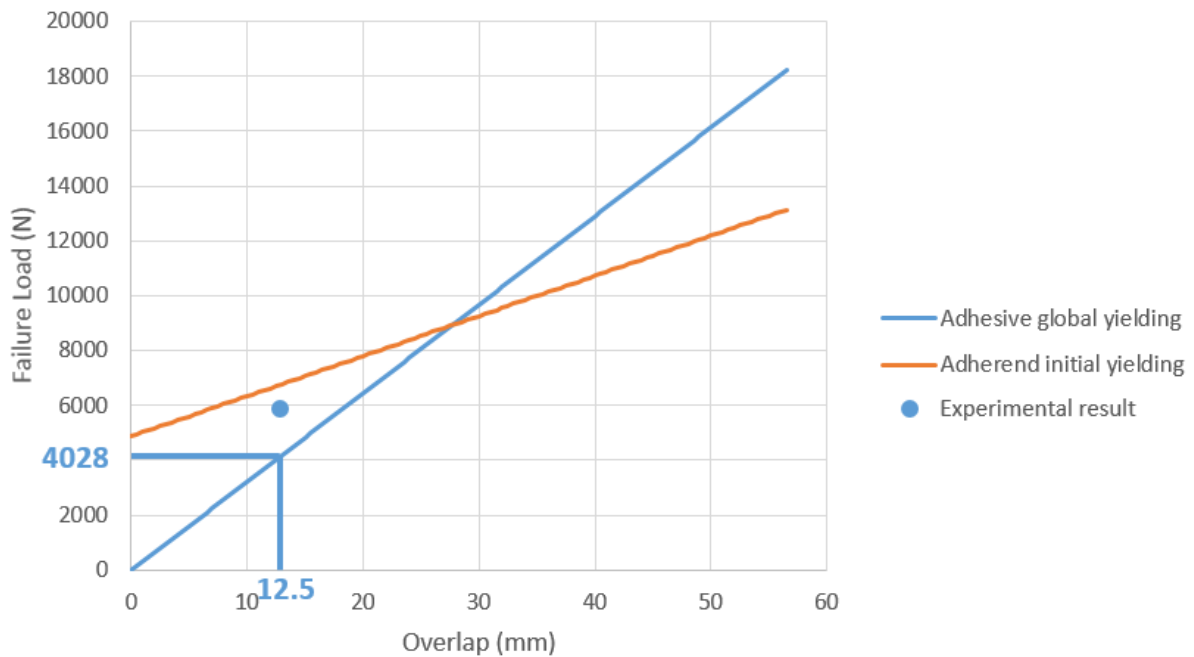


Figure 66. Maximum load prediction using Adams et al. predictive model for the static tests – SikaPower 4720 with 5 mm adherends.

Under impact, the properties of the materials are not the only parameters to change. As the strain-rate increases, so do the stress distributions along the adhesive

layer, a change that is not accounted for by the Adams et al. predictive model. This results in predicted failure loads that are significantly lower than the experimental values. The strength of the aluminium at high strain-rate also seems to be quite inaccurate since higher values of load for adherend initial yielding are to be expected (the SLJs with the Sika adhesive and 2 mm adherends should not fail by adherend yielding, for instance), so additional tests should be performed to properly obtain this value. This combined with the fact that the extrapolations were made from two strain-rates which are very far from the impact test speed, resulting in inaccurate properties, allow us to conclude these predictions are too imprecise to be taken into account. The only correct prediction (SLJs with the Sika adhesive and 2 mm adherends) was purely coincidental since the cause of failure should be the adhesive as opposed to what the prediction results show.

## 4.2. Absorbed energy under impact

Focusing on the impact tests, this section summarizes the amounts of energy absorbed in the impact tests, comparing the effect of each combination of properties on the joints' failure parameters. Results show that the XNR 6852E-2 adhesive joints are capable of absorbing a significantly higher amount of energy compared to the SikaPower 4720 ones (Figures 67 and 68).

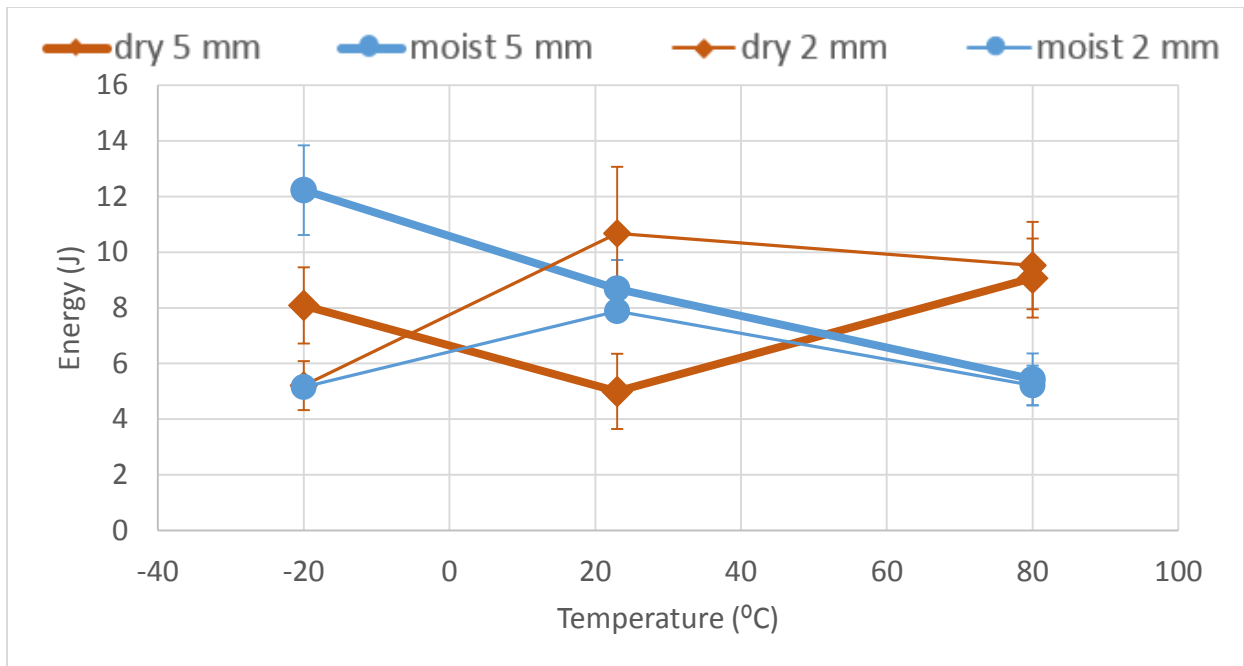


Figure 67. Energy absorbed under impact for the joints with the XNR 6852E-2 adhesive.

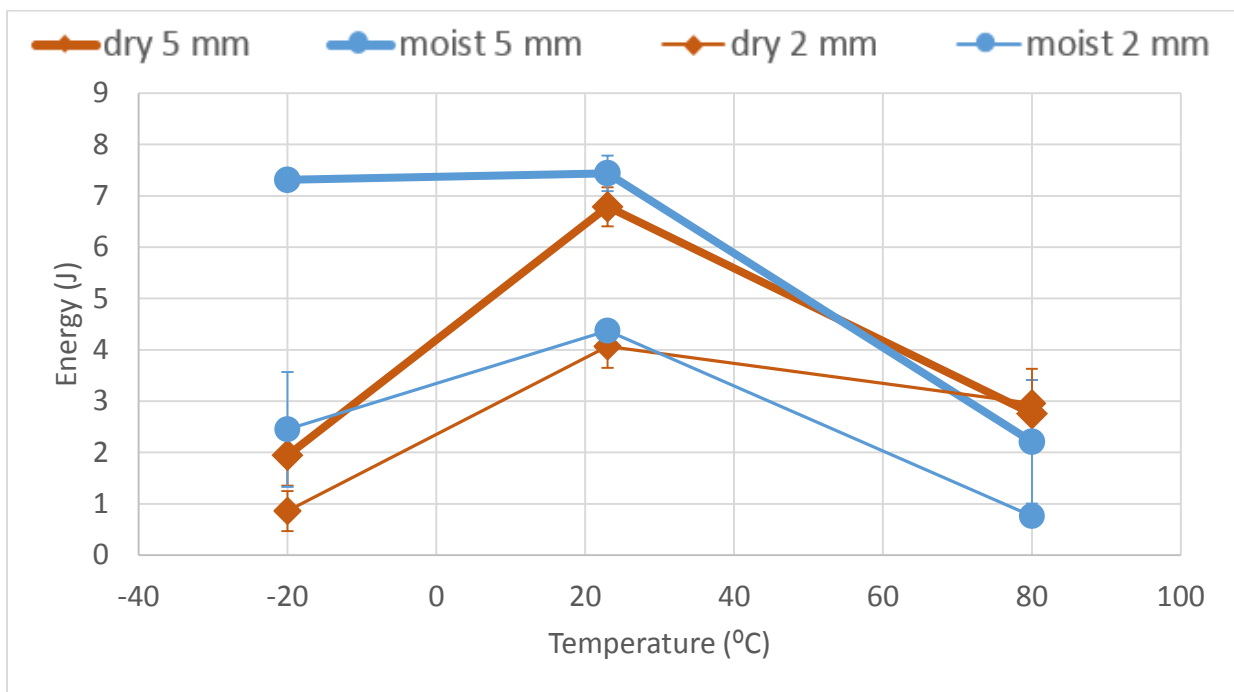


Figure 68. Energy absorbed under impact for the joints with the SikaPower 4720 adhesive.

With moisture, the joints' toughness seems to decrease as the temperature increases, showing the highest value at low temperature. This happens because of the plasticization of the adhesive and, with thick adherends where their yielding is not



a factor, the low temperature moist joints are capable of absorbing the most energy. With 2 mm thick adherends, where the stress peaks at the edges of the overlap are higher, the amount of absorbed energy was similar between the dry and moist joints. This is evident on the results of the Nagase adhesive but, while the pattern is still somewhat noticeable with Sika, it performed poorly at low temperatures, presenting adhesive failures (figure 69) for which no conclusions could be accurately made.



*Figure 69. Adhesive failure under impact of a SLJ with SikaPower 4720 at low temperature (2 mm adherends; dry).*

At room temperature the joints with thick adherends absorb more energy than their thin adherend counterparts (when adherend yielding is not perceptible) due to the difference in maximum stress in the adhesive layer. The moist joints absorb more energy than their dry counterparts due to the significantly higher elongation resulting from the higher ductility of the moist adhesive. Another reason is that the adhesive in the moist joints is more ductile at the ends of the overlap (where it has absorbed more water), resulting in a more uniform stress distribution, which is similar to what happens in a functionally graded joint. One clear exception to this rule is the dry joints made with 2 mm thick adherends and the Nagase adhesive. These present the highest load and therefore the highest adherend yielding which in turn absorbs an additional amount of energy relative to the other conditions (Figure 70).

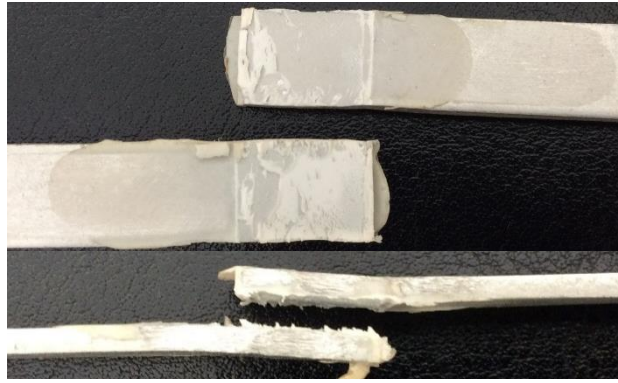


*Figure 70. Adherend yielding after impact on a joint made with the Nagase XNR 6852E-2 adhesive (2 mm adherends; dry; room temperature)*

At high temperature, the high plasticization of the adhesive causes the adherend thickness to lose relevance. The dry joints also absorb a higher amount of energy than their moist counterparts for both adhesives. This happens since a higher moisture level decreases the adhesives'  $T_g$  along with its mechanical properties at high temperature.

The SLJs' behaviour under impact can be further examined by analysing their absorbed energy as a function of maximum load (Figures 71-73).

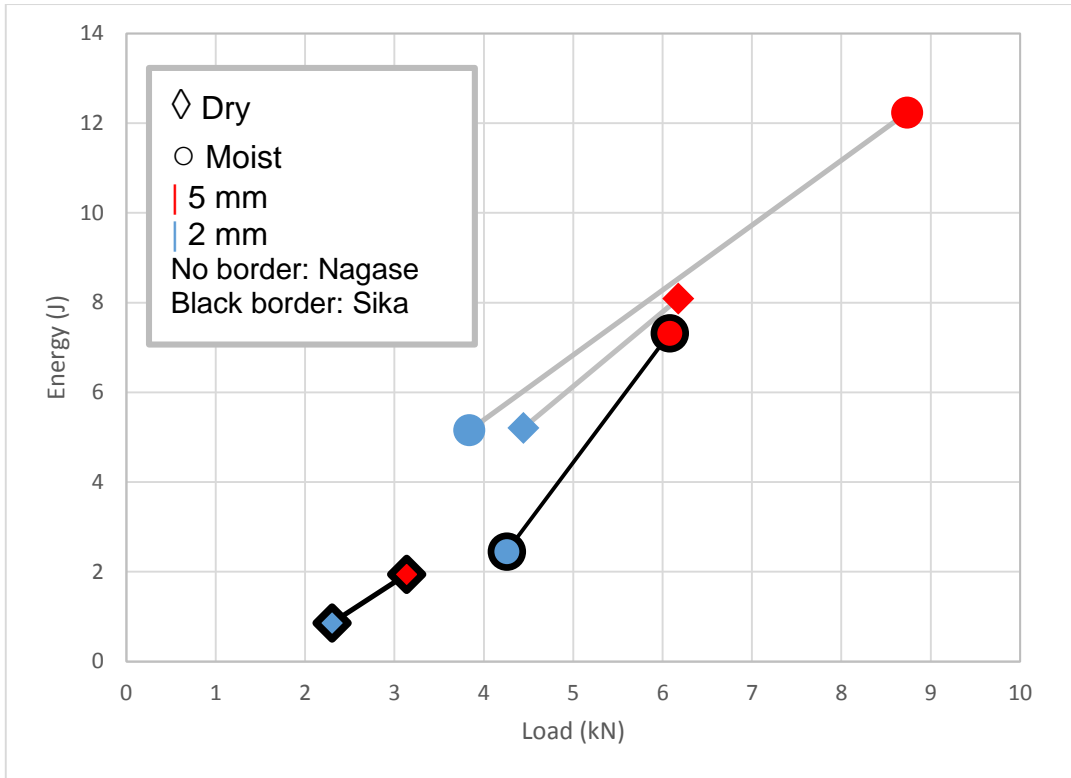


Figure 71. Energy absorbed as a function of maximum load at -20°C.

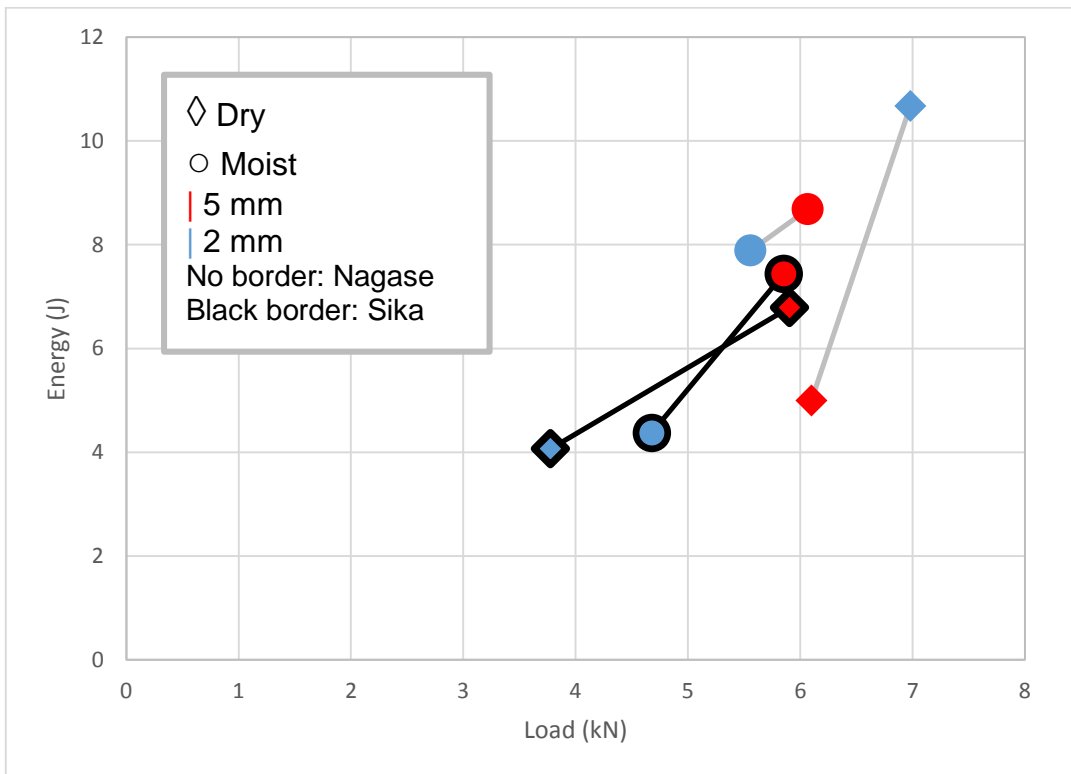


Figure 72. Energy absorbed Sika as a function of maximum load at room temperature.

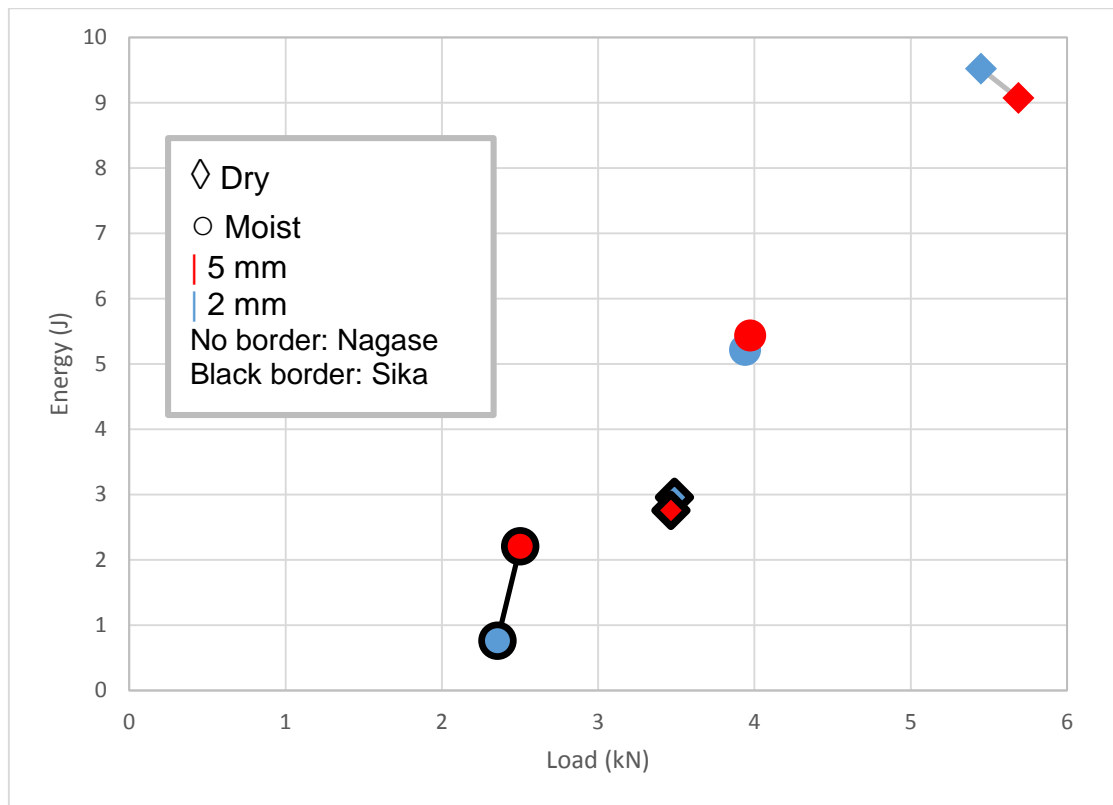


Figure 73. Energy absorbed as a function of maximum load at 80°C.

These graphs allow to observe the direct effect that the maximum load until failure has on the amount of energy the joints are capable of absorbing and how the Nagase adhesive is both capable of withstanding a higher load and absorbing a larger amount of energy than the Sika adhesive. At low temperature (Figure 71), it is clear how using a thicker adherend to reduce stress differential along the joint is a direct upgrade both in maximum load and energy absorbed. At high temperature (Figure 73), the effect of moisture reducing the adhesives'  $T_g$  is evident as well as how little effect the adherend thickness has upon the joint strength, as the points are paired up with their counterparts with different thicknesses.

## 5. Conclusions

The objective of this work was to verify how adhesively bonded joints made with two different adhesives used in the automotive industry behave under impact while several combinations of adverse conditions were applied to them, such as temperature and moisture. To study the effect of adherend yielding, two different substrate thicknesses were also used. The manufacturing process of the large quantity of required joints was optimized so that the tests could be performed as soon as possible. Several techniques were covered related to the manufacturing and testing process, such as adherend's surface preparation to improve adherence, water diffusion for tests with moisture and heating and cooling systems for tests with different temperatures.

The geometry of the joints allowed to correctly judge the effect of adherend yielding on the joint's behaviour, showing that the amount of energy absorbed may drastically increase. The joint thickness was correctly selected according to their geometry, although the small overlap length was not ideal to study the effect of the adhesives on the joints. A larger overlap would allow for a bigger variation in results and a better analysis of the joints' behaviour.

The implemented systems to heat up and cool down the joints before testing under different temperature conditions successfully allowed them to reach the required temperatures. At low temperature, the Sika adhesive failed at the interface and the Nagase adhesive had both interfacial and mixed failure modes. The brittle behaviour of the adhesives make for a poor performance at low temperature when dry. At high temperature the adhesives present a ductile behaviour and have a generally lower resistance and tensile strength.

Due to the reduced dimensions of the joints, a high enough moisture level to study its effects on the adhesive was easily obtained. The surface preparations also allowed for good adhesion even under moist conditions. The joints that were submerged showed a more plastic, ductile behaviour, withstanding generally lower maximum stresses but allowing for higher strains before failure, ultimately increasing the energy absorbed. At low temperature, combined with thick adherends, the moist joints absorbed a good amount of energy and sustained high failure loads despite their

bad adhesion. At high temperature, however, moisture lowered the adhesives'  $T_g$ , greatly harming the joints' performance. The amount of water content on an adhesive joint appears to have greater effect on its behaviour the higher the strain-rate applied on it.

As strain-rate increases, so does the maximum load the joints resist before failing. Under impact, the joints showed a generally better performance, although this may change with bad adhesion. It is important to understand how the adhesives' properties change with strain-rate and tests should be performed to determine these. The strong sensitivity of the adhesives to high strain-rate make it more difficult to predict their behaviour, presenting higher values than those expected from analytical models.

Lastly, the Nagase adhesive, besides having better mechanical properties, proves to behave better under different conditions. Its adhesion is better, even with moisture and it has a higher working temperature before beginning to degrade. All in all, and considering their performance alone, the Nagase XNR 6852E-2 adhesive demonstrates to be more adequate for the automotive industry than the SikaPower 4720.

## 6. Future Work

In order to quicken the joint manufacturing process and the water absorption of the joints to be tested under moist conditions, a small overlap and adherend width were used. To better study the effects of the adhesive on the joint, a larger overlap length would be recommended although the water absorption would take longer.

To better assess the results of the several tests, even though analytical methods were used to predict the expected values, more complex methods such as simulations using finite element method analysis software could be used to better and more accurately compare analytical and experimental values, especially at high strain-rates.

Since a large amount of properties were tested, it would be interesting to apply the analysis methods or the aforementioned simulations for these combinations. To do so, the properties for the adhesives under different strain-rates, temperatures and moisture levels would have to be determined by performing tests on bulk specimens for each adhesive.

Finally, the adhesives showed a difference in behaviour at high temperature that could be explained by the difference in  $T_g$  caused by the adhesive's moisture. It would therefore be interesting to learn the adhesives'  $T_g$  values to further investigate this phenomenon.





# References

- [1] L. F. M. d. Silva, A. Öchsner, and R. D. Adams, *Handbook of adhesion technology*: Springer-Verlag, 2011.
- [2] R. A. Mata, "Impact of adhesive joints for the automotive industry at low and high temperatures," MsC, IDMEC, University of Porto, 2014.
- [3] C. M. S. Canto, "Strength and fracture energy of adhesives for the automotive industry," MsC, FEUP, Porto, 2013.
- [4] S. R. Hartshorn, *Structural Adhesives: Chemistry and Technology*: Springer US, 2012.
- [5] W. A. Lees, *Adhesives in Engineering Design*: Springer Berlin Heidelberg, 2013.
- [6] L. F. M. da Silva and R. D. Adams, "Measurement of the mechanical properties of structural adhesives in tension and shear over a wide range of temperatures," *Journal of Adhesion Science and Technology*, vol. 19, pp. 109-141, 2005.
- [7] R. D. Adams, *Adhesive Bonding: Science, Technology and Applications*: Elsevier Science, 2005.
- [8] L. F. M. d. Silva, A. G. d. Magalhães, and M. F. d. S. F. d. Moura, *Juntas adesivas estruturais*. Porto: Publindústria, Edições Técnicas, 2007.
- [9] L. F. M. da Silva, P. J. C. das Neves, R. D. Adams, and J. K. Spelt, "Analytical models of adhesively bonded joints—Part I: Literature survey," *International Journal of Adhesion and Adhesives*, vol. 29, pp. 319-330, 2009.
- [10] L. F. M. da Silva, P. J. C. das Neves, R. D. Adams, A. Wang, and J. K. Spelt, "Analytical models of adhesively bonded joints—Part II: Comparative study," *International Journal of Adhesion and Adhesives*, vol. 29, pp. 331-341, 2009.
- [11] R. Adams, *Structural Adhesive Joints in Engineering*: Springer Netherlands, 2012.
- [12] Sugiman, "Combined Environmental and Fatigue Degradation of Adhesively Bonded Metal Structures," PhD, Mechanical, Medical and Aerospace Engineering Faculty of Engineering and Physical Sciences, University of Surrey, 2012.
- [13] L. Goglio and M. Rezaei, "Effect of Different Substrate Pre-Treatments on the Resistance of Aluminum Joints to Moist Environments," *The Journal of Adhesion*, vol. 89, pp. 769-784, 2013/10/03 2013.
- [14] *JointDesigner*. Available: <http://www.jointdesigner.com>
- [15] R. D. A. E. F. Karachalio, L. F. M. da Silva, "Single lap joints loaded in tension with ductile steel adherends," *International Journal of Adhesion and Adhesives*, vol. 43, pp. 96-108, 2013.
- [16] D. F. S. Saldanha, C. Canto, L. F. M. da Silva, R. J. C. Carbas, F. J. P. Chaves, K. Nomura, *et al.*, "Mechanical characterization of a high elongation and high toughness epoxy adhesive," *International Journal of Adhesion and Adhesives*, vol. 47, pp. 91-98, 2013.
- [17] L. F. M. da Silva, D. A. Dillard, B. Blackman, and R. D. Adams, *Testing Adhesive Joints: Best Practices*: Wiley, 2013.
- [18] L. F. M. da Silva and R. D. Adams, "Adhesive joints at high and low temperatures using similar and dissimilar adherends and dual adhesives," *International Journal of Adhesion and Adhesives*, vol. 27, pp. 216-226, 2007.
- [19] A. Deb, I. Malvade, P. Biswas, and J. Schroeder, "An experimental and analytical study of the mechanical behaviour of adhesively bonded joints for variable extension rates and temperatures," *International Journal of Adhesion and Adhesives*, vol. 28, pp. 1-15, 2008.

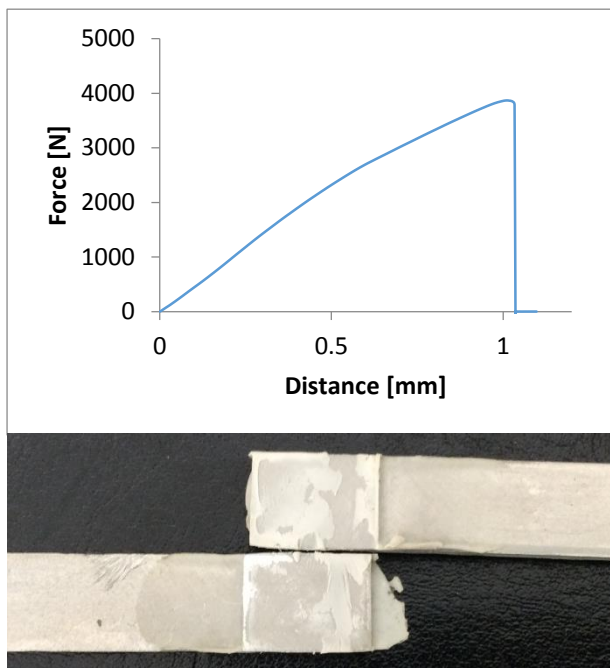
- [20] L. D. R. Grant, R. D. Adams, and L. F. M. da Silva, "Effect of the temperature on the strength of adhesively bonded single lap and T joints for the automotive industry," *International Journal of Adhesion and Adhesives*, vol. 29, pp. 535-542, 2009.
- [21] J. F. P. Owens and P. Lee-Sullivan, "Stiffness behaviour due to fracture in adhesively bonded composite-to-aluminum joints II. Experimental," *International Journal of Adhesion and Adhesives*, vol. 20, pp. 47-58, 2000.
- [22] J. Crank, *The Mathematics of Diffusion*: Clarendon Press, 1979.
- [23] M. Adamson, "Thermal expansion and swelling of cured epoxy resin used in graphite/epoxy composite materials," *Journal of Materials Science*, vol. 15, pp. 1736-1745, 1980/07/01 1980.
- [24] Y. Zhang, R. D. Adams, and L. F. M. da Silva, "Absorption and glass transition temperature of adhesives exposed to water and toluene," *International Journal of Adhesion and Adhesives*, vol. 50, pp. 85-92, 2014.
- [25] L.-R. Bao and A. F. Yee, "Effect of temperature on moisture absorption in a bismaleimide resin and its carbon fiber composites," *Polymer*, vol. 43, pp. 3987-3997, 2002.
- [26] J. F. Varajão, "Impact of CFRP adhesive joints for the automotive industry," MCs, FEUP, Porto, 2015.
- [27] V. Rudnev, D. Loveless, R. L. Cook, and M. Black, *Handbook of Induction Heating*: CRC Press, 2002.
- [28] R. J. C. Carbas, L. F. M. da Silva, and G. W. Critchlow, "Adhesively bonded functionally graded joints by induction heating," *International Journal of Adhesion and Adhesives*, vol. 48, pp. 110-118, 2014.
- [29] G. N. Gonzalez, *Aplicaciones del calentamiento por inducción electromagnética en el procesamiento de PRFV*, 2005.
- [30] DaWei Induction Heating Machine Co., Limited. Available: <http://www.dw-inductionheater.com/what-is-induction-heating.html>

# Appendix A: Results of the quasi-static tests

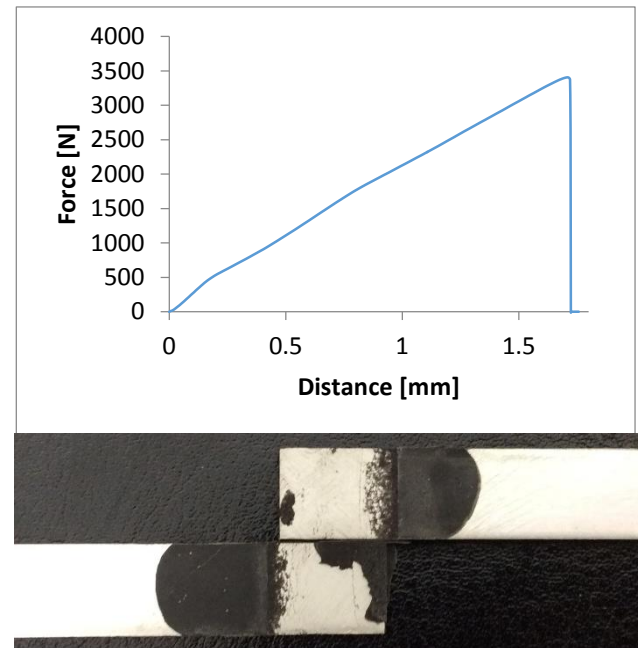
This appendix presents the individual results of the quasi-static tests for each of the combinations of conditions and adhesives. These graphs are the most indicative of the several tests performed for each condition. A photograph showing the failure mode of each joint is also presented, along with a side view in the cases where adherend yielding is visible.

## Nagase XNR 6852E-2

2 mm adherend; -20 °C; Dry

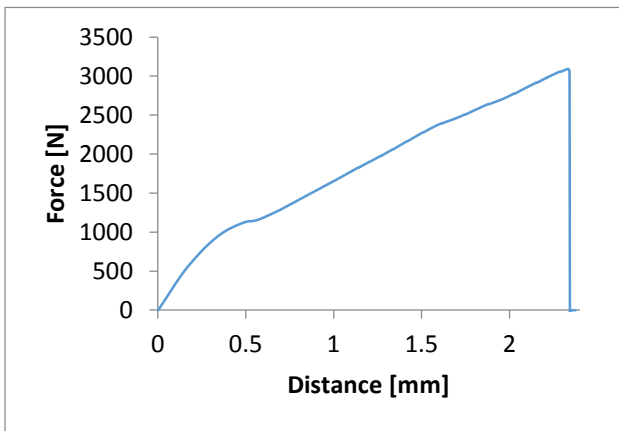


## SikaPower 4720

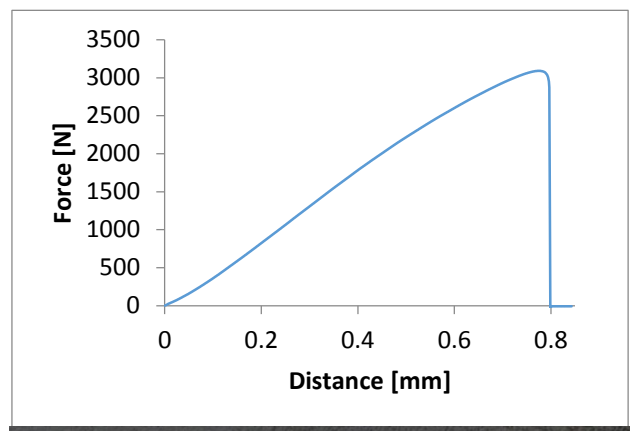


### Nagase XNR 6852E-2

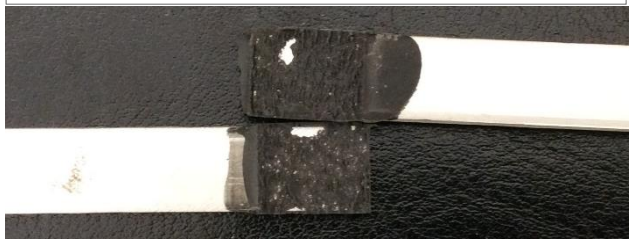
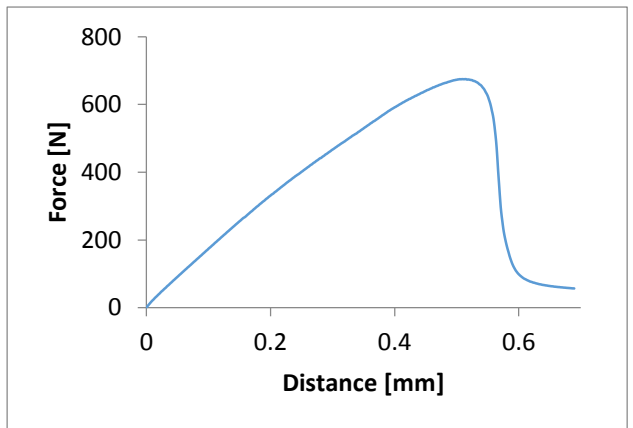
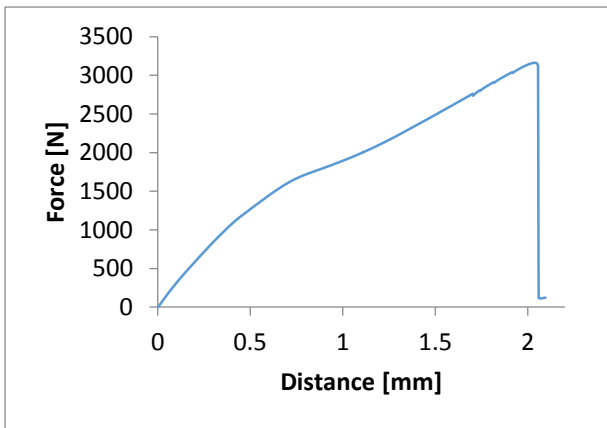
2 mm adherend; -20 °C; Moist



### SikaPower 4720

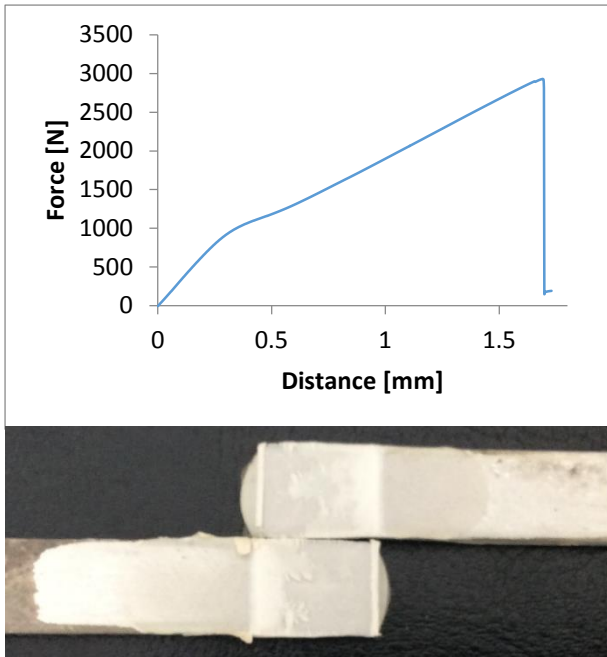


2 mm adherend; 80 °C; Dry

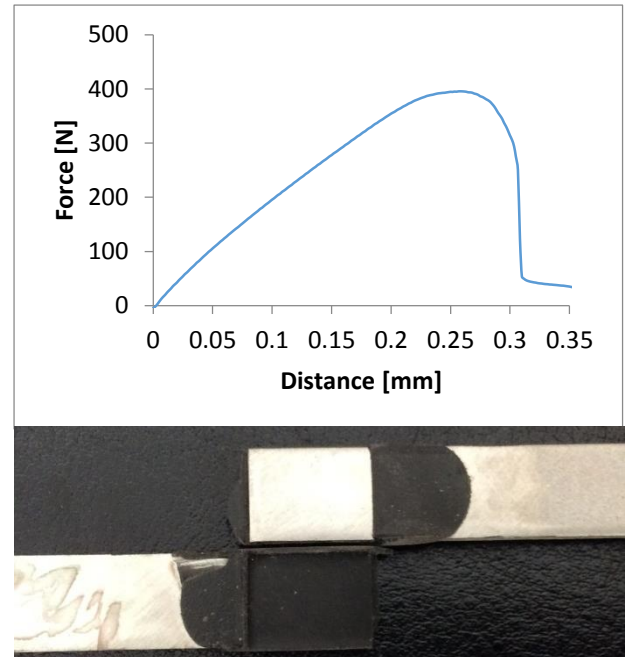


### Nagase XNR 6852E-2

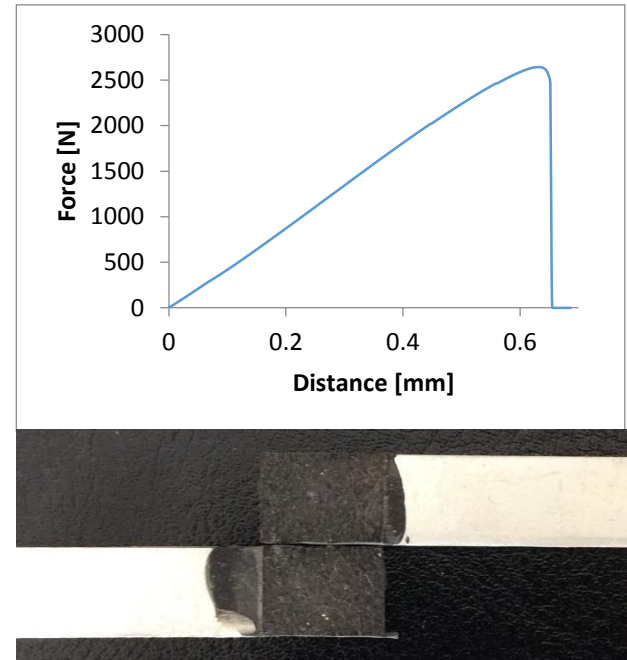
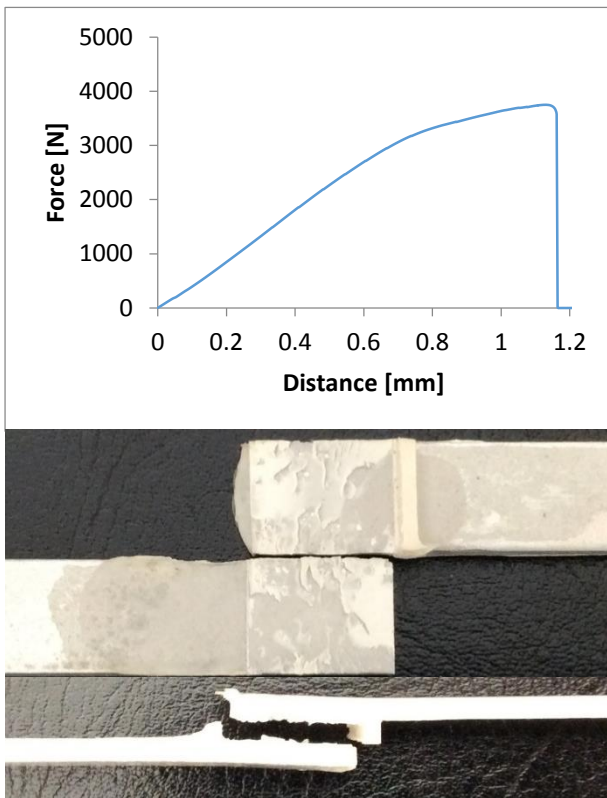
2 mm adherend; 80 °C; Moist



### SikaPower 4720

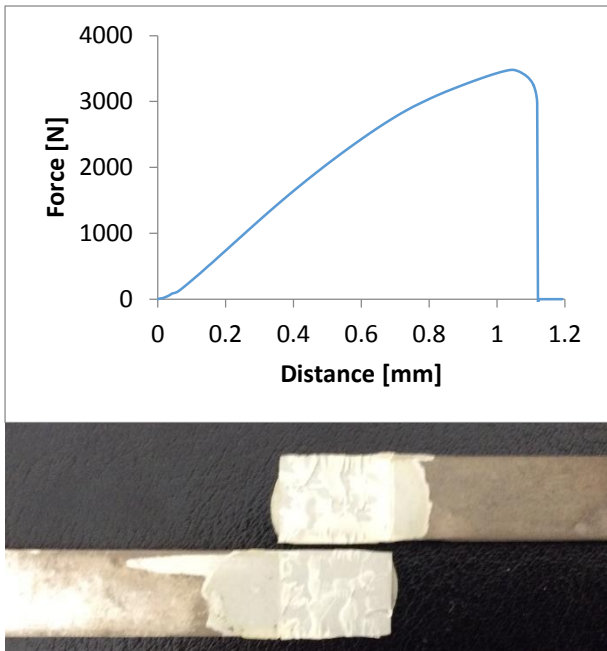


2 mm adherend; Room temperature; Dry

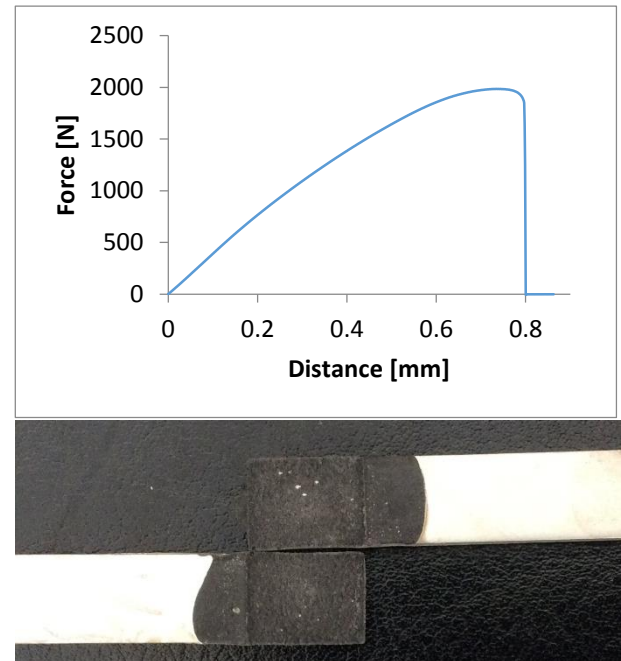


### Nagase XNR 6852E-2

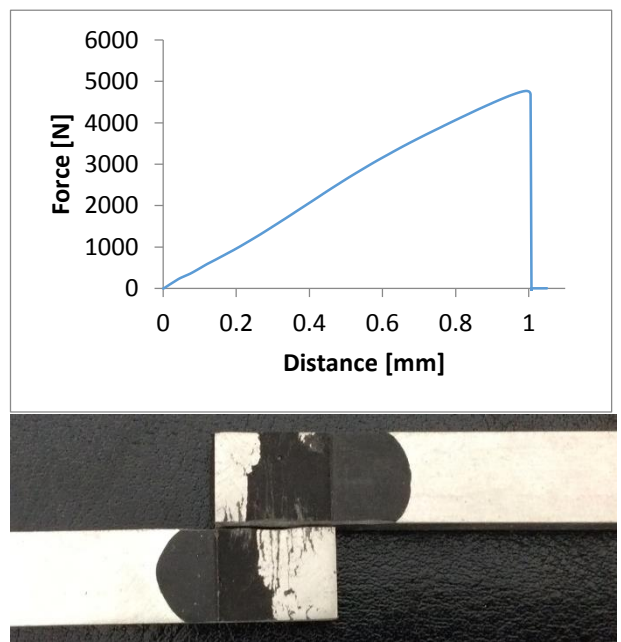
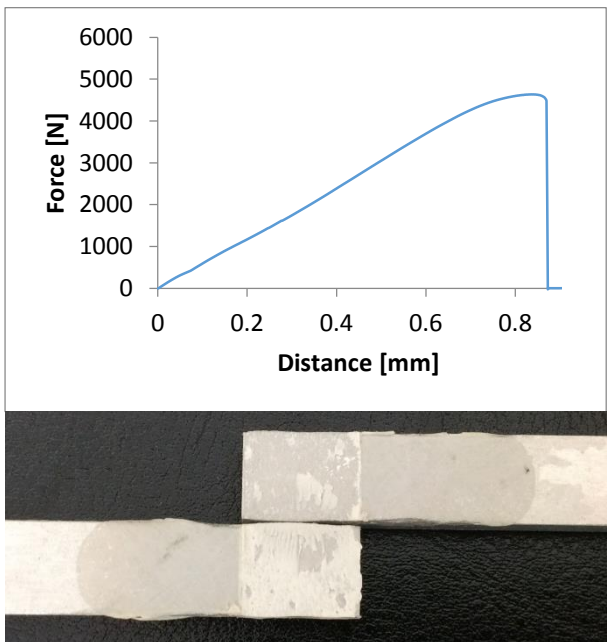
2 mm adherend; Room temperature; Moist



### SikaPower 4720

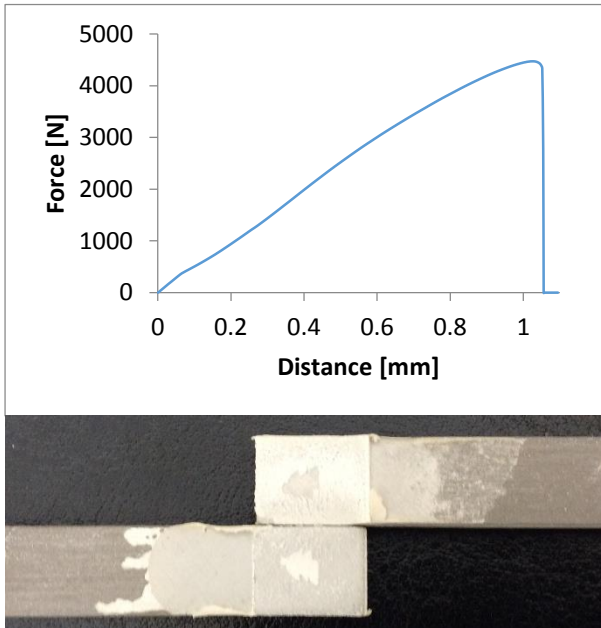


5 mm adherend; -20 °C; Dry

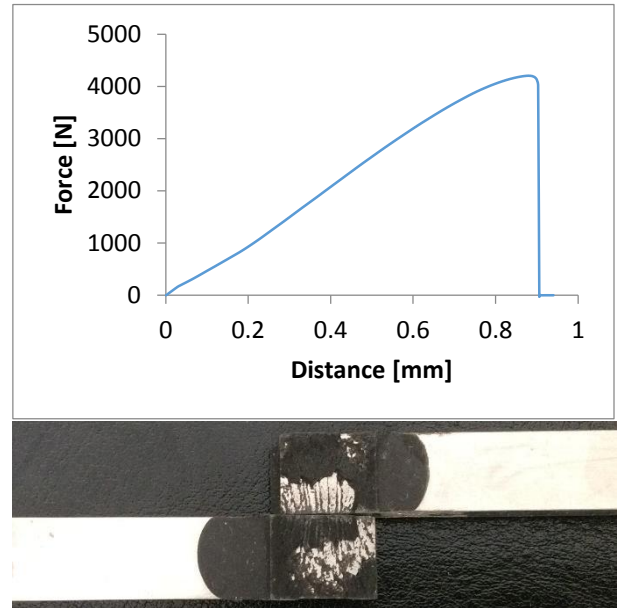


### Nagase XNR 6852E-2

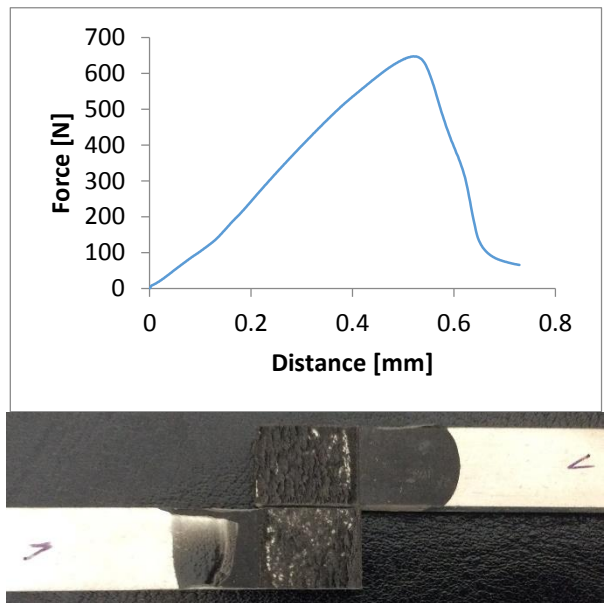
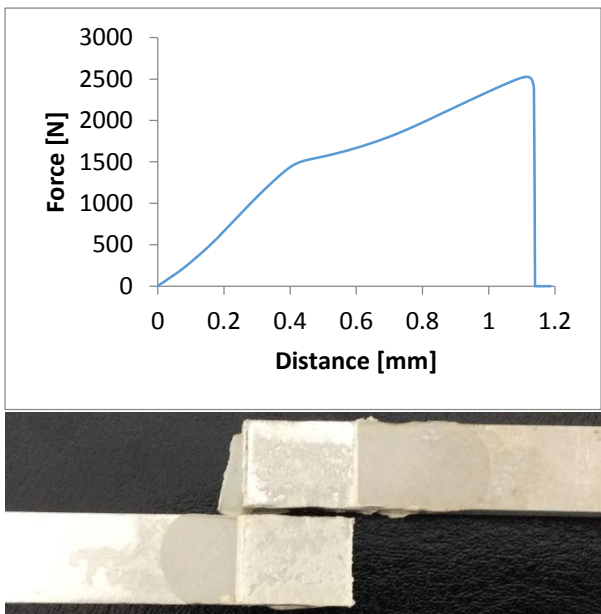
5 mm adherend; -20 °C; Moist



### SikaPower 4720

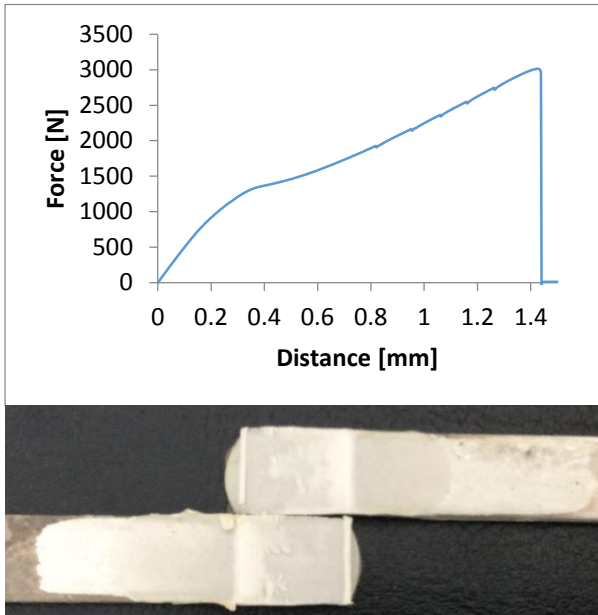


5 mm adherend; 80 °C; Dry

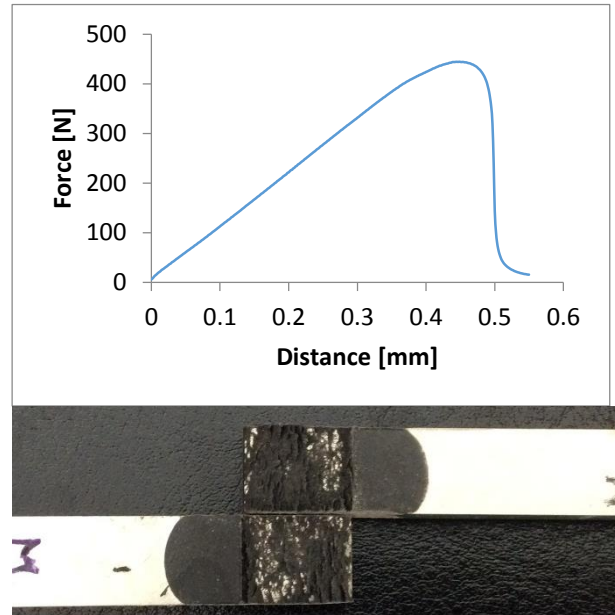


### Nagase XNR 6852E-2

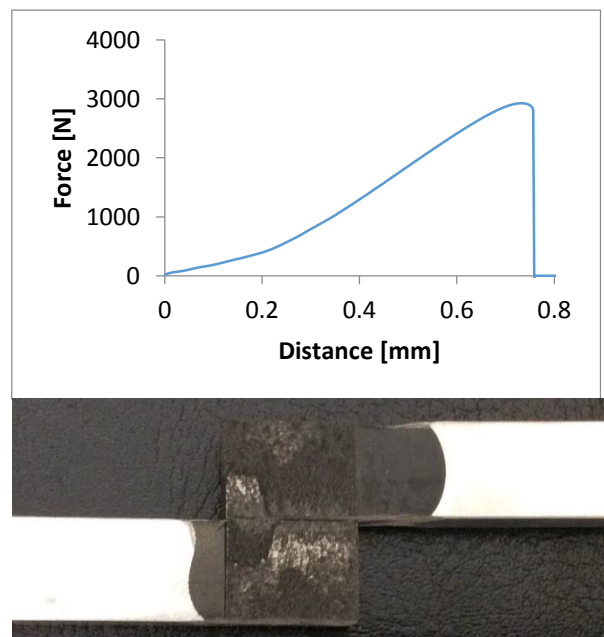
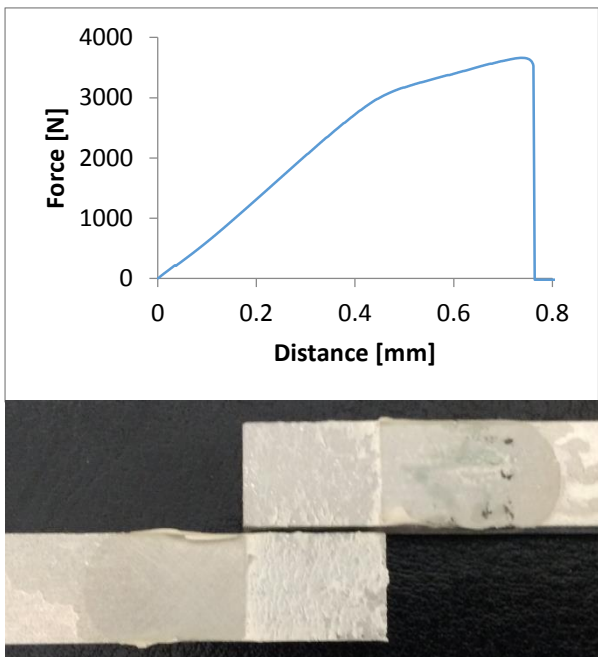
5 mm adherend; 80 °C; Moist



### SikaPower 4720



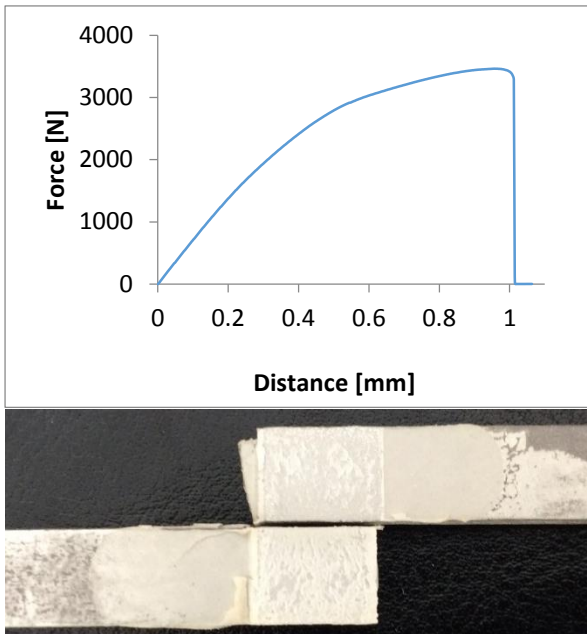
5 mm adherend; Room temperature; Dry



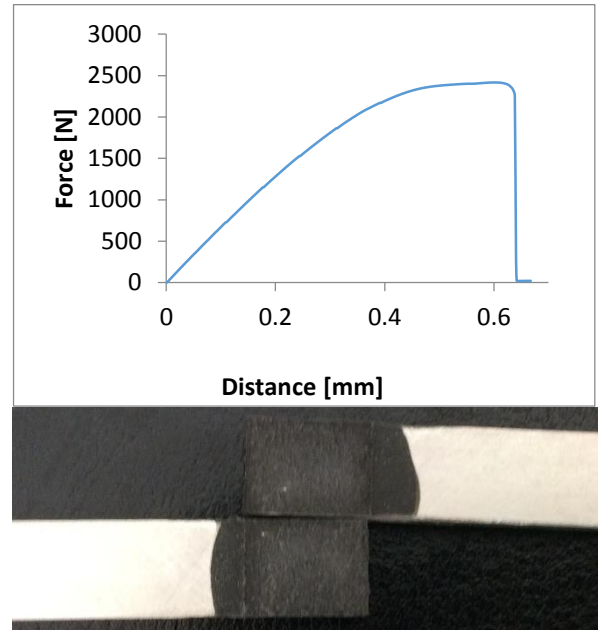


### Nagase XNR 6852E-2

5 mm adherend; Room temperature; Moist



### SikaPower 4720



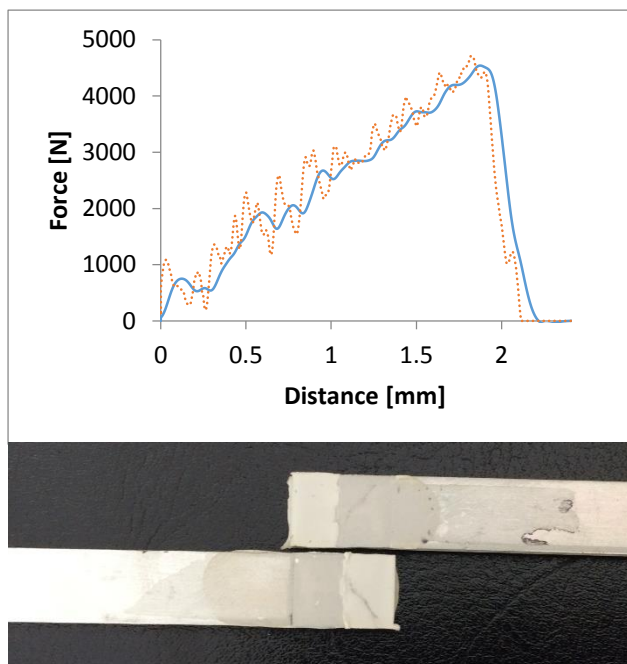


# Appendix B: Results of the impact tests

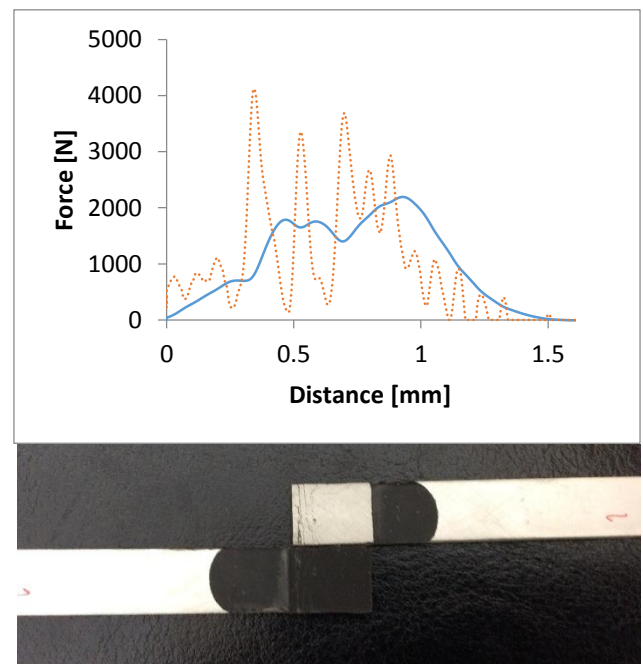
This appendix presents the individual results of the impact tests for each of the combinations of conditions and adhesives. These graphs are the most indicative of the several tests performed for each condition and are presented as given by the impact machine's software as well as using a built-in electronic filter which limits the frequency of vibrations so that the results can be more easily analysed. A frequency filter of 2000 Hz was used. It is also important to note that, to avoid results where the maximum force is affected by these vibrations, all values were obtained from the filtered values. A photograph showing the failure mode of each joint is also presented, along with a side view in the cases where adherend yielding is visible.

## Nagase XNR 6852E-2

2 mm adherend; -20 °C; Dry

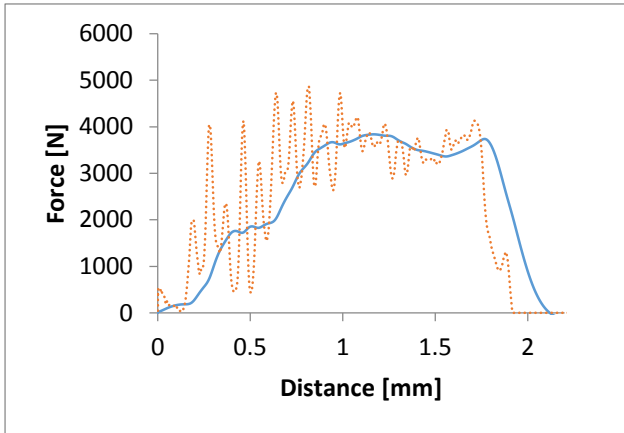


## SikaPower 4720

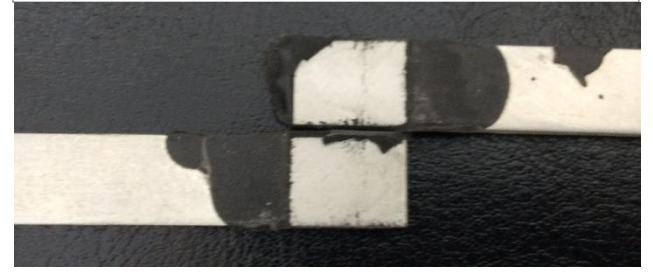
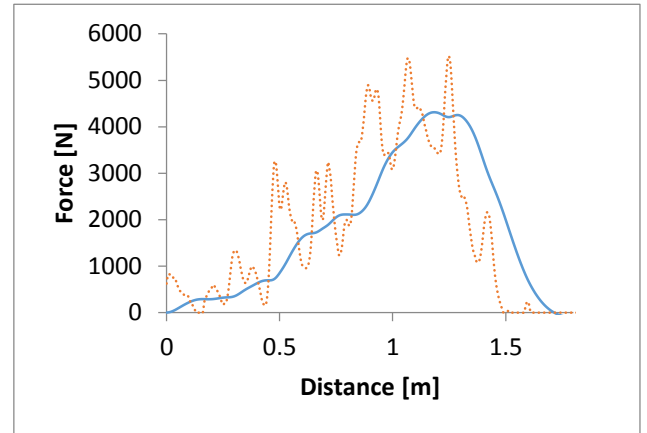


### Nagase XNR 6852E-2

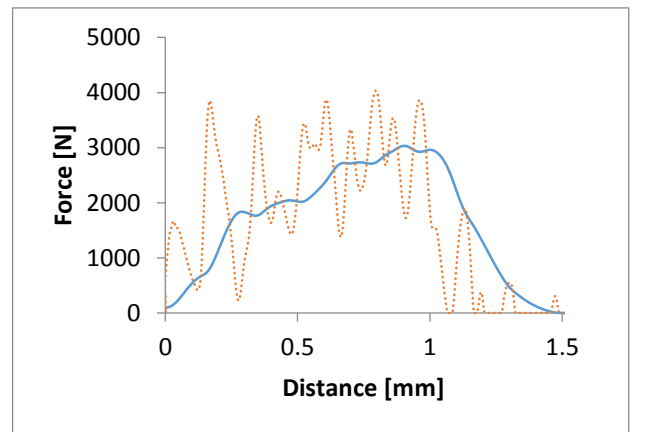
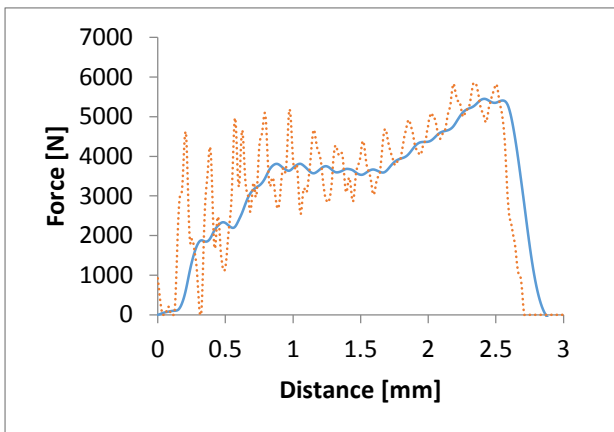
2 mm adherend; -20 °C; Moist



### SikaPower 4720

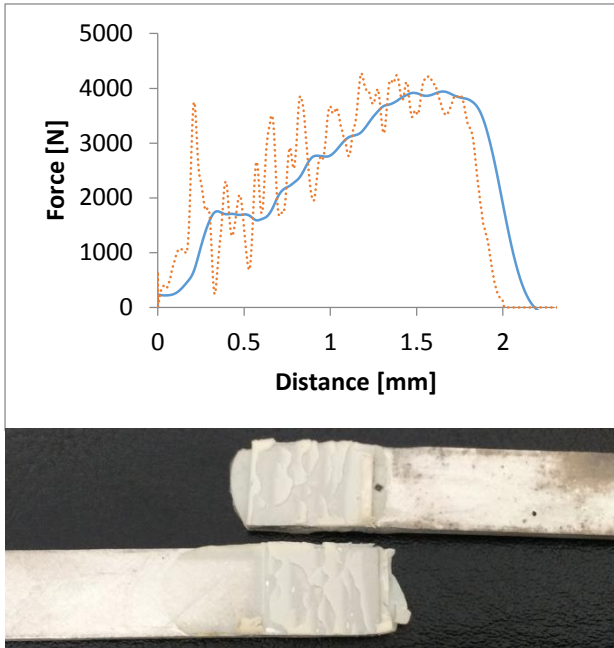


2 mm adherend; 80 °C; Dry

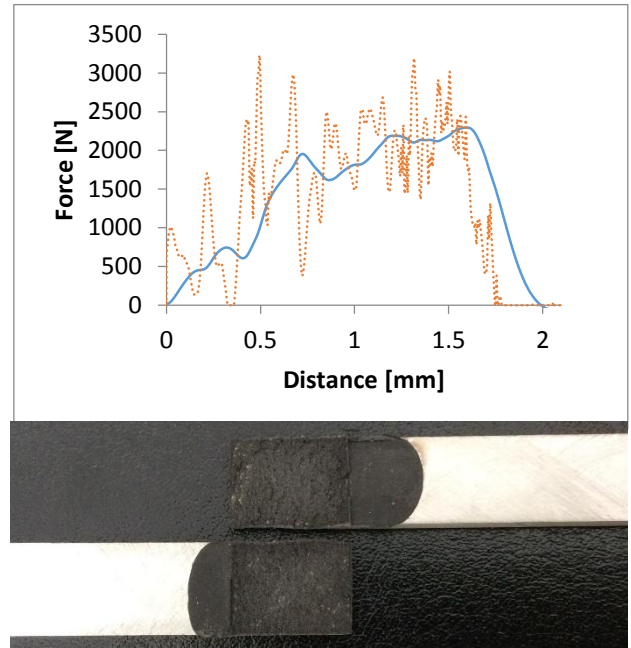


### Nagase XNR 6852E-2

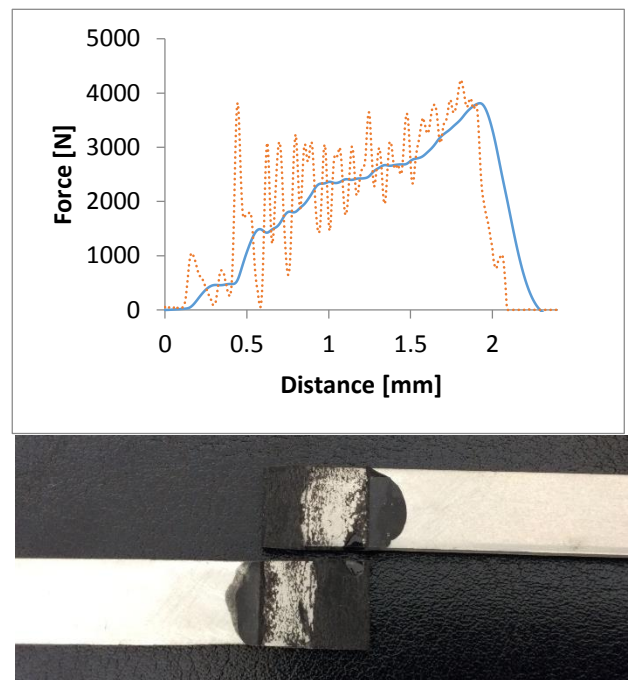
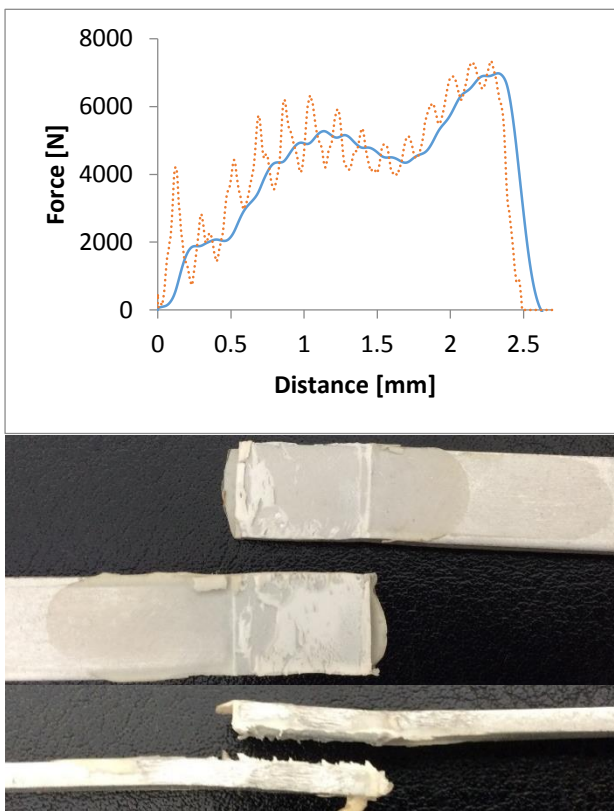
2 mm adherend; 80 °C; Moist



### SikaPower 4720

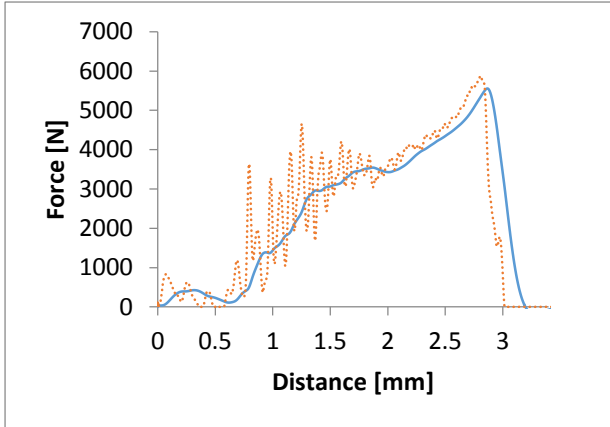


2 mm adherend; Room temperature; Dry

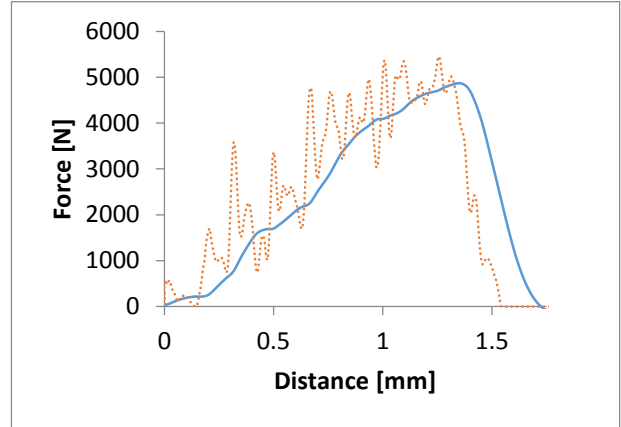


### Nagase XNR 6852E-2

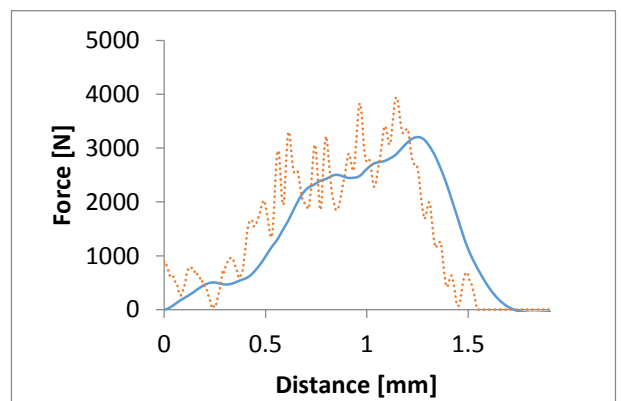
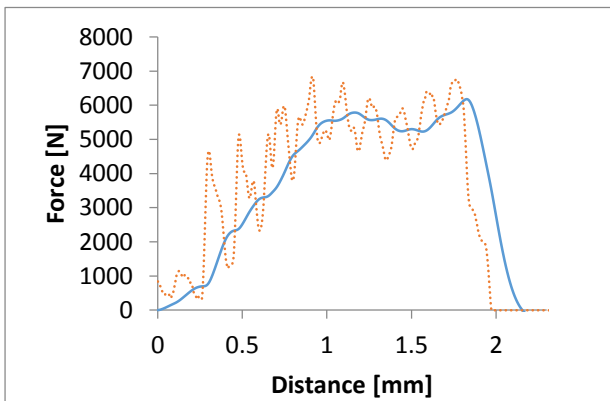
2 mm adherend; Room temperature; Moist



### SikaPower 4720

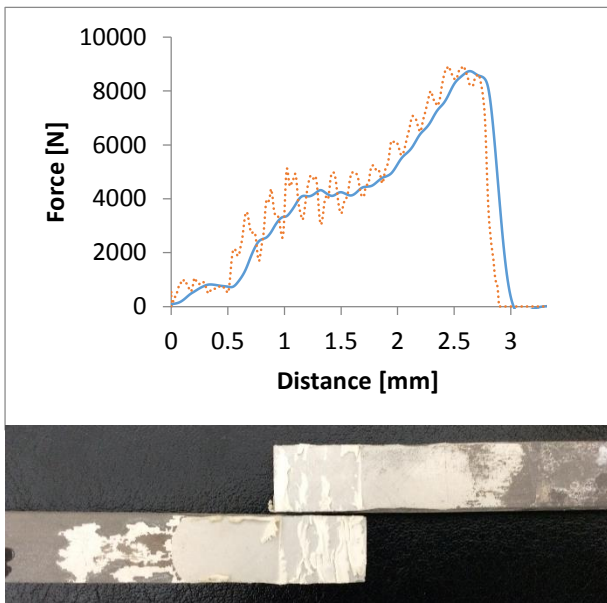


5 mm adherend; -20 °C; Dry

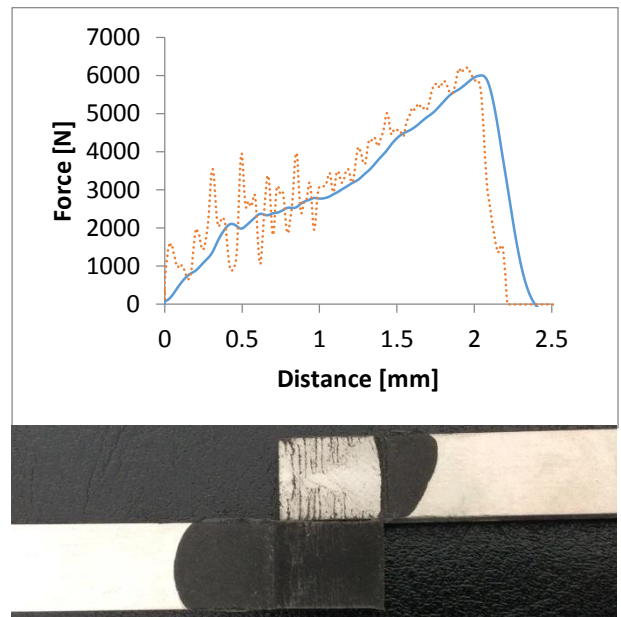


### Nagase XNR 6852E-2

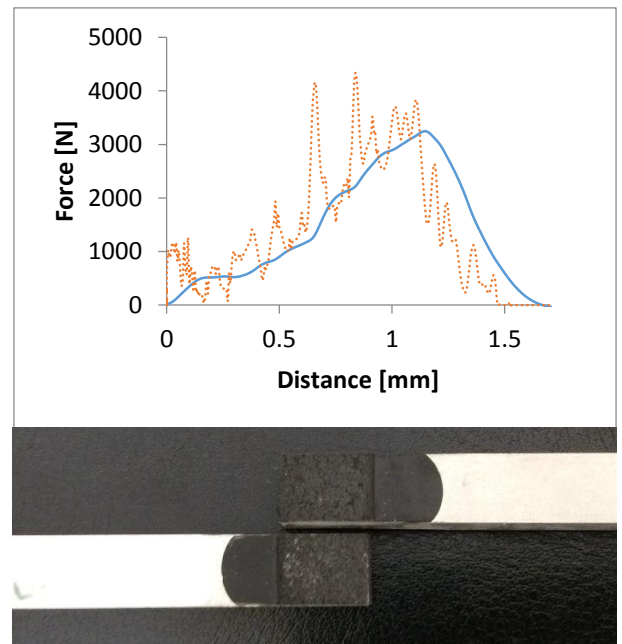
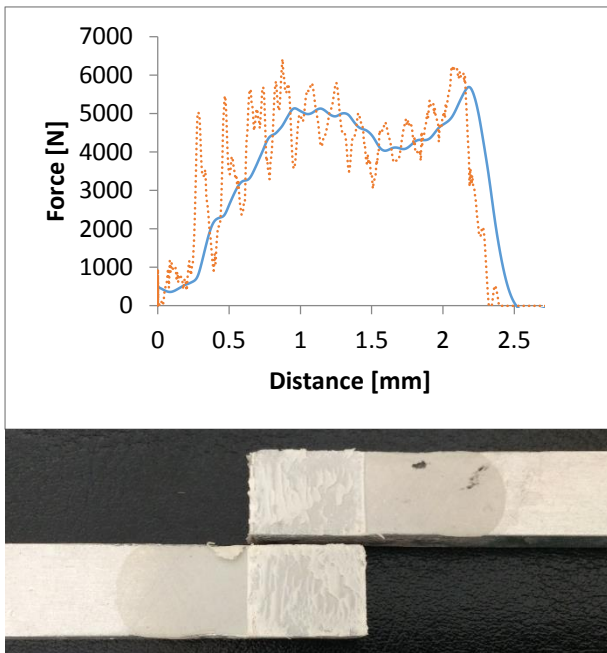
5 mm adherend; -20 °C; Moist



### SikaPower 4720

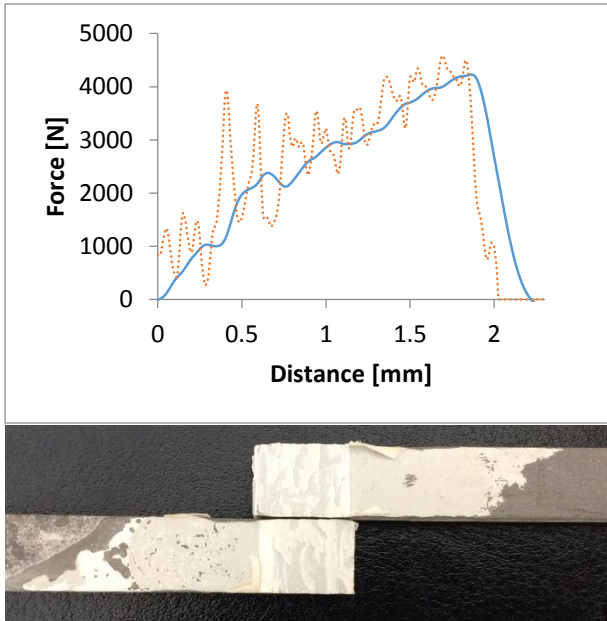


5 mm adherend; 80 °C; Dry

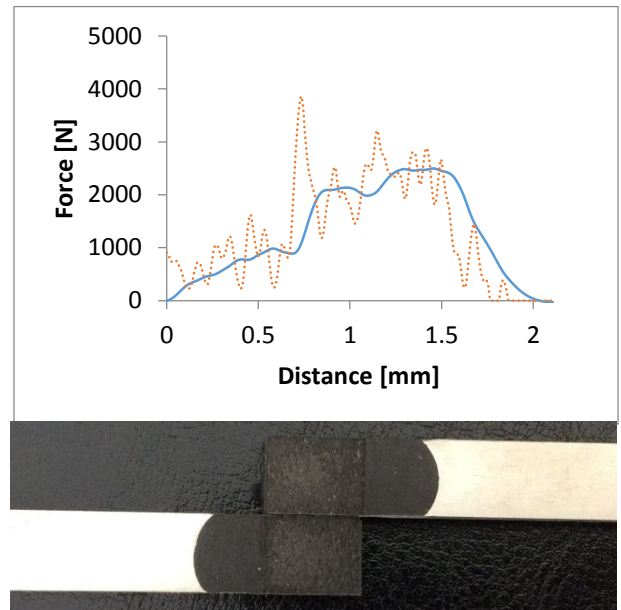


### Nagase XNR 6852E-2

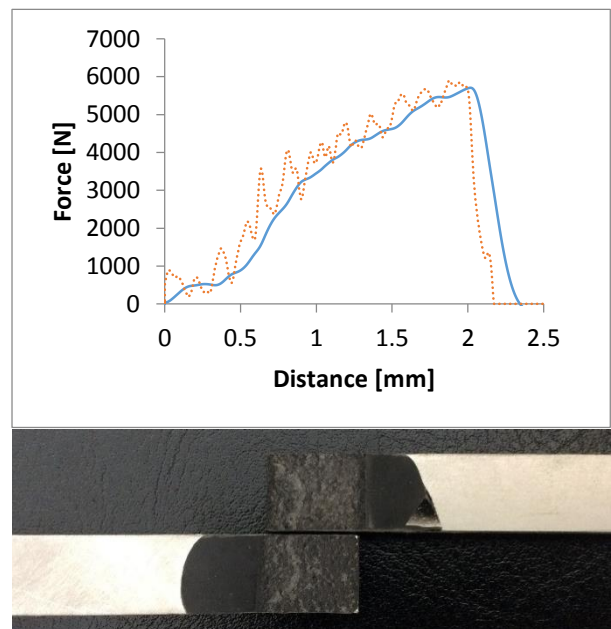
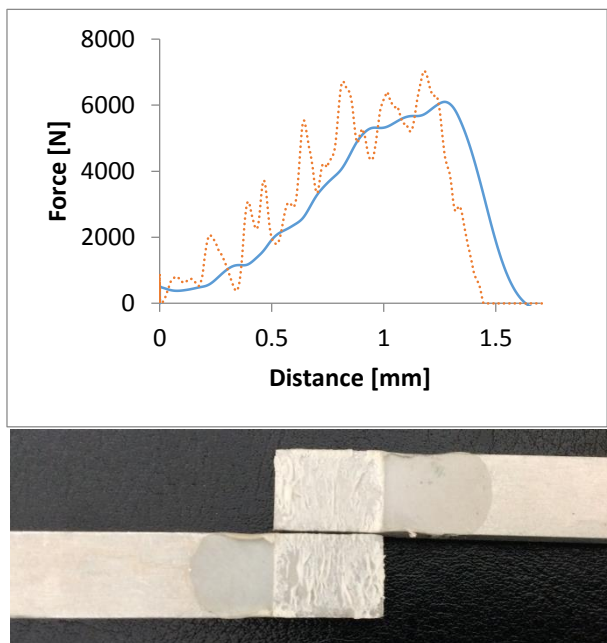
5 mm adherend; 80 °C; Moist



### SikaPower 4720



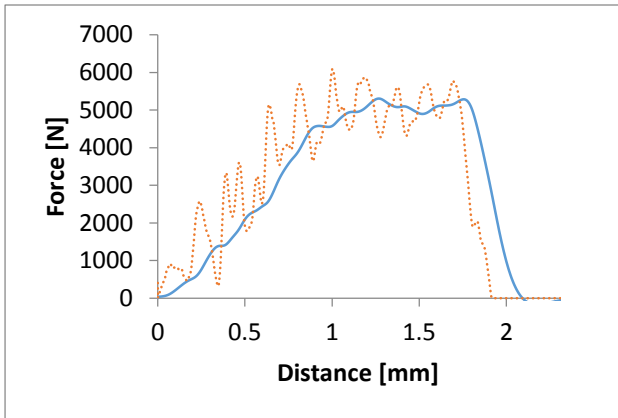
5 mm adherend; Room temperature; Dry





### Nagase XNR 6852E-2

5 mm adherend; Room temperature; Moist



### SikaPower 4720

